AD_____

GRANT NUMBER DAMD17-94-J-4468

TITLE: Mechanism of Aromatic Hydrocarbon Induced Mammary Tumorigenesis

PRINCIPAL INVESTIGATOR: Gail E. Sonenshein, Ph.D.

CONTRACTING ORGANIZATION: Boston University
Boston, Massachusetts 02118-2394

REPORT DATE: October 1997

TYPE OF REPORT: Annual

PREPARED FOR: Commander
U.S. Army Medical Research and Materiel Command
Fort Detrick, Frederick, Maryland 21702-5012

REPORT DOCUMENTATION PAGE

Form Approved
OMB No. 0704-0188

1. AGENCY USE ONLY *(Leave blank)*	2. REPORT DATE	3. REPORT TYPE AND DATES COVERED
	October 1997	Annual (30 Sep 96 - 29 Sep 97)

4. TITLE AND SUBTITLE
Mechanism of Aromatic Hydrocarbon Induced Mammary Tumorigenesis

5. FUNDING NUMBERS
DAMD17-94-J-4468

6. AUTHOR(S)
Gail E. Sonenshein, Ph.D.

7. PERFORMING ORGANIZATION NAME(S) AND ADDRESS(ES)
Boston University
Boston, Massachusetts 02118-2394

8. PERFORMING ORGANIZATION REPORT NUMBER

9. SPONSORING/MONITORING AGENCY NAME(S) AND ADDRESS(ES)
Commander
U.S. Army Medical Research and Materiel Command
Fort Detrick, Frederick, Maryland 21702-5012

10. SPONSORING/MONITORING AGENCY REPORT NUMBER

11. SUPPLEMENTARY NOTES

12a. DISTRIBUTION / AVAILABILITY STATEMENT
Approved for public release; distribution unlimited

12b. DISTRIBUTION CODE

13. ABSTRACT *(Maximum 200*

Recent evidence suggests that the rise in breast cancer rates reflects increased exposure to and bioaccumulation of environmental pollutants, such as 7,12-dimethylbenz(*a*)anthracene (DMBA). Female Sprague-Dawley rats treated with DMBA develop mammary (breast) tumor by about 15 weeks. Here experiments were proposed to elucidate the roles of the aromatic hydrocarbon (Ah) and estrogen receptors and the c-*myc* oncogene. Changes in the expression and function of these genes in normal and malignant tissue, and the regulation of any altered phenotype would be evaluated. Towards these goals, inappropriate activation of the NF-κB/Rel family of factors, which regulates c-*myc* expression, has been discovered in the rat breast neoplasias. Furthermore, NF-κB/Rel serves as a survival factor for breast cancer cells in *vitro*. Work, in progress, to address the temporal relationship between expression of these various genes and neoplastic transformation of mammary cells, has shown NF-κB/Rel activation precedes tumor formation. These findings suggest a potential mechanism for aberrant regulation of c-*myc* expression in breast cancer and for new therapeutic approaches.

14. SUBJECT TERMS	15. NUMBER OF PAGES
Breast Cancer NF-κB/Rel, c-*myc* oncogene; aromatic hydrocarbon receptor; environmental pollutants; hormone receptors; rat model	108
	16. PRICE CODE

17. SECURITY CLASSIFICATION OF REPORT	18. SECURITY CLASSIFICATION OF THIS PAGE	19. SECURITY CLASSIFICATION OF ABSTRACT	20. LIMITATION OF ABSTRACT
Unclassified	Unclassified	Unclassified	Unlimited

FOREWORD

Opinions, interpretations, conclusions and recommendations are those of the author and are not necessarily endorsed by the U.S. Army.

N/A Where copyrighted material is quoted, permission has been obtained to use such material.

N/A Where material from documents designated for limited distribution is quoted, permission has been obtained to use the material.

✓ Citations of commercial organizations and trade names in this report do not constitute an official Department of Army endorsement or approval of the products or services of these organizations.

✓ In conducting research using animals, the investigator(s) adhered to the "Guide for the Care and Use of Laboratory Animals," prepared by the Committee on Care and Use of Laboratory Animals of the Institute of Laboratory Resources, National Research Council (NIH Publication No. 86-23, Revised 1985).

____ For the protection of human subjects, the investigator(s) adhered to policies of applicable Federal Law 45 CFR 46.

✓ In conducting research utilizing recombinant DNA technology, the investigator(s) adhered to current guidelines promulgated by the National Institutes of Health.

✓ In the conduct of research utilizing recombinant DNA, the investigator(s) adhered to the NIH Guidelines for Research Involving Recombinant DNA Molecules.

✓ In the conduct of research involving hazardous organisms, the investigator(s) adhered to the CDC-NIH Guide for Biosafety in Microbiological and Biomedical Laboratories.

Paul E Lonenstein 10/27/97

PI - Signature Date

PROGRESS REPORT
TABLE OF CONTENTS

INTRODUCTION

Recent evidence suggests that the rise in breast cancer rates reflect increased exposure to and bioaccumulation of environmental pollutants, including polycyclic aromatic hydrocarbons such as 7,12-dimethylbenz(*a*)anthracene (DMBA). DMBA treatment of female Sprague-Dawley rats results in induction of mammary gland (breast) tumors. Mammary gland tumors, which develop by about 15 weeks after a single dose of DMBA, are generally well-differentiated and retain their hormonal responsiveness. In this application, we proposed to elucidate the roles of the receptors for the aromatic hydrocarbons, estrogen and prolactin hormones and the c-*myc* oncogene in a systematic, integrated fashion. Studies were proposed to evaluate changes in the expression and function of the aromatic hydrocarbon (Ah) and hormone receptors in normal and malignant tissue, and the regulation of any altered phenotype. We also proposed to monitor for potential dys-regulated expression of the c-*myc* oncogene, and elucidate the mechanisms mediating these changes. Multiple lines of evidence, including studies in transgenic mice, have demonstrated that the c-*myc* oncogene plays an important role in regulating changes that lead to neoplastic transformation of mammary epithelial cells. In summary, information on the nature of genetic alterations, and changes in cellular and molecular function involved in tumor progression should be forthcoming from these studies. Furthermore, identification of exogenous risk factors and key regulatory components may provide new targets for prevention and treatment of breast cancer. Progress has been made on all of the specific aims. In this report, an introduction is given first to set the stage with regards to the current understanding of the rat model as well of the role of the Ah and estrogen receptors and of the expression of the c-*myc* oncogene in neoplastic transformation.

Mammary Gland Tumorigenesis in Rats

It has been estimated that known risk factors such as genetics, diet, and endogenous estrogen levels account for approximately 30% of human breast cancer cases (1,2). However, changes in these factors appear unable to explain the apparent recent increases in breast cancer mortality and incidence. It has been suggested that some of the rise in breast cancer rates reflects increased exposure to and bioaccumulation of lipophilic environmental pollutants such as polycyclic aromatic hydrocarbons (PAH) like DMBA and related organochlorines (1,2). This conclusion has been drawn in part from epidemiologic studies associating elevated breast cancer rates with PAH exposure (3-6) and from studies demonstrating increased levels of aromatic hydrocarbons in breast carcinomas (7,8), and in sera from breast cancer patients (5). Given the potentially critical role that PAH may play in human breast cancer, the use of the DMBA/rat mammary tumor model to study tumorigenesis should be viewed as particularly relevant to human disease.

Rat models for breast cancer are widely used. The DMBA single dose model has permitted elucidation of factors that act at initiation of neoplasia in the gland and at the subsequent steps on tumor development. Review of papers from our own and other laboratories shows good agreement on the characteristics of tumorigenesis induced in female Sprague-Dawley (S-D) rats by DMBA with only the variations that can be expected on the basis of biological variability or differences in protocols (9-21). Under the auspices of the International Life Sciences Institute (ILSI), Dr. Rogers and 4 other experts on the DMBA model recently made a comprehensive review and evaluation of the model and of tumors induced (16). The mammary

gland tumors induced in rats comprise a spectrum of morphology from benign, typical fibroadenomas and adenomas to papillomas with hyperplastic, atypical or dysplastic epithelium and significant stromal and myoepithelial components, to tumors that are architecturally and cytologically malignant and invade adjacent normal tissue. Metastases from even the most anaplastic tumors are rare (16).

Aromatic Hydrocarbon Receptor-Dependent Tumorigenesis

The most proximal event in PAH tumorigenesis is the binding of environmental chemicals such as DMBA, benzo[*a*]pyrene, 2,3,7,8-tetrachlorodibenzo-*p*-dioxin (TCDD), and polychlorinated biphenyls (PCBs) to a cytosolic aromatic hydrocarbon receptor (AhR) (22-24). Therefore, rather than scrutinize the toxicology of a myriad of carcinogenic chemicals (e.g. there are over 200 possible PCB isomers and congeners) it is prudent to focus on a common, critical element in the transformation pathway, AhR activation. Molecular analysis of AhR structure and function has only recently been facilitated by the cloning of the murine AhR gene (22,23) and the gene coding for a requisite accessory molecule called "Arnt" (25). The AhR and Arnt are highly conserved throughout evolution (24-26).

Like most other members of a family of DNA-binding protein receptors (e.g. the estrogen, progesterone, and glucocorticoid receptors), unbound AhR is associated with a heat shock protein which may repress receptor nuclear translocation (27). Upon binding with PAH, hsp90 dissociates and the receptor complexes with an accessory molecule "Arnt," the "aromatic hydrocarbon nuclear translocating" factor (24). Formation of this heterodimer appears to be mediated by helix-loop-helix motifs present on the AhR and on Arnt (22,24). Arnt-dependent AhR activation results in receptor binding to specific Ah response elements located within an enhancer element (28). AhR binding to these core recognition sequences induces transcription of a battery of genes which code for enzymes involved in PAH metabolism (29,30). A hallmark of this transcriptional activity is the induction of cytochrome P-450IA1 mRNA synthesis and P-450 enzyme activity (29-33). Oxidation of PAH by P-450 and subsequent metabolism by P-450-dependent "phase II" enzymes (e.g. UDP glucuronyltransferase, NAD[P]H:menadione oxidoreductase, aldehyde dehydrogenase, and glutathione transferase) result in the production of reactive oxygen intermediates (e.g. diol-epoxides) which form DNA adducts, induce DNA damage, and ultimately elicit cell transformation. The role of pro-oxidant production and DNA-adduct formation in human and rat mammary neoplasias following DMBA exposure has been well documented (1,11,34,35). The extent to which this pathway is activated, as measured by P-450IA1 levels, has been correlated with human cancer risk (36-39).

AhR activity may be particularly relevant to breast cancer given the documented "cross-talk" between AhR- and ER-dependent cell activation pathways. AhR ligands such as TCDD, PCBs, dibenzo-*p*-dioxins (PCDDs) and dibenzofurans (PCDFs) regulate ER (40-47) or prolactin receptor (48) levels. These regulatory activities are AhR-dependent and are frequently manifest in human breast cancer cell lines. Interestingly, trichlorodibenzofuran, an AhR ligand, induces a time- and dose-dependent increase in cytosolic and nuclear ER and progesterone receptor levels despite its failure to directly bind either the ER or the PR (49). Thus, the potential role of aromatic hydrocarbons as "xenoestrogens" may in part reflect indirect activation of the ER through the AhR. Communication in the opposite direction, from the ER-dependent to the AhR-dependent pathway, has also been documented (41,50-52). That is, activation of the ER pathway increases activity of the AhR pathway.

AhR ligands also appear to promote transformation by activating intracellular factors and proto-oncogenes. For example, PAH exposure *in vitro* or *in vivo* results in amplification of the c-*erb*-2, c-*myc*, *c-fos*, *c-jun* and *Ha-ras* proto-oncogenes (92-95). The extent to which and the mechanisms by which the AhR mediates these activities are unclear. However, Dr. Sherr's laboratory has recently generated data demonstrating NF-κB activation *in vitro* following AhR binding. More importantly, Dr. Sonenshein's laboratory has demonstrated NF-κB activation in PAH-induced mammary tumors (see below). Collectively the data suggest that binding of the AhR by ligands induces a network of interactions involving the AhR, hormone receptors, transcription factors like NF-κB, and the oncogenes, such as c-*myc*. Therefore, we have taken an integrated approach toward analyzing regulation of these biomarkers during breast cancer development.

Role of Estrogen Receptors in Mammary Gland Cancer

It is well established that normal growth and differentiation of the mammary gland is dependent on estrogens and prolactin (15,16,53,54). Estrogens have been implicated in the etiology and development of human breast cancer (55-57). Growth of human breast cancer is often estrogen-responsive, and the presence of estrogen receptor (ER) in human breast tumors forms the basis for the use of antiestrogens for breast cancer prevention and treatment (58). Currently, ER is used as a prognostic factor in management of breast cancer patients.

The development of the hormone responsive, DMBA-induced, mammary tumor model has contributed significantly to our understanding of the role of estrogens in breast cancer (59). While administration of estrogens to ovariectomized animals stimulates tumor growth and development, ovariectomy or treatment with antiestrogens causes rapid regression of established tumors and inhibits development of new tumors in response to DMBA (56,57). It is important to note that ovarian and other hormones of pregnancy have a protective effect against DMBA-induced carcinogenesis. This protective effect is attributed to hormone-induced differentiation, which eliminates the target cell for DMBA or decreases the cellular susceptibility to tumorigenesis (15).

Approximately one third of all human breast cancer patients respond to some form of hormone therapy. DMBA-induced tumors express ER, progesterone receptor (PR) and prolactin receptors (57,58,60,61). The hormone responsiveness of DMBA-induced tumors provides a model for investigation of the role of hormones contributing to tumorigenesis.

Estrogens regulate cell growth and function by modulating gene expression through binding of the activated hormone-receptor complex to its responsive elements (ERE). Functional studies have demonstrated that ER consists of several functional domains (62,63). The N-terminal region (region A/B) contains a transactivation domain and is thought to be important for gene and cell specificity (62,63). The DNA binding domain is essential for ER recognition and specific binding to the ERE. The DNA-binding domain is also involved in nuclear translocation, dimerization and transactivation (62). Deletion of the DNA binding region or mutations in the dimerization domain or the transactivation domains eliminate ER function (63). Mutations in the hormone binding domain reduce ER function or result in a constitutively active receptor even in the absence of hormone. These mutations have been described in several human breast cancers (64).

It is unknown whether exposure of mammary gland cells to PAH produce structural or functional changes in the estrogen and progesterone receptors. It would be important to

determine if DMBA-induced tumors express altered estrogen receptors which may contribute to the process of carcinogenesis. Given the role of estrogens in the development of mammary gland carcinogenesis, any changes in ER receptor levels, structural integrity or function, in response to DMBA, may provide relevant information to the role of these receptors in breast cancer.

The c-Myc Oncogene

The c-*myc* oncogene, the cellular homologue of the transforming gene of the avian myelocytomatosis virus, has been implicated in control of cell proliferation, neoplastic transformation, and more recently in apoptosis or programmed cell death. The c-*myc* gene encodes two phosphoproteins, initiated at independent translational start sites, that localize to the nucleus (67,68). These normal cellular proteins are believed to function as transcription activators. They contain a region rich in basic amino acids (basic region), a helix-loop helix (HLH) and a leucine zipper (LZ) domain at the carboxy terminus (69). They bind a specific sequence of DNA: CACGTG (70,71). A Myc binding partner, called Max, interacts with Myc (72); the heterodimer binds and transactivates this DNA sequence more efficiently than homodimers of Myc (70,73). Evidence from many laboratories, including our own, has demonstrated that c-*myc* plays a key role in control of cell proliferation, as well as neoplastic transformation (rev. in 74). In one of the first examinations of the cell cycle expression of c-*myc,* we demonstrated that c-*myc* mRNA levels are low in normal cells in quiescence and increase early during the G0 to G1 transition (75). This induction of c-*myc* expression is required for cells to enter S phase. Cycling cells maintain constant levels of c-*myc* expression (76).

Altered expression of c-*myc* is a hallmark of transformed cells (rev. in 77). Several types of genetic alterations of c-*myc* have been noted within tumors, including point mutations within exons 1 and 2, gene amplification, gene rearrangements, and retroviral insertions (68,74,77,78). As we first demonstrated several years ago, fibroblasts transformed by DMBA display overexpression of c-*myc* RNA, even when quiescent (75). This misregulation of c-*myc* expression occurred in the absence of gene rearrangement or amplification (75). Work from many laboratories, including our own (79-81), has elucidated two major sites of regulation of c-*myc* RNA expression, gene transcription and mRNA stability. Changes in the rate of c-*myc* gene transcription are responsible for many of the increases and decreases in mRNA expression (79,80).

The role of aberrant c-*myc* expression in neoplastic transformation was confirmed when transgenic mice bearing the normal and variant forms of the c-*myc* gene under the control of an immunoglobulin enhancer were found to develop B cell tumors (82). Since the tumors were of monoclonal origin, the now generally accepted model was proposed that overexpression of c-*myc* is an early event and that subsequent activation of additional oncogenes is involved in tumor formation. Mammary tumors are similarly characterized by overexpression of c-*myc*. As high as 80% of the human breast cancers in some studies were found to overexpress c-*myc* at the RNA or protein level (83-86). For many of these tumors, c-*myc* genes were present in large copy numbers indicating amplification. In others, c-*myc* genes were detected as single copies (84), indicating that the overexpression of c-*myc* was due to altered regulation. A direct role of c-*myc* in transformation of mammary cells has been demonstrated. Transgenic mice carrying c-*myc* genes under the control of promoters expressed in mammary cells, either the mammary tumor virus (MTV) (87) or the whey acidic acid (WAP) promoter (88), develop mammary tumors exclusively.

BODY AND CONCLUSIONS

The finding/or progress relevant to each Specific Aim is detailed in the section after the aim. Figures and Tables have been included at the end of the text.

SPECIFIC AIM 1

Using the rodent model of DMBA-induced mammary tumorigenesis to investigate the pathogenesis of breast cancer: We will determine the effects of DMBA on the temporal relationships between DNA synthesis and expression of the aromatic hydrocarbon, estrogen and prolactin receptors, and the c-*myc* oncogene at the RNA and protein levels. To assess RNA expression, isolated RNA preparations will be characterized using Northern blot or RT-PCR analysis. Furthermore, in situ hybridization will be performed to assess expression in specific cells. Marker protein levels will be evaluated using immunohistochemistry. In addition, AhR will be monitored by AhR-DNA binding and P-450 enzyme levels and ER function via progesterone receptor levels.

PROGRESS:

Immunohistochemistry

In order to perform the immunohistochemical analysis of these proteins, we developed procedures for their detection. Progress in this area is summarized below:

Normal mammary glands and mammary gland tumors, as well as uteri and livers in some cases, were collected from 540 rats studied in separately supported, long-term carcinogenesis studies, one of which included rats killed at early periods (6 hours to 3 weeks) after DMBA administration.

These tissues were used to:

1) develop immunohistochemical methods for demonstration of estrogen receptor (ER), aromatic hydrocarbon receptor (AhR), proliferating cell nuclear antigen (PCNA) and NF-κB subunit p65 in formalin-fixed, paraffin-embedded sections.

2) develop an image analysis program to study the ER and PCNA staining in a semiquantitive manner in normal and neoplastic glands.

3) develop biochemical and molecular techniques to study the mRNA species for the estrogen and aromatic hydrocarbon receptors and for c-*myc* oncogene using RT-PCR and in situ hybridization.

Livers from normal mice, studied in a separately supported experiment, and cell lines from mouse hepatocellular carcinomas carried in Dr. Sherr's laboratory were used to develop an immunohistochemical method to stain the AhR that was subsequently applied to the rat tissue.

The rats used for these studies are from three carcinogenesis studies. They are female, Sprague-Dawley rats (Charles River Laboratories, Wilmington, MA) fed from weaning the AIN76-A diet and housed individually in environmentally controlled quarters. They were given a single intragastric dose of DMBA, 25 mg/kg (Expt 1) or 15 mg/kg (Expts 2 and 3), at 55 days of age. They were weighed and palpated for tumor weekly and killed by CO2 inhalation 16-18

weeks after DMBA exposure. (A few rats were killed at 10-15 weeks in each experiment because they bore large or ulcerated tumors).

At necropsy, all tumors and normal mammary glands were dissected rapidly. Tumors were weighed and sectioned rapidly for:

1) immediate freezing in dry ice for biochemical and molecular studies.
2) fixation and processing for histology and immunohistochemistry.

Normal glands were not weighed but were frozen or fixed as above.

All tumors that exceeded 0.3g in weight were divided. One section was fixed in 10% neutral buffered formalin (NBF) (Expt 1) or paraformaldehyde (Expts 2 and 3) for histologic and immunohistochemical analysis; one section was frozen in dry ice for biochemical analysis. The fixed tissues subsequently underwent alcoholic dehydration and a paraffin infiltration process and then were embedded in paraffin. Normal glands were prepared in the same way. The sections were mounted on 3-aminoproplytriethoxysilane (Silane) coated slides. The following stains are being performed on consecutive three micron sections taken from each block.

Hematoxylin & Eosin (H&E): Each slide was stained as a routine H&E.
Feulgen Staining: This stain is used to evaluate DNA content of cells. The RIAS Feulgen Biological Stain Kit for DNA Evaluation from Roche Image Analysis Systems was used. The procedure has been outlined in the progress report for year 1 of this grant.
Estrogen Receptor (ER) Staining: Dako's ER clone 1D5 is a mouse monoclonal antibody used to detect estrogen receptor in the cell, using procedures outlined in the progress report for year 1 of this grant.
Proliferating Cell Nuclear Antigen (PCNA) Staining: BioGenex's PCNA clone 19A.2 is used to stain cells which are actively proliferating. It recognizes cells in all stages, except for G0. The procedure used was outlined in the progress report for year 1 of this grant
Aromatic Hydrocarbon Receptor (AhR) Staining: A polyclonal rabbit antibody to the mouse AhR, obtained by Dr. Sherr from Dr. Richard Pollenz, has been shown to cross-react with rat AhR in western blots and to detect murine AhR by immunohistochemistry. NF-κB p65 staining: Santa Cruz Biotechnology rabbit polyclonal antibody.

Results

The histology and immunohistochemical (IHC) results are being evaluated and the results entered into a central file that will, ultimately, contain all the morphological, biochemical and molecular data collected by all the participating laboratories for each tumor, gland and animal. The partially completed morphological data are given below.

Immunohistochemical Studies of AhR and NF-κB in the Mammary Gland and 7,12-dimethylbenz(a)anthracene-induced Tumors:

AhR staining in tissues from Expts. 1 and 2 combined are shown in Table 1. Very few epithelial cells in either normal glands or tumors show nuclear staining for the AhR; there is cytoplasmic staining and staining of infiltrating mononuclear cells. Some nuclear staining was present in virtually all the tumors examined, regardless of their histology. Nuclear staining was detected in only a few histologically normal glands from control rats or DMBA-treated rats.

If a gland did contain cells with positive nuclei, the number of positive cells expressed per 10,000 cells was similar to the number of positive cells in the tumors.

For NF-κB p65 subunit the results are shown separately because a different staining protocol was used in expt. 1 than in expts. 2 and 3. In expt. 1 few normal glands were evaluated; some staining was detected in the nuclei as well as in infiltrating mononuclear cells. The results in the tumors suggested that translocation might be greater in malignant than benign tumors (Table 2). In expt. 2, tumors were more likely to show nuclear translocation than normal glands, and normal glands from a few DMBA -treated rats showed translocation (Table 3). However, there was no detectable effect of tumor histology (benign or malignant) on NF-κB p65 subunit nuclear translocation in this experiment.

There is wide variation in the results for both AhR and NF-κB p65 subunit, and we are now completing the analysis of the third experiment to evaluate more completely nuclear translocation of these two entities.

We are studying also changes in the glands early after DMBA exposure in rats fed the control AIN-76 A diet or fed a high N-6-polyunsaturated fat diet (23.5% corn oil), which promotes DMBA-induced mammary tumorigenesis.

Rats were necropsied at 6 hours, 24 hours, 1 week, 3 weeks, or 9 weeks after a single gavage of 15 mg/kg DMBA. Beginning three days after DMBA, one-half of the rats initially fed AIN-76A diet (corn oil 5%), were fed the high fat diet which is nutritionally balanced and comparable to the AIN-76A diet. NF-κB p65 subunit nuclear translocation 3 weeks after DMBA was higher in the DMBA-treated rats fed control diet than in the DMBA-treated rats fed the high fat diet (P=0.005). Virtually all DMBA-treated rats showed translocation that time. In contrast, only one of five rats fed the high fat diet but not given DMBA showed translocation (Table 4). Evaluation of slides from the other groups and times is proceeding.

Estrogen and Progesterone Receptors in the Mammary Glands and 7,12-dimethylbenz(a)anthracene-induced Mammary Gland Tumors in Female Sprague-Dawley Rats:

Expt. 1: Seventeen weeks after administration of vehicle (group C1) or 7,12-dimethylbenz(a)anthracene (DMBA), 25 mg/kg by gastric gavage (C2) at 8 weeks of age, 180 female Sprague-Dawley rats fed a purified control diet, AIN-76A, were killed by CO_2 inhalation. All mammary gland tumors and grossly normal glands were excised. One section was immediately taken from each tumor and fixed in 10% neutral buffered formalin for subsequent alcoholic dehydration and embedding in paraffin for histologic, immunohistochemical, and in-situ hybridization analyses. The remaining tissue was immediately frozen on dry ice for molecular and biochemical analyses. All samples were marked with an identification number for later comparisons. Using the standard dextran-coated charcoal, receptor-ligand binding assays for estrogen and progesterone receptors (ER, PR), each tumor and normal gland was analyzed for ER and PR content.

Normal mammary glands from DMBA treated rats showed no effect of DMBA on ER expression, but there was a suggestive increase in PR expression with DMBA ($p=0.07$). Compared to normal mammary glands, DMBA-induced benign and malignant tumors had significantly increased levels of ER and PR (<0.05) (Table 5).

Assays of additional tissues from expts. 2 and 3 are in progress.

Expt. 3. This experiment (see above) was designed in part to examine ER and PR expression in the mammary gland at intervals beginning 6 hours after DMBA administration and ending 9 weeks later, the time at which tumors first appear. At necrospy all mammary glands were excised. Three sections were immediately fixed in cold 4% paraformaldehyde for subsequent alcoholic dehydration and embedding in paraffin for histologic, immunohistochemical, and in situ hybridization analyses. The remaining tissue was immediately frozen on dry ice for molecular and biochemical analyses. Uteri from the rats in the 9-week group were also excised and frozen for biochemical analyses. All samples were marked with an identification number for later comparisons. Using the standard dextran-coated charcoal, receptor-ligand binding assays for ER and PR, mammary glands were analyzed for ER and PR content.

In DMBA-treated rats fed the control diet (C4), ER expression appears to be slightly decreased compared to vehicle-treated rats (C1) 24 hours, 1 week and 3 weeks after DMBA. This decrease was abolished in DMBA-treated rats fed a high N-6-PUFA diet (CF4). In the vehicle-treated rats fed the high fat diet (CFI) there was no detectable effect of diet. (Figure 1).

In DMBA-treated rats fed the control diet (C4) PR expression was the same as in vehicle controls (C1). In DMBA treated rats fed the high PUFA diet (CF4), PR levels appear to be slightly decreased at 1 week and 3 weeks after DMBA. In vehicle-treated rats (CF1) PR levels were the same as in rats fed control diet (Figure 2).

We are currently undertaking the following:

1. Completion of dextran-coated charcoal, receptor-ligand binding assays for tumors and normal tissues (mammary glands and uteri) in the animals in the second experiment that were killed 16-18 weeks after DMBA, to extend these findings and determine the specificity of the effects seen in the mammary glands.
2. Correlation of biochemical ER and PR results with immunohistochemical evaluation of ER and PR .
3. Correlation of the ER and PR results with NF-κB and c-*myc* data from Dr. Sonenshein's laboratory.
4. Creation of a database for each specimen in the experiments, so that all results can be easily summarized and correlated. This database will include the following information: experiment number, rat identification number, site of tumor, histologic diagnosis, treatment (DMBA, diet), and measurements of ER, PR, NF-κB, c-*myc* and AhR.

Analysis of c-*myc* Oncogene mRNA Levels in Mammary Tumors

Using *in situ* hybridization, we have detected increased expression of c-*myc* transcripts in the tumor tissue compared to normal mammary glands. These experiments have been performed using a clone encoding a genomic fragment of the rat c-*myc* gene, including the first 195 bp of exon III, and were described in last year's Progress Report. RNA probes were prepared in both orientations. The antisense probe can detect c-*myc* mRNA whereas the sense probe serves as a control for background hybridization. As an additional control, an antisense rat α1(I) collagen probe, which hybridizes specifically with cells of fibroblastic rather than epithelial origins, was similarly used. The c-*myc* antisense probe hybridized to the epithelial cell layer surrounding the ducts in the normal mammary gland in contrast to the hybridization pattern of the collagen probe. The control c-*myc* sense probe failed to hybridize, as expected, demonstrating the specificity of the hybridization for this oncogene. Furthermore, the intensity of hybridization was routinely found to be higher in the tumors isolated 15 weeks following exposure to DMBA compared to the normal mammary gland. Thus c-*myc* mRNA expression is elevated in the tumor tissue and potentially in the pre-malignant mammary tissue as well.

To begin to assess the kinetics of the induction of the levels of c-*myc* expression in the tumor tissue, we are in the process of isolating RNA from mammary glands of rats administered DMBA for various periods of time ranging from 6 hours to 9 weeks, i.e., preceding the appearance of tumors. All mammary glands were harvested and combined from control and DMBA-treated rats. These RNA preparations are being process for Northern blot analysis to monitor c-*myc* mRNA levels. This should provide valuable information on the kinetics of induction of c-*myc* gene expression. Furthermore, we try to correlate the appearance of this message with activation of NF-κB/Rel, a transcription factor implicated in regulation of c-*myc* gene transcription; aberrant activation of NF-κB/Rel has been observed in rat tumors, see Aim 3 below.

SPECIFIC AIM 2

Using the rodent model of DMBA-induced mammary tumorigenesis to investigate the pathogenesis of breast cancer: We will determine the ability of DMBA to result in production of mutated ER and c-*myc* genes by assessment of DNA and/or protein structural integrity.

PROGRESS:

Studies on Expression of a Novel Nuclear Matrix Protein in Estrogen Receptor-Negative Breast Cancer

There is an urgent need for identification of node-negative patients whose tumors have a metastatic potential. Several tumor markers have been used in assessing tumor changes linked to poor prognosis. These include loss of ER and PR, high blood vessel count (angiogenesis), amplification of *erbB2/HER2/neu* gene and decreased activity of *nm23* gene. None of these markers alone, however, predict, with complete reliability, which node-negative patients will be likely to relapse. Recently, we have identified a novel protein while screening for variant ER

proteins using site-directed monoclonal ER antibodies. Importantly, this protein was found to be absent in ER^- cells and thus represents a potential marker. Below the studies on this 55 kDa protein, termed *nmt55* are described.

The 55 kDa nuclear *nmt55* protein was identified and characterized from human breast tumors and MCF-7 cell line. Measurements of estrogen (ER) and progesterone (PR) receptors, by ligand binding assays, in cytosols of 63 human breast tumors permitted classifications of these tumors into four phenotypes (ER^+/PR^+, ER^+/PR^-, ER^-/PR^-, ER^-/PR^+). *nmt55* protein expression in these tumors, as determined from Western blot analyses, showed a statistically significant association ($p=0.001$) with tumor hormonal phenotype. A review of the pathological characteristics of tumors analyzed suggested that lack of *nmt55* expression was significantly associated with mean tumor size ($p < 0.03$), mean ER ($p= 0.001$) and mean PR ($p <0.002$), but was not associated with tumor stage, grade or type. To further study this protein, we cloned and sequenced a 2.5-kb cDNA. The complete predicted open reading frame encodes a predicted protein with 471 amino acids and a calculated molecular mass of 54,169 Da. These data area consistent with molecular mass obtained by gel electrophoresis. The deduced amino acid sequence exhibited unique regions rich in glutamine, histidine, arginine, and glutamic acid. Northern blot analysis of RNA from MCF-7 cells and ER^+/PR^+ human breast tumors showed a 2.6 kb mRNA. Southern blot analysis suggested that presence of a single copy of this gene. Chromosomal mapping, using fluorescent in situ hybridization (FISH), located *nmt55* gene to the X chromosome, region q13. The extensive homology between *nmt55* and RNA binding proteins suggested that *nmt55* may be involved in hnRNA splicing. The strong association observed between expression of *nmt55*, tumor hormonal phenotype, mean tumor size, mean ER, and mean PR content suggests that loss of *nmt55* expression may be related to events involved in hormone-insensitivity, tumor differentiation and unregulated tumor cell growth and metastases (see enclosed publication, Traish et al., 1997).

To investigate the possible regulatory role of *nmt55* in cellular function, we have used gel shift mobility assays to determine the putative DNA binding elements for this protein. Using homology sequences with other nuclear proteins, we have shown that *nmt55* binds to intercisternal A-particle proximal enhancer element (IPE), with specific DNA sequence, GATCATCAGGGAGTGACACGTCCGA. As shown in Figure 3, nmt 55 bound IPE probe specifically (lane 3) since unlabeled IPE (lane 2) competed for binding of proteins to the IPE probe. To further determine that this IPE probe represent a binding site for *nmt55* and further characterize sequence requirements for binding, interaction of *nmt55* with IPE probe was carried out in the presence of mutated sequence of IPE and with DNA representing the cAMP response elements (CRE). As shown in lanes 4, mutated IPE (mt2) reduced *nmt55* binding to IPE probe. Mutated IPE (mt3) and CRE did not compete for IPE probe binding to *nmt55* (lanes 5 and 7). Mutated IPE (mt4) was very effective in displacing IPE probe from *nmt55* (lane 6).

Identification Of Proteins That Associate With *nmt55*

To determine if *nmt55* associates with members of RNA splicing proteins, we carried out experiments in which cells were labeled with ^{35}S methionine, proteins extracted and immunprecipitated with monoclonal and polyclonal antibodies. Figure 4, lane 7 represents ^{35}S methionine labeled total nuclear extracts. Incubation with pre-immune serum (lane 1) did not

show a strong band at molecular weights of 55 and 100 kDa, while immunoprecipitation with antibody NMT5 (lane 2) showed a strongly labeled protein band at 100 and 55 kDa, respectively. This suggests that *nmt55* associates with a 100 kDa protein. Similarly, immunoprecipitation with pre-immune serum or with antibody NMT4 provided similar results (lanes 3 and 4). Using unrelated antibody (ER-213) raised against ER, only a weakly labeled band was detected (lane 5). In contrast, immunoprecipitation with NMT1 antibody (lane 6) showed strongly labeled bands at 100 and 55 kDa, respectively.

To confirm this finding, parallel samples were immunoprecipitated with NMT1 monoclonal antibodies, electrophoresed and electrotransfered and the proteins were detected using specific antibodies to either *nmt55* or the 100 kDa PSF (Polypyrimidine tract binding protein Splicing Factor) protein. As shown in Figure 5, lanes 1 and 2, antibodies raised against PSF detected a specific 100 kDa band in the co-immunoprecipitate, suggesting that *nmt55* is associated with PSF. Lanes 3 and 4 demonstrate the presence of *nmt55* in the co-immunoprecipitates. Immunoprecipitation with antibodies to PSF also resulted in detection of *nmt55* protein in the co-immunoprecipitate. These observations indicate that *nmt55* associates with polypyrimidine tract binding protein PSF.

Detection of Estrogen Receptors in Human Breast Tumors by Immunoblotting

With the advent of improved mammograpy techniques in early detection of breast cancer, tumor size is expected to be smaller. This reduces the amount of tissue available to perform conventional ligand binding assays for receptor analysis. New methods of receptor detection in smaller tissue sample size or in needle aspiration biopsies are becoming necessary. Immunochemical assays utilizing specific antibodies are the alternatives to the classical ligand binding assays. To this end, we have developed site-directed monoclonal antibodies, which were proven useful for immunohistochmistry and in immunoblotting. We have compared detection of estrogen receptor by ligand binding assays and by western blots in the extracts of 40 human breast tumors. Using antibody EVG-F9, and western blots, we were able to detect comparable values of estrogen receptors to those determined by ligand binding assays. This suggests that western blot analyses can be performed on small tissue sample or needle aspirated of breast cancer.

Studies on Estrogen Receptor Activation and Phosphorylation

We have found that treatment of MCF-7 cells in culture with estradiol results in phophorylation of ER, as determined by western blot analysis using specific site-directed monoclonal antibodies to ER. The phosphorylation of ER correlates with receptor activation *in situ.* We have taken advantages of this assay system and analyzed the binding properties and the ability of polychlorinated biphenyls (Figure 6) to activate ER in intact cells. As shown in Figure 7, polychlorinated biphenyls bind to ER with moderate affinity and cause ER activation, as demonstrated by the reduced electrophoretic mobility of ER (Figure 8). This new assay system provides new and simple assay for screening compounds with potential estrogenic activity.

Expression of ER and PR in Older Breast Cancer Patients

We have examined the expression of estrogen (ER) and progesterone receptors (PR) and the distribution of tumor phenotypes as a function of age in breast cancer patients. ER and PR concentrations were determined in tissue biopsies from 1739 specimens of patients with primary breast cancer, using ligand-binding assays. Tumors were classified as receptor positive (ER^+) or negative (ER^-) and PR^+ or PR^- based on the presence or absence of receptor binding activity. Tumors were stratified into four phenotypes based on the combined ER and PR status: ER+ PR+; ER^+ PR^-; ER^- PR^+; and ER^- PR-. Significant positive associations were found between ER and age ($p=0.0001$) and between PR and age ($p=0.0002$). The median ER levels were statistically different age groups, with the greatest levels older versus younger patients. The prevalence of ER^+PR^+ tumor phenotype increased with age. In contrast, the prevalence of ER^-PR- and ER^- PR^+ tumor phenotypes decreased with age. The median PR to ER ratio decreased with age ($p=0.0001$) and this trend was attributed to increased ER levels with age. The prevalence of ER^- PR^- and ER^-PR^+ tumor phenotypes in younger patients suggest that hormonal regulation of ER gene expression may be responsible for the observed disparity of tumor phenotypes in breast cancer. A copy of the manuscript which is submitted to Cancer Detection and Prevention is enclosed (Ashba et al.).

SPECIFIC AIM 3

The mechanism(s) leading to increased expression of hormone or Ah receptor or c-*myc* genes will be elucidated. Results will be correlated with morphologic studies of the glands and tumors.

PROGRESS:

We hypothesized that mis-regulation of gene expression induced by DMBA was most likely to result from altered control of transcription. Control of transcription is mediated by binding of trans-acting factor(s) to cis-regulatory elements. Thus, increased transcription is most likely due either to 1) a mutation in the gene itself (affecting binding of a nuclear transcription factor), or 2) a mutation in a gene encoding a factor that regulates its transcription. In model 2, activation of a transcription factor via the oxidative stress pathway induced by DMBA could provide the stimulus for overexpression. For the control of c-*myc* gene transcription, NF-κB represents an excellent candidate for this model, since this family of factors are induced by oxidative stress (89), and we have shown this family of factors plays a major role in regulation of c-*myc* transcription (90,91).

Mammary Tumors Display Aberrant Activation of NF-κB/Rel Transcription Factors That Promote Cell Survival

We have measured the expression of NF-κB/Rel factors in tumor tissue from the DMBA treated rats as well as the levels in normal mammary gland. Consistent with our hypothesis, we have observed very high levels of factor expression in nuclei of 85% of the tumors that we have examined. As expected NF-κB/Rel was not detected in normal mammary glands. (A manuscript

has now been accepted for publication on this work in the Journal of Clinical Investigation: Sovak, M.A., Bellas, R.E., Kim, D.W., Zanieski, G.J., Rogers, A.E., Traish, A.M., and Sonenshein, G.E., 1997; a copy of this manuscript, which will be referred to as Sovak et al., 1997, is enclosed). The data demonstrating the EMSA assays on the nuclear extracts is shown in Figure 4 of Sovak et al., 1997. These findings are consistent with the results we reported in the Progress Report for last year. Furthermore, when we compared the expression of NF-κB/Rel factors in untransformed vs transformed human breast epithelial cells. We found that breast cancer cancer lines express high constitutive levels of nuclear NF-κB/Rel whereas untransformed human breast epithelial cells express only low levels of nuclear Rel activity (Figure 1, Sovak et al., 1997). We have also found that primary human breast cancer tissue specimens contain nuclear NF-κB/Rel subunits, as judged by immunoblotting (Figure 5 and Table 1, Sovak et al., 1997). Since Rel factors regulate expression of c-*myc* (2-4), we tested the activity of this factor using transient transfection. We determined that an NF-κB element driven construct in 578T cells and the c-*myc* promoter in MCF-7 cells was transactivated by binding of these endogenous NF-κB/Rel factors (Figure 2, Sovak et al., 1997). These results indicate that the aberrantly activated NF-κB/Rel is functional. Thus these results are consistent with the hyphothesis presented in our application and suggest a mechanism by which exposure to environmental carcinogens leads to overexpression of the c-*myc* oncogene. Importantly, recent evidence from our laboratory suggests that NF-κB/Rel provide survival signals for B cells and hepatocytes (96-99), and this finding has been confirmed by several other laboratories. Importantly, inhibition of NF-κB/Rel activity leads to the induction of a cell death program. Thus, we tested the effects of specific inhibition of this transcription factor in 578T cells using a microinjection strategy. Using either microinjection of specific antibodies, oligonucleotide or specific inhibitor proteins of NF-κB/Rel binding, we induced apoptosis of 578T breast cancer cells (Figure 3, Sovak et al., 1997). These findings suggest aberrant NF-κB/Rel activity may play a role in tumor progression, and that importantly it represents a possible therapeutic target in the treatment of these tumors.

NF-κB/Rel is Activated in the Mammary Gland Prior to Tumor Formation

More recently, we are have performed analysis of mammary gland tissue isolated during a time course experiment; glands were isolated after 6 hours, 1 day, 1 week, 3 weeks and 9 weeks following DMBA treatment to determine the kinetics of activation of NF-κB/Rel and c-*myc* RNA levels. No detectable increase in basal NF-κB/Rel binding levels was seen at 6 hours, 1 day or 1 week after treatment. However, 2 of 5 rats displayed detectable levels of NF-κB/Rel binding prior to tumor formation (data not shown). This finding suggests that activation of this factor is an early event. These preliminary findings suggest that NF-κB/Rel subunit expression may represent a marker(s) for early detection of pre-metastatic breast disease. As discussed above, immunohistochemistry of the DMBA induced tumors indicates nuclear localization of the p65 subunit in some of the tumors. Additional immunohistochemistry will be performed to determine which NF-κB/Rel subunits are activated. The results should provide insights into the pathway leading to DMBA-induced neoplastic transformation of the mammary gland in rats, and provide a new therapeutic approach to treatment and diagnosis of this disease.

REFERENCES

1. Morris, J.J., and Seifter, E. The role of aromatic hydrocarbons in the genesis of breast cancer. Med. Hypothesis 38:177-184 (1992).
2. DiAugustine, R., and Davis, D.L. A holistic approach to breast cancer. Environ. Health Perspect. 101:116-120 (1993).
3. Dusich, K., Sigurson, F., Hall, W.N., and Dean A.G., Cancer rates in a community exposed to low levels of creosote components in municipal water. Minn. Med. 63:803-806 (1980).
4. Willett, W. The search for the causes of breast and colon cancer. Nature 338:389-394 (1989).
5. Wolff, M.S., Toniolo, P.G., Lee, E.W., Rivera, M., and Dubin, N. Blood levels of organochlorine residues and risk of breast cancer. J. Natl. Cancer Inst. 85:648-652 (1993).
6. Manz, A., Berger, J., Dwyer, J.H., Flesch-Janys, D., Nagel, S., and Waltsgott, H. Cancer mortality among workers in chemical plant contaminated with dioxin. Lancet 338:959-964 (1991).
7. Wassermann, M., Nogueira, D.P., Tomatis, L, Mirra, A.P., Shibata, H., Arie, G.,Cucos, S. and Wassermann, D. Organochlorine compounds in neoplastic and adjacent apparantly normal breast tissue. Bull. Environ. Contam. and Toxicol. 15:478-483 (1976).
8. Falk, Jr. F., Ricci, Jr., Wolff, M.S., Godbold, J. and Deckers, P. Pesticides and polychlorinated biphenyl residues in human breast lipids and their relation to breast cancer. Arch. Env. Health 47:143-146 (1992).
9. Rogers, A.E., Conner, B., Boulanger, C., Lee, S. Mammary tumorigenesis in rats fed diets high in lard. Lipids 21:275-280 (1986).
10. Clinton, S.K., Imrey, P.B., Alster, J.M., Simon, J., Truex, C.R., Visek, W.J. The combined effects of dietary protein and fat on 7,12-dimethylbenz[a]anthracene-induced breast cancer in rats. J. Nutr. 114:1213-1223 (1984).
11. Hirose, M., Masuda, A., Inoue, T., Fukushima, S., Ito, N. Modification by antioxidants and p,p-diamino-diphenylmethane of 7, 12-dimethylbenz(a)anthracene-induced carcinogenesis of the mammary gland and ear duct in CD rats. Carcinogenesis, 7:1155-1159 (1986).
12. Chan, P.C., Dao, T.L. Enhancement of mammary carcinogenesis by a high-fat diet in Fischer, Long-Evans, and Sprague-Dawley rats. Cancer Res. 41:164-167 (1981).
13. Lee, S.Y., Walsh, C.T., NG, S.F. and Rogers, A.E. Toxicokinetics of 7,12-Dimethylbenz(a)anthracene (DMBA) in Rats Fed High Lard or Control Diets. J. Nutri. Growth and Cancer 3:167-176 (1986).
14. Lee, S.Y., Ng, S.F., Busby, W.F. and Rogers, A.E. Mammary gland DNA synthesis in rats fed high lard or control diets. J. Nutr, Growth & Cancer 4:167-174, (1987).
15. Russo, J. and Russo, I.H. Biological and molecular basis of mammary carcinogenesis. Laboratory Investigations, 587:112-137 (1987).
16. Russo, J., Russo, I.H., van Zwieten, M.J., Rogers, A.E. and Gusterson, B.A. Classification of neoplastic and nonneoplastic lesions of the rat mammary gland. (eds T. C. Jones, U. Mohr, R.D. Hunt), In: Pathology of Laboratory Animals Integument and Mammary Glands, Springer-Verlag Berlin Heidelberg, 275-304 (1989).

17. Rogers, A.E., Lee, S.Y. Chemically induced mammary gland tumors in rats: modulation by dietary rat. In: Dietary fat and cancer. Ip C, Birt DF, Rogers AE, Mettlin C (eds) Liss, New York (1986).
18. Rogers, A.E. Factors that modulate chemical carcinogenesis in the mammary gland of the female rat. (eds T. C. Jones, U. Mohr, R.D. Hunt), In:Pathology of Laboratory Animals. Integument and Mammary Glands, Springer-Verlag, Berlin, Heidelberg, 304-314 (1989).
19. Rogers, A.E. Commentary: Diet and Carcinogenesis in laboratory rodents, Carcinogenesis, (in press).
20. Wetsel, W.C., Rogers, A.E., Newberne, P.M. Dietary fat and DMBA mammary carcinogenesis in rats. Cancer Detect Prev. 4:535-543 (1981).
21. Clinton, S.K., Alster, J.M., Imrey, P.B., Nandkumar, S., Truex, C.R., Visek, W.J., Effects of dietary protein, fat and energy intake during an initiation phase study of 7,12-dimethylbenz[a]anthracene-induced breast cancer in rats. J. Nutr. 116:2290-2302 (1986).
22. Ema, M., K. Sogawa, N. Watanabe, Y. Chujoh, N. Matsushita, O. Gotoh, Y. Funae, and Y. Fujii-Kuriyama. cDNA cloning and structure of mouse putative Ah receptor. Biochem. and Biophys. Research Comm. 184:246-253 (1992).
23. Burbach, K.M. A. Poland, C.A. Bradfield. Cloning of the Ah-receptor cDNA reveals a distinctive ligand-activated transcription factor. Proc. Natl. Acad.Sci. USA 89:8185-8189 (1992).
24. Hoffman, E.C., Reyes, H. F-F Chu, F. Sander, L.H. Conley, B.A.Brooks, O. Hankinson. Cloning of a factor required for activity of the Ah (dioxin) receptor. Science 252:954-958 (1992).
25. Poland, A., E. Glover, and C.A. Bradfield. Characterization of polyclonal antibodies to the Ah receptor prepared by immunization with a synthetic peptide hapten. Mole. Pharmacol. 39:20-26 (1990).
26. Bank P.A., Yao, E.F., Phelps, C.L., Harper, P.A., and Denison, M.S. Species-specific binding of transformed Ah receptor to a dioxin responsive transcriptional enhancer. Eur. J. Pharmacol. 228:85-94 (1992).
27. Perdew, G.H. Association of the Ah receptor with the 90-kDa heat shock protein. J. Biol. Chem. 263:13802-13805 (1988).
28. Gasiewicz, T.A. and G. Rucci. Alpha-naphthoflavone acts as an antagonist of 2,3,7,8-tetrachlorodibenzo-p-dioxin by forming an inactive complex with the Ah receptor. Mole. Pharmacol. 40:607-612 (1991).
29. Nebert, D.W. and F.J. Gonzalez. P450 genes: Structure, evolution and regulation. Ann. Rev. Biochem. 56:945-993 (1987).
30. Conney, A.H. Induction of microsomal enzymes by foreign chemicals and carcinogenesis by polycyclic aromatic hydrocarbons: G.H.A. Clowes Memorial lecture. Canc. Res. 42:4875-4917 (1982).
31. Buening, M.K., R.L. Chang, M-T Huang, J.G. Fortner, A.W. Wood, A.H. Conney. Activation and inhibition of benzo(a)pyrene and aflatoxin B_1 metabolism in human liver microsomes by naturally occuring flavonoids. Canc. Res. 41:67-72 (1981).
32. Le Bon, A.M., M.H. Siess, M. Suschetet. Inhibition of microsome-mediated binding of benzo(a)pyrene to DNA by flavonoids either in vitro or after dietary administration to rats. Chemico-Biol. Interact. 83:65-71 (1992).

33. Nebert, D.W., D.D. Patersen, A.J. Fornace, Jr. Cellular responses to oxidative stress:The [Ah] gene battery as a paradigm. Env. Health Perspectives 88:13-25 (1990).
34. Russo, J., Tay, L.K., Ciocca, D.R. and Russo, I.H. Molecular and cellular basis of the mammary gland susceptibility to carcinogenesis. Environ. Hlth Perspect. 49:185-199 (1983).
35. Daniel, F.B. and Joyce, N.J. 7,12-dimethyl-benzanthracene-DNA adducts in Sprague-Dawley and Long-Evans female rats: the relationship of DNA adducts to mammary cancer. Carcinogenesis 5:1021-1026 (1984).
36. Nebert, D., D.D. Petersen, A. Puga. Human AH locus polymorphism and cancer: inducibility of CYP1A1 and other genes by combustion products and dioxin. Pharmacogenetics 1:68-78 (1991).
37. Caparaso N., M.T. Landi, P. Vineis. Relevance of metabolic polymorphisms to human carcinogenesis: evaluation of epidemiologic evidence. Pharmacogenetics 1:4-19 (1991).
38. Kouri, R.E., McKinney, C.E., Slomiany, D.J., Snodgrass, D.R., Wray, N.P., and McLemore, T.L., Positive correlation between high aryl hydrocarbon hydroxylase activity and primary lung cancer as analyzed in cryopreserved lymphocytes. Canc. Res. 42:5030-5037 (1982).
39. Marshall, E. Toxicology goes molecular. Science 259:1394-1399 (1993).
40. Harris, M. T. Zacharewski and S. Safe. Effects of 2,3,7,8-tetrachlorodibenzo-p-dioxin and related compounds on the occupied nuclear estrogen receptor in MCF-7 human breast cancer cells. Cancer Res. 50:3579-3584 (1990).
41. Vickers, P.J., M.J. Dufresne, K.H. Cowan. Relation between cytochrome P450IA1 expression and estrogen receptor content of human breast cancer cells. Mole. Endocrinol. 3:157-164 (1989).
42. Zacharewski, T, M. Harris, S. Safe. Evidence for the mechanism of action of the 2,3,7,8-tetrachlorodibenzo-p-dioxin-mediated decrease of nuclear estrogen receptor levels in wild-type and mutant mouse hepa-1c1c7 cells. Biochem. Pharmacol. 41:1931-1939 (1991).
43. Lin, F.H., S.J. Stohs, L.S. Birnbaum, G. Clark, G.W. Lucier, J.A. Goldstein. The effects of 2,3,7,8-tetrachlorodibenzo-p-dioxin (TCDD) on the hepatic estrogen and glucocorticoid receptors in congenic strains of Ah responsive and Ah nonresponsive C57BL/6J mice. Tox. and Applied Pharm. 108:129-139 (1991).
44. Umbreit, T.H., M.A. Gallo. Physiological implications of estrogen receptor modulation by 2,3,7,8-tetrachlorodibenzo-p-dioxin. Tox. Lett. 42:5-14 (1988).
45. Gierthy, J.F., Bennett, J.A., Bradley, L.M., and Cutler, D.S. Correlation of *in vitro* and *in vivo* growth suppression of MCF-7 human breast cancer by 2,3,7,8-tetrachlorodibenzo-p-dioxin. Canc. Res. 53:3149-3153, (1993).
46. Umbreit, T.H. and Gallo, M.A. Physiologal implications of estrogen receptor modulation by 2,3,7,8-tetrachlorodibenzo-*p*-dioxin. Toxicol. Lett. 42:5-14 (1988).
47. Rigdon, R.H. and Neal J. Relationship of leukemia to lung and stomach tumors in mice fed benzo[a]pyrene. Proc. Soc. Exptl. Biol. Med. N.Y., 130:146-148 (1969).
48. Jones, M.K., Weisenburger, W.P., Sipes, I.G. and Russell, D.H. Circadian alterations in prolactin, corticosterone, and thyroid hormone levels and down-regulation of prolactin receptor activity by 2,3,7,8-tetrachlorodibenzo-p-dioxin. Toxicol. Appl. Pharmacol. 87:337-350 (1987).

49. Dickerson, R., Howie, L., and Safe, S. The effect of 6-nitro-1,3,8-trichlorodibenzofuran as a partial estrogen in the female rat uterus. Toxicol. and App. Pharmacol. 113:55-63 (1992).
50. Lucier, G.W., A. Tritscher, T. Goldsworth, J. Foley, G. Clark, J. Goldstein, and R. Maronpot. Ovarian hormones enhance 2,3,7,8-tetrachlorodibenzo-p-dioxin-mediated increases in cell proliferation and preneoplastic foci in a two-stage model for rat hepatocarcinogenesis. Cancer Res. 51:1391-1397 (1991).
51. Kociba, R.J., Keyes, D.G., Beyer, J.E., Carreon, R.M., Wade, C.E., Dittenber, d.A., Kalnins, R.P., Frauson, L.E., Park, C.N., Barnard, S.D., Hummel, R.A., and Humiston, C.G., Results of a two-year chronic toxicity and oncogenicity study of 2,3,7,8-tetrachlorodibenzo-p-dioxin in rats. Toxicol. Appl. Pharmacol. 46:279-303 (1978).
52. National Toxicology Program. Bioassay of 2,3,7,8-Tetrachlorodibenzo-p-dioxin for Possible Carcinogenicity (Gavage Study). Technical Report Series No. 102. Research Triangle Park, N.C.: National Toxicology Program, (1982).
53. Lyons WR Li CH and Johnson RE. The hormonal control of mammary growth and lactation. Rec. Prog. Horm. Res. 14: 219-240, 1958.
54. Meites J and Nicoll CS. Adenohypophysis: Prolactin. Ann Rev Physiol. 28:57-68 (1966).
55. MacMahon B Cole P Brown B.J. Etiology of breast cancer A review. J. Natl. Cancer Inst. 50:21-24 (1973).
56. Wotiz HH, Beebe DR, and Muller RE, Effects of estrogen on DMBA-induced breast tumors. J. Steroid Biochemistry 20:1067-1075 (1984).
57. Kelly PA, Asselin J Labrie F and Turcot-Lemay L. Endocrine regulation of growth and hormone receptor levels of DMBA-induced mammary tumors. in Steroid Receptors and Management of Cancer eds Lipmann M and Thompson B. 1979 pp. 4-29.
58. McGuire W. L. Prognostic factors for recurrence and survival in human breast cancer. Breast Cancer Research Treatment 10:5-9 (1987).
59. Huggins, C., Grand, L.C., and Brillantes, F.P. Mammary cancer induced by a single feeding of polynuclear hydrocarbons and its suppression. Nature (London) 189:204-208 (1961).
60. McGuire WL Chamness GC Costlow ME and Shepherd RE. Subcellular Biochemistry of Estrogen in breast cancer. In " Hormones and Cancer" eds McKerns KW 1974, P75-102.
61. Leung, B.S., Sasaki, G.M. and Leung, J.S. Estrogen-prolactin dependency in 7,12-dimethyl-benz(a)anthracene-induced tumors. Cancer Res. 35:621-627 (1975).
62. Beato M, Gene regulation by steroid hormones. Cell 56:335-344 (1989).
63. Kumar V, Green S Staub A Berry M Jin J R and Chambon P. Functional domains of the human estrogen receptor. Cell 51:941-951 (1987).
64. Fuqua, S.A.W., Fitzgerald, S.D., Chamness, G.C., Tandon, A.K., McDonnell, D.P., Nawaz, Z., O'Malley, W.B. and McGuire, W.L. Variant human breast tumor estrogen receptor with constitutive transcriptional activity. Cancer Res. 51:105-109, (1991).
65. Kelly PA Bradly C Shiu R P C Meites J and Friesen HG. Prolactin binding to rat mammary tumor tissue. Pro. Soc. Exp. Biol. Med. 146:816-820, 1974
66. DeSomber, E.R, Kledzik, G.S., Marshall, S and Meites J. Estrogen and prolactin receptor concentrations in rat mammary tumors and response to endocrine ablations. Cancer Res. 36:354-358 (1976).

67. Hann, S. R., H.D. Abrams, L.R. Rohrschneider, and R.N. Eisenman. Proteins encoded by the v-*myc* and c-*myc* oncogenes: identification and localization in acute leukemia virus transformants and bursal lymphoma cell lines. Cell 34:789-798 (1983).
68. Hann, S. R., M. W. King, D.L. Bentley, C.W. Anderson, and R.N. Eisenman. A non-AUG translational initiation in c-myc exon1 generates an N-terminally distinct protein whose synthesis is disrupted in Burkitt's lymphoma. Cell 52:185-195 (1988).
69. Luscher, B. and R.N. Eisenman. New light on Myc and Myb. I.Myc. Genes Dev. 4:2025-2035 (1990).
70. Blackwell, T. K., L. Kietzner, E.M. Blackwood, R.N. Eisenman, and H. Weintraub. Sequence-specific DNA binding by the c-Myc protein. Science 250:1149-1152 (1990).
71. Prendergast, G. C. and E.B. Ziff. Methylation sensitive sequence-specific DNA binding by the c-Myc basic region. Science 251:186-189 (1991).
72. Blackwood, E. M. and R.N. Eisenman. Max: a helix-loop-helix zipper protein that forms a sequence-specific DNA-binding complex with Myc. Science 251:1211-1217 (1991).
73. Kretzner, L., E. Blackwood, and R.N. Eisenman. Myc and Max proteins possess distinct transcriptional activities. Nature 359:426-429 (1992).
74. Spencer, C. A. and M. Groudine, Control of c-myc regulation in normal and neoplastic cells. Adv. Cancer Res. 56:1-48 (1991).
75. Campisi, J., H. E. Gray, A. B. Pardee, M. Dean, and G. E. Sonenshein, Cell cycle control of c-myc but not c-ras expression is lost following chemical transformation, Cell 36:241-247 (1984).
76. Dean, M., R. A. Levine, W. Ran, M. S. Kindy, G. E. Sonenshein, and J. Campisi, Regulation of c-myc transcription and mRNA abundance by serum growth factors and cell contact, J. Biol. Chem. 261, 9161-9166 (1986).
77. Cole, M. The myc oncogene: its role in transformation and differentiation. Ann. Rev. Genet. 20:361-384 (1986).
78. Cesarman, R. Dalla-Favera, D. Bentley, and M. Groudine. Mutations in the first exon are associated with altered transcription of c-myc in Burkitt lymphoma. Science 238:1272-1275 (1987).
79. Buckler, A.J., Rothstein, T.L. and Sonenshein, G.E. Transcriptional control of c-*myc* gene expression during stimulation of murine B lymphocytes. J. Immunol. 145:732-736 (1990).
80. Levine, R., J. McCormack, A. Buckler, and G.E. Sonenshein. Transcriptional and posttranscriptional control of c-*myc* gene expression in WEHI 231 cells. Mol. Cell. Biol. 6:4112-4116 (1986).
81. Kindy, M. and Sonenshein, G.E. Regulation of oncogene expression in cultured aortic smooth muscle cells, J. Biol. Chem. 261:12865-12868 (1986).
82. Adams, J., A.W. Harris, C.A. Pinkert, L.M. Corcoran, W.S. Alexander, S. Cory, R.D. Palmiter, and R.L. Brinster. The c-myc oncogene driven by immunoglobulin enhancers induces lymphoid malignancy in transgenic mice. Nature 318:533-538 (1985).
83. Roux-Dosseto, M., S. Romain, N. Dussault, C. Desideri, L. Piana, P. Bonnier, N. Tubiana, and P.M. Martin. c-myc gene amplification in selected node-negative breast cancer patients correlates with high rate of early relapse. Eur. J. Cancer 28A:1600-1604 (1992).
84. Pavelic, Z., P. Steele, and H. Preisler. Evaluation of c-myc proto-oncogene in primary human breast carcinomas. Anticancer Res. 11:1421-1428 (1991).

85. Berns, E., J. Klijn, W. van Putten, I. van Staveren, H. Portengen, and J. Foekens. c-myc amplification is a better prognostic factor than HER2/neu amplification in primary breast cancer. Cancer Res. 52:1107-1113 (1992).
86. Borg, A., B. Baldetorp, M. Ferno, H. Olsson and H. Sigurdsson. c-myc amplification is an independent prognostic factor in postmeopausal breast cancer. Eur. J. Cancer.51:687-691 (1992).
87. Stewart, T.A., P.K. Pattengale, and P. Leder. Spontaneous mammary adenocarcinomas in transgenic mice that carry and express MTV/myc fusion genes. Cell 38:627-637 (1984).
88. Schoenenberger, C.-A., A-C. Andres, B. Groner, M. van der Valk, M. LeMeur, and P. Gerlinger. Targeted c-myc expression in mammary glands of transgenic mice induces mammary tumors with constitutive milk protein gene transcription. EMBO J. 7:169-175 (1988).
89. Schreck, R., Rieber, P. and Baeuerle, P. A. Reactive oxygen intermediates as apparent widely used messengers in the activation of the NF-κB transcription factors and HIV-1. EMBO J. 10:2247-2258 (1991).
90. Kessler, D.J., M.P. Duyao, D.B. Spicer, and G.E. Sonenshein. NF-κB-like factors mediate interleukin 1 induction of c-myc gene transcription in fibroblasts. J.Exp. Med. 176: 787-792 (1992).
91. Duyao, M.P., Kessler, D.J., Spicer, D., Bartholomew, C., Cleveland, J., Siekevitz, M., and Sonenshein, G.E. Transactivation of the c-*myc* promoter by HTLV-1 *tax* is mediated by NFκB. J. Biol. Chem. 267:16288-16291 (1992).
92. Bombick DW, Jankun J, Tullis K, Matsumura F. 2,3,7,8-Tetrachlorodibenzo-p-dioxin causes increases in expression of c-erb-A and levels of protein-tyrosine kinases in selected tissues of responsive mouse strains. Proc. Natl. Acad. Sci. USA, 85:4128 (1988).
93. Sadhu DN, Merchant M, Safe SH, Ramos KS. Modulation of protooncogene expression in rat aortic smooth muscle cell by benzo[a]pyrene. Arch. Biochem. and Biophysics. 300:124-131 (1993).
94. Pratt MAC, Kralova J, McBurney NW. A dominant negative mutation of the alpha retinoic acid receptor gene in a retinoic acid-nonresponsive embryonal carcinoma cell. Mol. Cell. Biol. 10:6445-6453 (1990).
95. Rubin E, Farber J L. Pathology Second Edition. J.B. Lippincott Company, Philadelphia, p. 959 (1994).
96. Wu, M., Lee, H., Bellas, R. E., Schauer, S. L., Arsura, M., Katz, D., FitzGerald, M., Rothstein, T. L., Sherr, S. H., and Sonenshein, G. E. Inhibition of NF-κB/Rel induces apoptosis of murine B cells. EMBO J. 15:4682-4690 (1996).
97. Arsura, M., Wu, M., and Sonenshein, G. E. TGF-β1 inhibits NF-κB/Rel activity inducing apoptosis of B cells: Transcriptional activation of IκB-α. Immunity 5:31-40 (1996).
98. Bellas, R.E., FitzGerald, M.J., Fausto, N., and Sonenshein, G.E. Inhibition of NF-κB activity induces apoptosis in murine hepatocytes. Amer. J. Pathol. 151:891-896 (1997).
99. Arsura, M., FitzGerald, M.J., Fausto, N., and Sonenshein, G.E. Nuclear Factor-κB/Rel blocks transforming growth factor β1-induced apoptosis if murine hepatocyte cell lines. Cell Growth Diff.8:1049-1059 (1997).

Table 1: IHC of AhR Nuclear Translocation in Normal (Non-DMBA-Treated Rat) Mammary Gland Epithelium and in DMBA-Induced Mammary Gland Tumors

Group	No. Samples	Positive Nuclei/10,000 Cells*		Positive Cases/ Total Cases
		All Cases	Positive Cases	
Normal Glands, Control Rats	8	2+3.9,(0)	8+2.3,(8)	2/8
Histologically Normal Glands, DMBA-Treated Rats	12	0	0	0/12
Benign Tumors	26	11+11,(9)	12+11,(9)	24/26
Malignant Tumors	52	9.9+7.7,(8)	10+7.6,(9)	49/52

* Mean + S.D., (Median)

Table 2: IHC of NF-KB P65 Nuclear Translocation in Normal (Non-DMBA-Treated Rat) Mammary Gland Epithelium and in DMBA-Induced Mammary Gland Tumors. [Experiment 1]

Group	No. Samples	Positive Nuclei/ 10,000 Cells*		Positive Cases/ Total Cases
		All Cases	Positive cases	
Normal Glands, Control Rats	3	65.6+66.5,(64)	126+115,(126)	2/3
Benign Tumors	15	0.35+0.9,(0)	2.6+0.02,(2)	2/15
Malignant Tumors	67	3+4.8,(1.14)	5.7+5,(4)	38/67

* Mean + S.D., (Median)

Table 3: IHC Detection of NF-KB P65 Nuclear translocation in Histologically Normal (Non-DMBA and DMBA-Treated Rat) Mammary Glands Epithelium and in DMBA-Induced Mammary Gland Tumors. [Experiment 2]

Group	No.Sample	Positive Nuclei/ 10,000 Cells*		Positive Cases/ Total Cases
		All Cases	Positive Cases	
Normal Glands Control Rats	5	0	0	0/5
Histologically Normal Glands, DMBA-Treated	12	51+119,(0)	256+150,(256)	2/12
Benign Tumors	11	48.7+46,(49)	53.5+41,(49)	10/11
Malignant Tumors**	18	31+67,(4.7)	31+67,(4.7)	18/18

* Mean + S.D., (Median)

Table 4: IHC Detection of NF-KB P65 Nuclear Translocation in Histologically Normal Mammary Glands Epithelium (Non-DMBA and DMBA-Treated Rat) Three Weeks after DMBA Exposure.

Group	No.Samples	Positive Nuclei/10,000 Cells*		Positive Cases/ Total Cases
		All Cases	Positive Cases	
High Fat Diet,No DMBA	5	0.22+0.5, (0)	1.14	1/5
Control Diet+DMBA	5	22+11.7,(21)	22+11.7,(21)	5/5
High Fat Diet +DMBA	5	2 + 1.7, (1.6)	2.6 + 1.5, (2.4)	4/5

- Mean + S.D., (Median)

Table 5:
Estrogen and Progesterone Receptors in Mammary Glands and DMBA-induced Tumors in Female S-D Rats

I. Histologically Normal Mammary Glands:

Group	DMBA	No. of Glands	Receptors* ER	PR
C1	0	7	10±16	6±9
C2	+	50	9±12 (p=0.8)	26±28 (p=0.07)

II. DMBA-induced Mammary Gland Tumors (Group C2):

Tumors Histology	No.	Receptors* ER	PR
Benign	14	34±27	172±105
Malignant	63	36±25	257±159

*Mean ± S.D.; ER, estrogen receptor; PR, progesterone receptor; both reported as fmol/mg protein

Figure 1

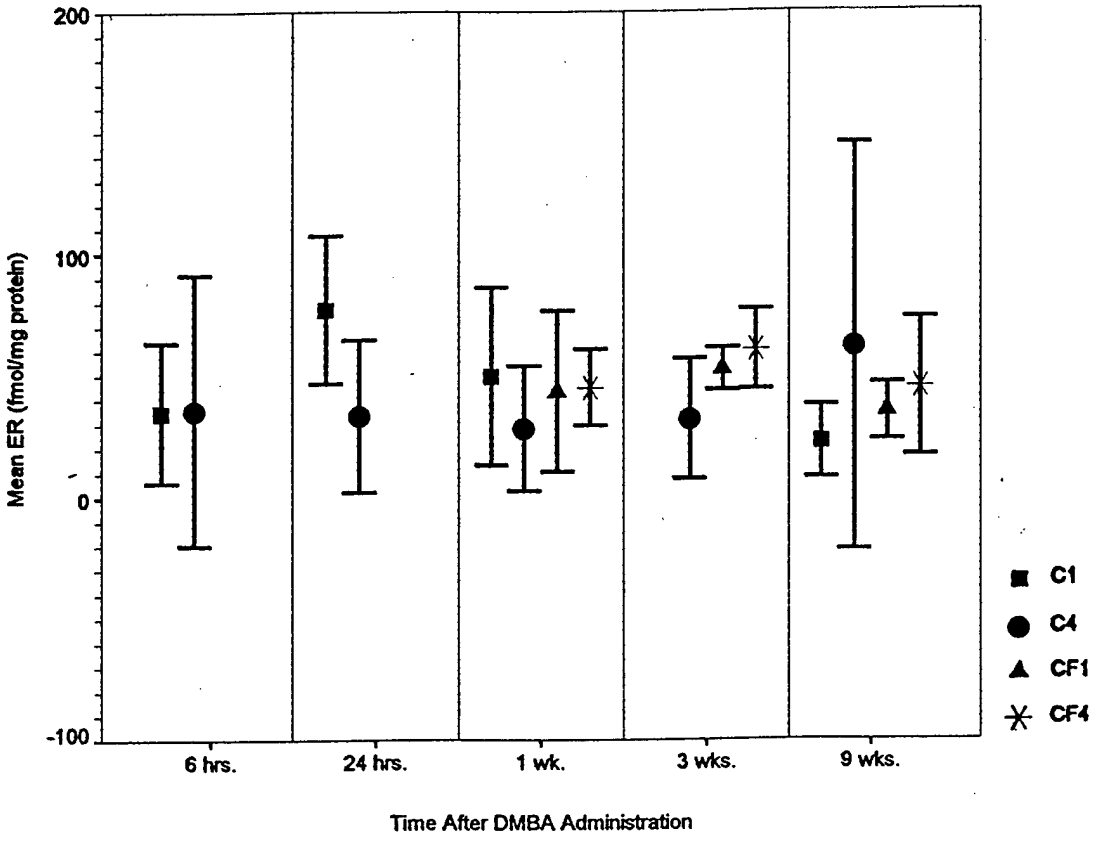

Figure 2

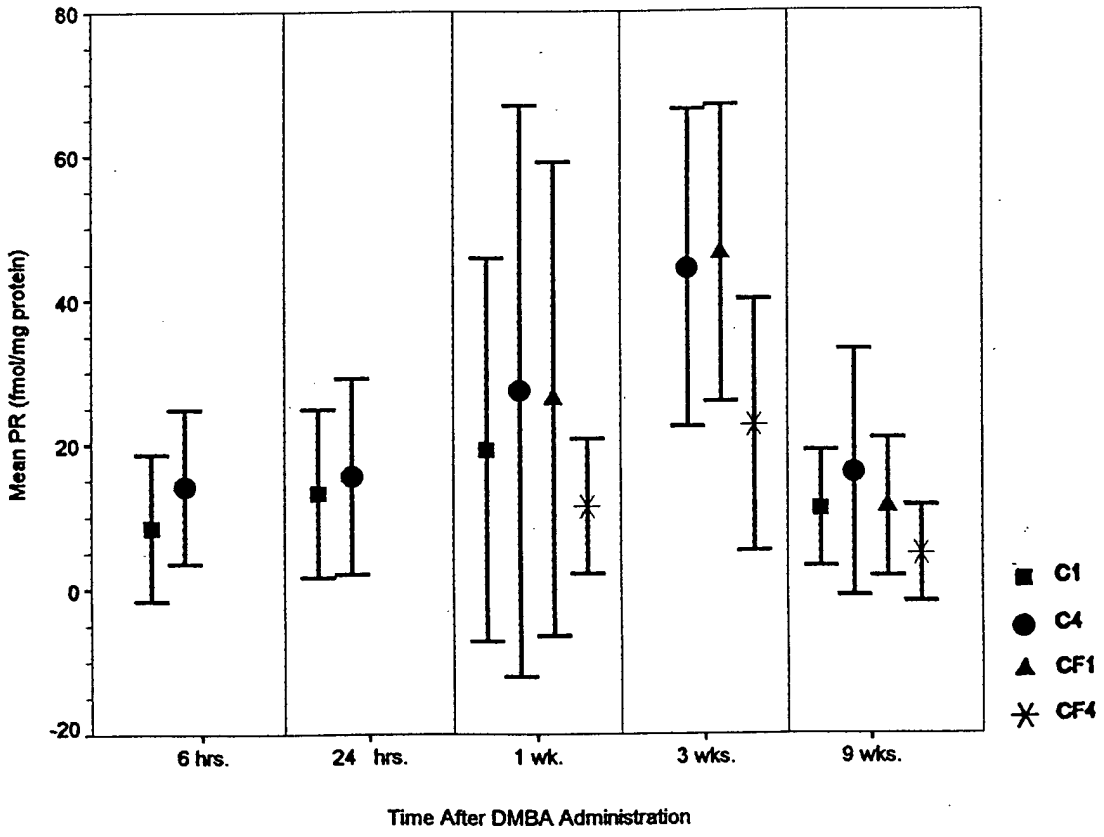

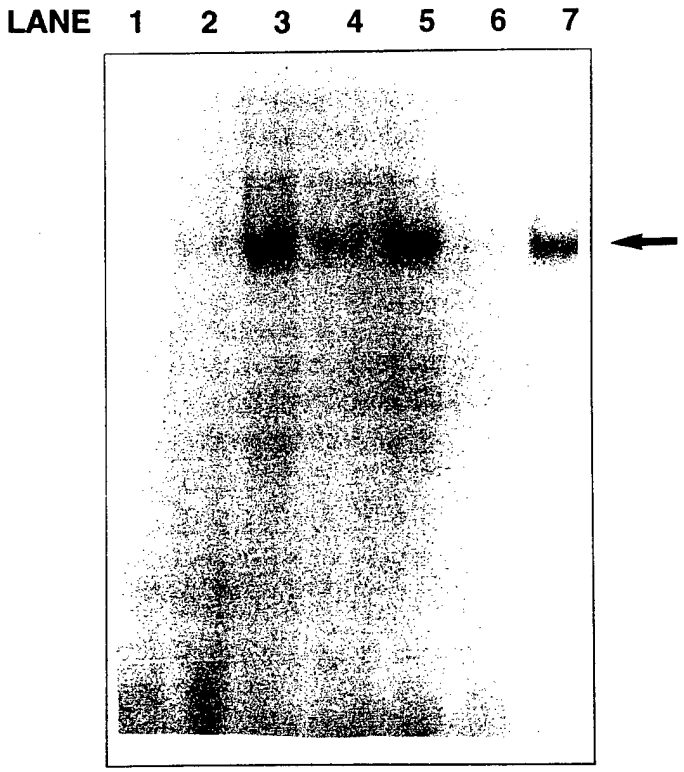

Figure 3

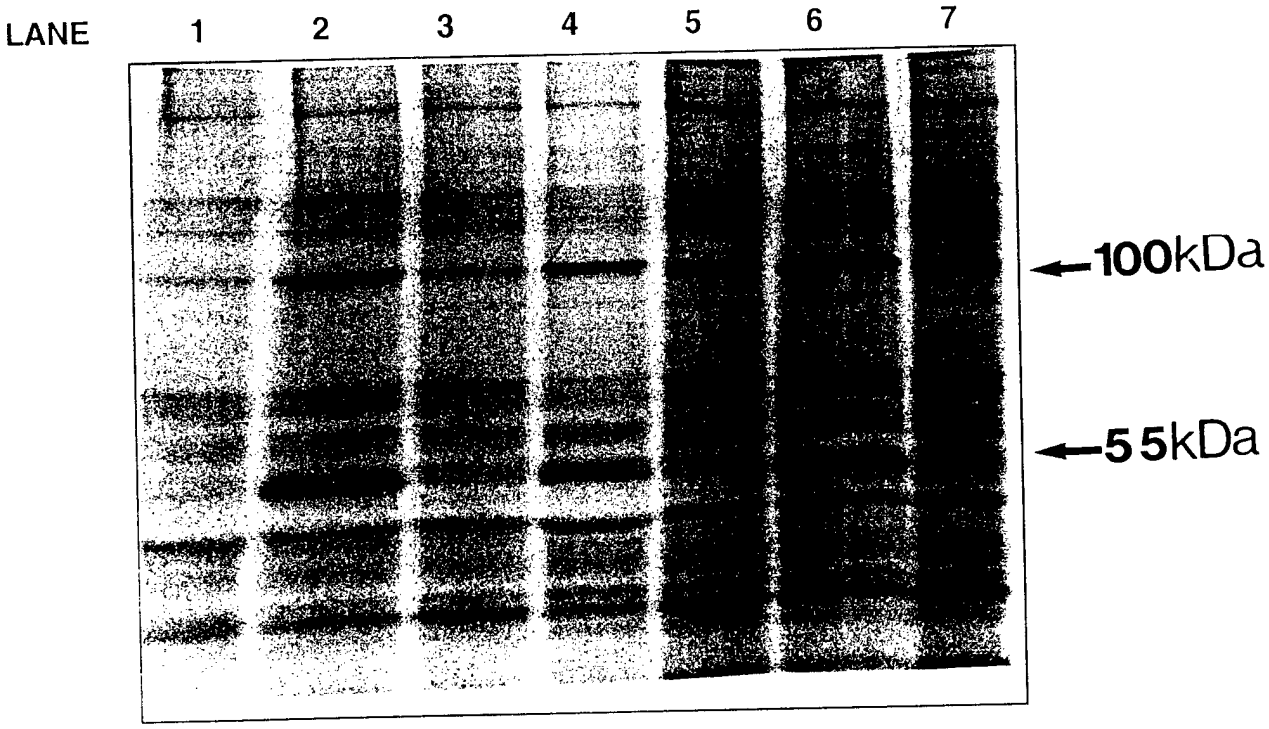

Figure 4

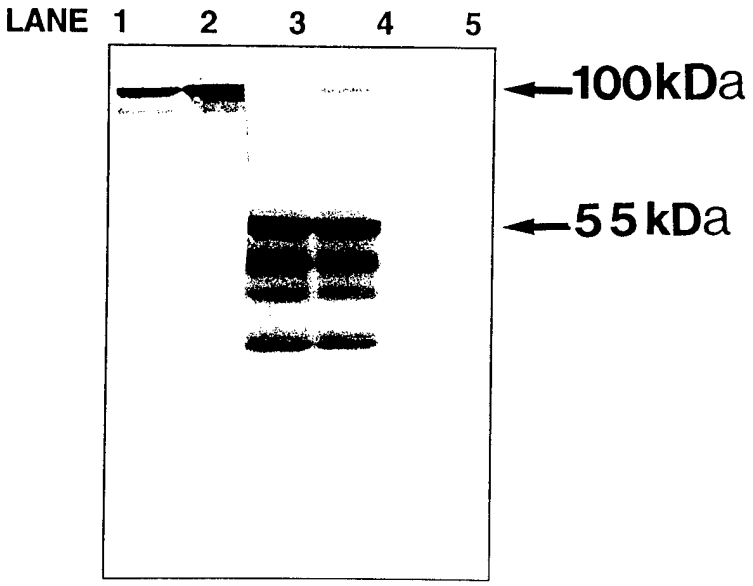

Figure 5

The chemical structure of the polychlorinated biphenyls.

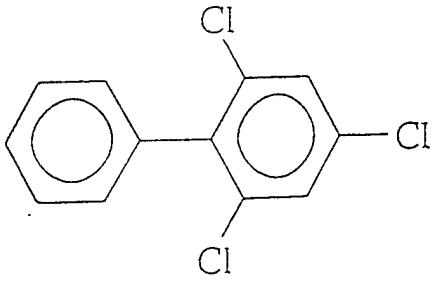

2,4,6-trichlorobiphenyl

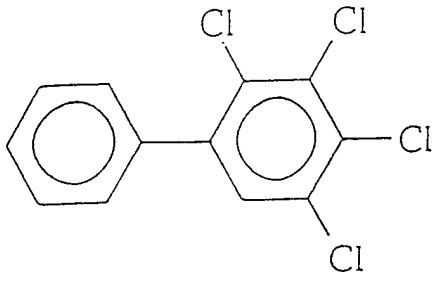

2,3,4,5-tetrachlorobiphenyl

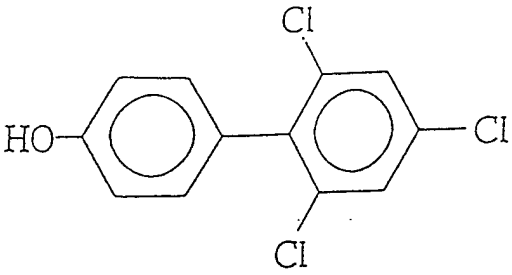

4-hydroxy-2',4',6'-trichlorobiphenyl

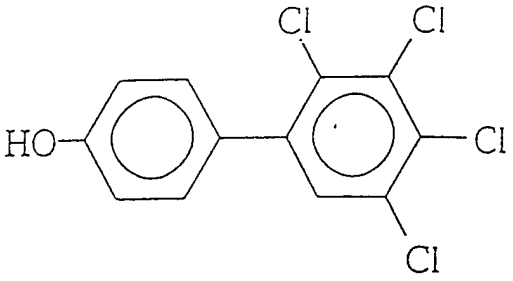

4-hydroxy-2',3',4',5'-tetrachlorobiphenyl

Figure 6

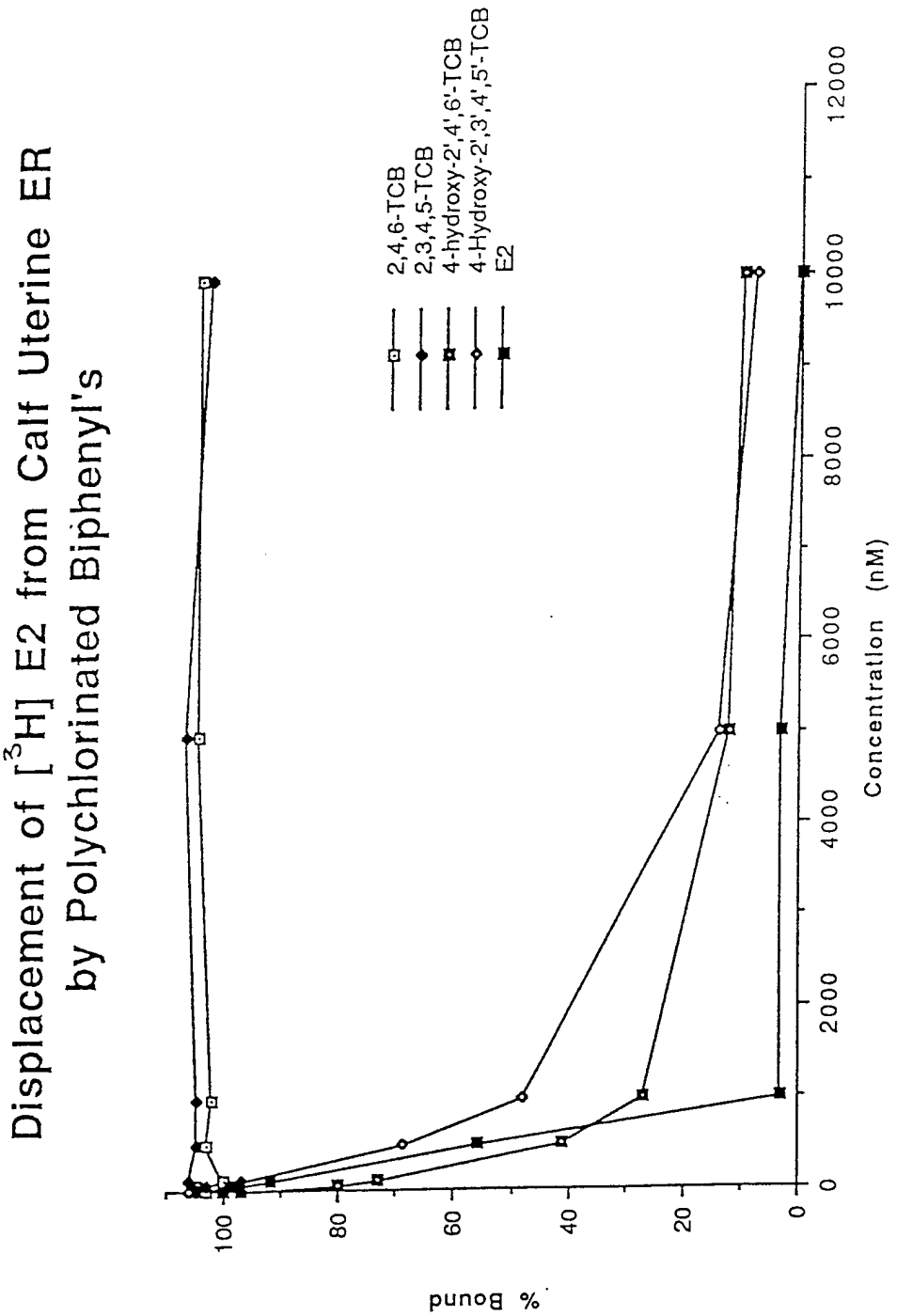
Displacement of [3H] E2 from Calf Uterine ER
by Polychlorinated Biphenyl's
2,4,6-TCB
2,3,4,5-TCB
4-hydroxy-2',4',6'-TCB
4-Hydroxy-2',3',4',5'-TCB
E2
% Bound
100
80
60
40
20
0
0
2000
4000
6000
8000
10000
12000
Concentration (nM)

Figure 7

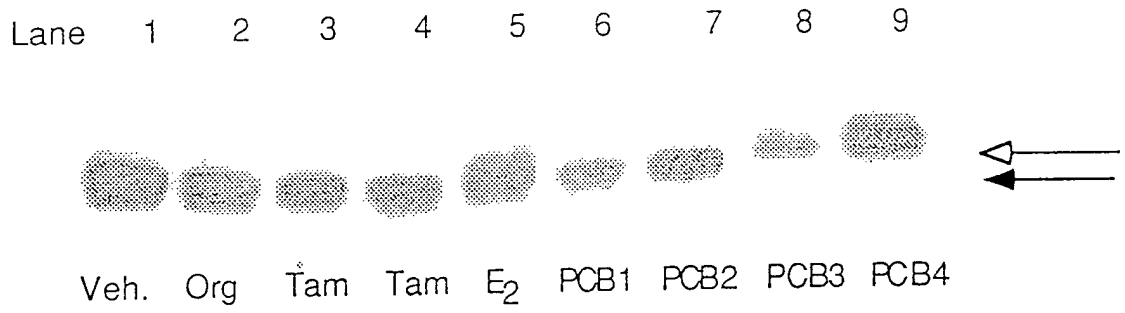

Figure 8

Diagnostic Molecular Pathology 00(0): 000–000, 1997

Loss of Expression of a 55 KDa Nuclear Protein (*nmt55*) in Estrogen Receptor-Negative Human Breast Cancer

Abdulmaged M. Traish, Yue-Hua Huang, Jacqueline Ashba, Mary Pronovost, Matthew Pavao, David B. McAneny, and Robert B. Moreland

We have identified and characterized a 55 kDa nuclear protein (referred to as *nmt55*) from human breast tumors and MCF-7 cell line, using site-directed monoclonal antibodies. Measurements of estrogen receptors (ER) and progesterone receptors (PR), by ligand binding assays, in cytosols of 63 human breast tumors permitted classifications of these tumors into four phenotypes (ER+/PR+, ER+/PR−, ER−/PR−, ER−/PR+). Nuclear protein (*nmt55*) expression in these tumors, as determined from Western blot analyses, showed a statistically significant association ($p = 0.001$) with tumor hormonal phenotype. Review of the pathologic characteristics of tumors analyzed suggested that lack of *nmt55* expression was significantly associated with mean tumor size ($p < 0.03$), mean ER ($p = 0.001$) and mean PR ($p < 0.002$), but was not associated with tumor stage, grade, or type. To further study this protein, we cloned and sequenced a 2.5 kb cDNA using a monoclonal antibody to *nmt55*. The complete predicted open reading frame encodes a protein with 471 amino acids and a calculated molecular mass of 54,169 Da. The deduced amino acid sequence exhibited unique regions rich in glutamine, histidine, arginine, and glutamic acid. Northern blot analysis of RNA from MCF-7 cells and ER+/PR+ human breast tumors showed a 2.6 kb mRNA. Southern blot analysis suggested the presence of a single copy of this gene. Chromosomal mapping, using fluorescent in situ hybridization (FISH), located *nmt55* gene to the X chromosome, region q13. The extensive homology between *nmt55* and RNA binding proteins suggested that *nmt55* may be involved in hnRNA splicing. The strong association observed between expression of *nmt55*, tumor hormonal phenotype, mean tumor size, mean ER, and mean PR content suggests that loss of *nmt55* expression may be related to events involved in hormone insensitivity, tumor differentiation, and unregulated tumor cell growth and metastases.

Key Words: Breast tumors—Estrogen receptor—55 kDa nuclear protein—RNA-binding protein—Splicing factors.

Diagn Mol Pathol 00(0): 000–000, 1997.

The development of breast cancer is thought to be a multistage process (9). The progression of this disease is associated with cellular and molecular changes. Thus, initiation and progression may be associated with loss of chromosomal material and ultimately specific gene function(s). Some of these cellular and molecular changes may be associated with tumor cell acquisition of metastatic ability. Discovery of tumor-specific genes that lead to tumor metastasis is important in the development of strategies for treatment of breast cancer patients. There is an urgent need for identification of node-negative patients whose tumors have a metastatic potential. Several tumor markers are used in assessing tumor changes linked to poor prognosis. These include loss of estrogen receptors (ER) and progesterone receptors (PR) (18–20), high blood vessel count (angiogenesis) (13), amplification of *erbB2/HER2/neu* gene (29,33) and decreased activity of *nm23* gene (2). None of these markers alone predict, with complete reliability, which node-negative patients will be likely to relapse.

Positive and negative regulators of metastasis are likely to exist in breast cancer. During malignant progression, breast cancer cells may acquire cellular transforming functions required for abnormal growth and loss of regulatory gene functions (e.g. tumor suppressor genes). The existence of specific genes responsible for suppression of tumor metastasis has been reported (27). Over the past several years, a number of proteins were implicated in the aberrant growth of human breast cancer cells, such as epidermal growth factor receptor (EGFR) (33,41). The *erbB2* protein is under investigation for its possible use as a response variable for monitoring the efficacy of chemotherapy. Similarly, other proteins are thought to be involved in the process of metastasis, such as *p53* (a transcriptional factor with tumor suppressor properties) (41) and *nm23* (a putative metastatic suppressor) (2). While these proteins may have some prognostic value, they have yet to be utilized clinically for lack of sufficient information on these markers.

In our efforts to screen human breast tumors for ER

Manuscript received October 28, 1996; revision accepted May 19, 1997.

From the Departments of Biochemistry (A.M.T., J.A., M.P.), Urology (Y-H.H., R.B.M.), and Surgical Oncology (M.P., D.B.McA.), Boston University School of Medicine, Boston, MA.

Address correspondence and reprint requests to Abdulmaged Traish, Ph.D., Department of Biochemistry, Boston University School of Medicine, W607, 80 East Concord St., Boston, MA 02118, U.S.A.

variants using a monoclonal antibody raised to a 15-amino acid polypeptide, representing a unique sequence of the acidic/basic (A/B) region of human ER, we observed that this antibody cross-reacted with a 55 kDa nuclear protein present only in a subset of human breast cancer tissues. In this study identifies and characterizes this protein to assess its potential role in human breast cancer. We have identified, characterized, and cloned the cDNA for *nmt55* protein. One striking observation is that tumors that did not express ER and PR also lacked expression of *nmt55* protein. Because ER expression is used as a prognostic factor in management of breast cancer patients, it is possible that the loss of *nmt55* expression may represent the state of tumor differentiation.

MATERIALS AND METHODS

Clinical Material

Human breast cancer tissue was obtained from patients undergoing surgery for treatment of breast cancer, as described previously (39). Two breast normal tissue specimens were obtained from subjects who had undergone breast reconstruction surgery. This study was approved by the Institutional Review Board of Boston University Medical Center Hospital. Human breast cancer cell line MCF-7 was obtained from the American Type Tissue Culture Collection (ATCC). Monoclonal antibody NMT-1 (36,38) was developed to a unique peptide encompassing amino acids 140–154 in the A/B region of the human estrogen receptor.

Estrogen and Progesterone Receptor Assays

The concentrations of unoccupied ER and PR were determined by ligand binding analyses as described previously (35–39). Radiolabeled estradiol was used as a ligand for ER and radiolabeled ORG 2058 was used as ligand for PR (35–39). All assays were performed in The Hormone Receptor Assay Laboratory at Boston University Medical Center. The binding data were normalized in femtomoles per milligram (fmol/mg) of cytosol proteins. We have chosen cutoff values for ER as 10 fmol/mg protein and for PR as 2 fmol/mg proteins. These cutoff values reflect the sensitivity of the assays using the appropriate ligands. Tumors were stratified into four groups according to their ER and PR status: 1) ER+PR+, 2) ER−PR−, 3) ER+PR−, and 4) ER−PR+. Similar tumor stratifications were reported based on ligand binding and gel shift assays (6,18–20,30).

Statistical Analysis

Statistical analyses were performed to determine the association between *nmt55* protein expression, ER and PR expression, and tumor pathologic characteristics. Two-sample *t*-test procedures were used to compare the mean values of ER and PR concentrations and tumor size with presence or absence of *nmt55*. We also conducted chi-square analyses to examine possible differences between tumor characteristics (stage, grade, tumor hormonal phenotypes, and tumor type) and *nmt55* protein status. Multiple logistic regression analyses were performed to assess the association of *nmt55* presence with ER and PR concentrations, adjusting for tumor characteristics. All statistical analyses were performed using mainframe SAS version 6.11 at Boston University.

Sodium Dodecyl Sulphate-Polyacrylamide Gel Electrophoresis and Western Blot Analysis

Polyacrylamide gel electrophoresis (PAGE) and Western blot analyses were carried out as described previously (37). Briefly, cytosols and nuclear KCl extracts were prepared in the appropriate buffers, as described (35–39) and electrophoresed on 10% sodium dodecyl sulphate (SDS)/PAGE according to the method of Laemmli (16). The proteins were electrotransferred onto nitrocellulose membranes. Strips of the nitrocellulose membranes were then incubated in buffer TBST (50 mM Tris-HCl, pH 8.0, 0.15 M NaCl, 0.5% Tween 20) containing 5% nonfat dry milk to block nonspecific binding sites for 1 h at 37°C and then probed for 2 h at 30°C with the appropriate dilution of the antibody in the same buffer containing 5% nonfat milk.

Bacterial Strains

Escherichia coli strain XL1 Blue (genotype F′::Tn10 *proAB lacI*^{q}Δ {*lacZ*} M15/*recA1 endA1 gyrA96* {Nal^r}*thi- hsdR17* {r_k^- m_k+} *supE44 relA1 lac* {Stratagene}) was used for all lambda phage experiments and DH5α (genotype F′/*endA1 recA1 relA1 hsdR17* {r_k^- m_{k+}}, *supE44, gyrA* {Nal^r}, *thi-1,* Δ{*lacIZYA-argF*} *U169 deoR* {ϕ*80 dlac*Δ [*lacZ*]*M15*}) (Life Sciences Inc.) was used in the transfection and preparation of plasmid DNAs.

Library Screening and Subcloning

A lambda ZAP II (Stratagene) cDNA library of MCF-7 cells (complexity-1 × 10^7, generous gift of Dr. Mark Sobel, NCI) was screened using expression cloning with isopropylthiogalactose (IPTG)-induction (21) and Mab NMT-1 (36,38). Recombinant phage were plated at a density of ~50,000 pfu/150 mm Petri dish. Plaque lifts were prepared and probed (135 mm nitrocellulose, Schleicher and Scheull) as described (21). To avoid selecting ER clones, the nitrocellulose membranes were soaked in 0.1% SDS in Western blot buffer, and then

washed with buffer containing 10% methanol. This treatment denatures ER protein and does not permit detection of ER on Western blots by NMT-1. Positive plaques were isolated and purified to homogeneity. pBluescript plasmids corresponding to the positive phage were excised, according to the manufacturer's instructions. Polymerase chain reaction (PCR), using T3 and T7 RNA polymerase promoter primers (Stratagene) was carried out to determine insert sizes. The primers used flank, the cloned sequences in pBluescript. Polymerase chain reaction followed by agarose gel electrophoresis revealed two clones with approximate sizes of 2.5 kb and 1.7 kb for the inserts. Restriction analysis with XhoI and EcoRI (the sites for insertion of the cDNA into lambda ZAPII) revealed a complex pattern indicating either internal EcoRI and/or XhoI restriction sites. Induction of bacteria harboring the plasmid (pBluescript *nmt55*) with 2 m*M* IPTG for 5 h followed by isolation and lysis of the bacteria in SDS sample buffer, SDS-PAGE, and Western blotting resulted in an immunoreactive ~60 kDa band, in agreement with a predicted 55 kDa protein. The 1.7 kb clone yielded a smaller protein product indicative of an internal methionine start site (data not shown).

Nucleotide Sequencing of cDNA Clones

Plasmids were prepared from candidate bacteriophage clones by cotransfection of XL-1 Blue with the helper M13 phage R408 (Stratagene) and the lambda phage. The resulting phagemids were transfected into DH5α, positive clones selected on ampicillin containing plates, screened, and plasmids were prepared. The insert DNA was sequenced in both directions using primers every 300 bp at the Boston University DNA Core Facility, using an Applied Biosystems International (ABI) 3000 DNA sequencer.

Expression of *nmt55* in Bacteria

Cultures of DH5α harboring the appropriate plasmids were grown to late log phase (A600 ~ 1A). We have observed that bacteria harboring the 2.5 kb cDNA clone did not grow when induced with IPTG, suggesting a detrimental effect of the gene product in bacteria. To overcome this, cells were grown for 3 h prior to induction with IPTG, and then induced with 200 m*M* IPTG with shaking at 300 rpm 37°C for 5 h. Aliquots of bacteria cultures were centrifuged in 1.5 ml microfuge tubes and the cell pellets lysed by boiling in 1× SDS-PAGE sample buffer. After 5 min of centrifugation to remove cell debris, aliquots of the supernatants were electrophoresed on 10% SDS-PAGE, electrotransferred, and processed for Western blot analysis.

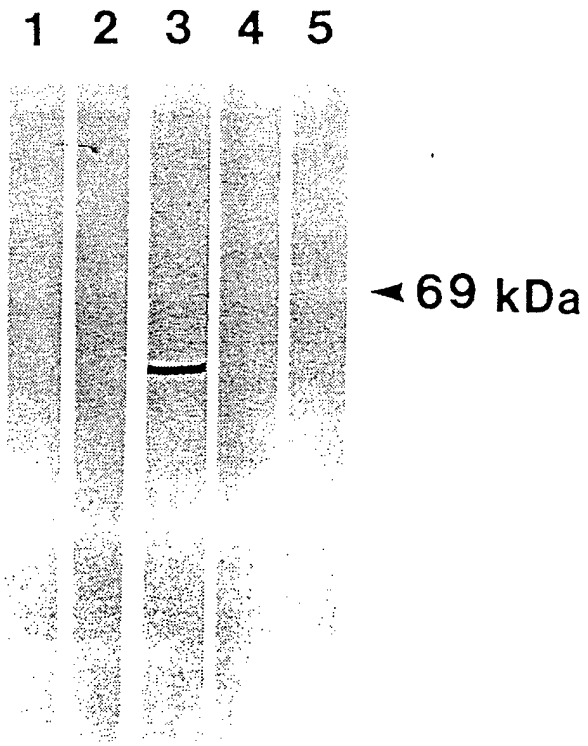

FIG. 1. Western blot analysis of MCF-7 cells nuclear and cytosolic extracts with MAb NMT-1. Nuclear KCl-extracts Lanes (lanes 1, 2, 3, and 5) and cytosol (lane 4) were analyzed by sodium dodecyl sulphate polyacrylamide gel electrophoresis (SDS/PAGE), transferred onto nitrocellulose membranes and subjected to immunoblotting. The arrow represents the migration of bovine serum albumin (BSA, 69 kDa). Lane 1 was immunoblotted with preimmunserum; Lane 2 represents immunoabsorption of the antibody with the synthetic immunogenic peptide; Lanes 3 and 4 were immunoblotted with NMT-1 antibody; Lane 5 was immunoblotted with antibodies against RARa.

RNA Preparation and Northern Blot Analysis

Total RNA from MCF-7 cells and human breast tumor tissues was prepared by homogenization in guanidinium isothiocyanate followed by phenol/chloroform extraction and isopropanol precipitation (3). Total RNA (10–20 μg) was electrophoresed on 1% formaldehyde-MOPS agarose gels and then transferred onto nylon-reinforced nitrocellulose membranes. Membranes are treated with ultraviolet light (Stratalinker, Stratagene; 1200 watt/cm^2) to immobilize the nucleic acids. Double-stranded DNA probes for Northern blot analysis were labeled with α-[^{32}P] dCTP using T7 DNA polymerase and random primers. Specific activities range from 10^8 to 10^9 cpm/μg. Double-stranded DNA probes include a 499 bp SacI/BglII fragment of human *nmt55*, and a 545 bp HindIII/XbaI fragment of human glyceraldehyde-3-phosphate dehydrogenase (GAPHD) (34). The probe used for this analysis was a 499 bp SacI/BglII fragment, representing the unique carboxyl terminus of *nmt55*. This probe was chosen to avoid possible cross-hybridization with other

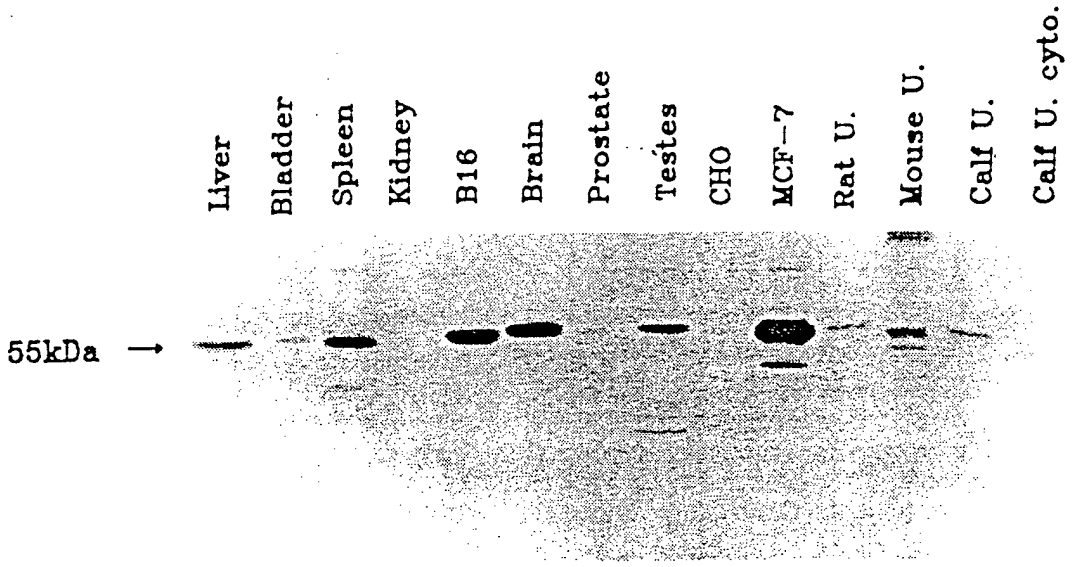

FIG. 2. Distribution of *nmt55* in tissues and cells. Rat uterine tissue was obtained from mature female animals. Mice uterine tissue were obtained from mature mice. The uteri were stripped of fat and mesenteric tissue and kept frozen at –80°C until use. Calf uterine tissues were obtained from a local slaughter house, placed on dry ice, and transported to the laboratory. Rat kidney, bladder, spleen, brain, testis, liver, and prostate were obtained from mature male animals. B16 melanoma cells were a gift from Dr. Richard Niles (Marshall University, WV). CHO cells were obtained from Dr. M. Brann (University of Vermont). Human breast cancer tissues were obtained from patients undergoing surgery for breast cancer. Tissues were placed on dry ice and transported to the laboratory where they are stored at –80°C until experimentation. Nuclear KCl-extracts from several tissues and cells were electrophoresed, electrotransferred onto nitrocellulose, and immunoblotted with MAb NMT-1.

RNA binding factors such as polypyrimidine splicing factor (PSF) (7,24). Hybridizations were carried out at 67°C for 2 h in Quickhyb (Strategene). Following low (2× SSC 0.1% SDS, 25°C) and high stringency (0.2× SSC 0.1% SDS, 65°C) washes, membranes were exposed to Amersham Hyperfilm for 24–48 h at –70°C. RNA samples were normalized for loading using GAPHD (34).

Southern Blot Analysis of Genomic DNA

Human placental genomic DNA (20 μg) was digested with restriction endonucleases (EcoRI, Hind III, NcoI, and PstI; genomic grade, high concentration), and electrophoresed on 1% agarose gels (17). The gels are transferred onto nylon-reinforced nitrocellulose membranes, and treated with ultraviolet light (Stratalinker, Stratagene; 1200 watt/cm^2) to immobilize the nucleic acids. Double-stranded DNA probes for Southern blot analysis are prepared as described in the experiments for Northern blot analysis (above), using a 499 bp Sac/BglII fragment of human *nmt55*. Hybridizations are carried out at 67°C for 2 h. Following low (2× SSC 0.1% SDS, 25°C) and high-stringency washes (0.2× SSC 0.1% SDS, 65°C), membranes are exposed to Hyperfilm for 24–48 h at –70°C.

Chromosomal Mapping

Slides Preparation

Lymphocytes from human blood were cultured in minimal essential medium (MEM) supplemented with 10% fetal bovine serum and phytohemagglutinin (PHA) at 37°C for 68–72 h. The lymphocyte cultures were treated with BrdU (0.18 mg/ml, Sigma) to synchronize the cell population. The synchronized cells were washed three times with serum-free medium to release the block and recultured at 37°C for 6 h in MEM with thymidine (2.5 μg/ml, Sigma). Cells were harvested and slides were made using standard procedures including hypotonic treatment, fixed and air dired.

Fluorescent In Situ Hybridization

Biotinylation of the cDNA probe (2.5 kb) with dATP using BRL BioNick labeling kit (15°C, 1 h) was carried out as described (10). In situ hybridization was performed by the fluorescent in situ hybridization (FISH) method as described by Heng et al. (11,12). Slides were baked at 55°C for 1 h and after RNase treatment, DNA on the slides was denatured 70% formamide in 2× SSC for 2 min at 70°C and dehydrated by ethanol. Probes were denatured at 75°C for 5 min in a hybridization mix

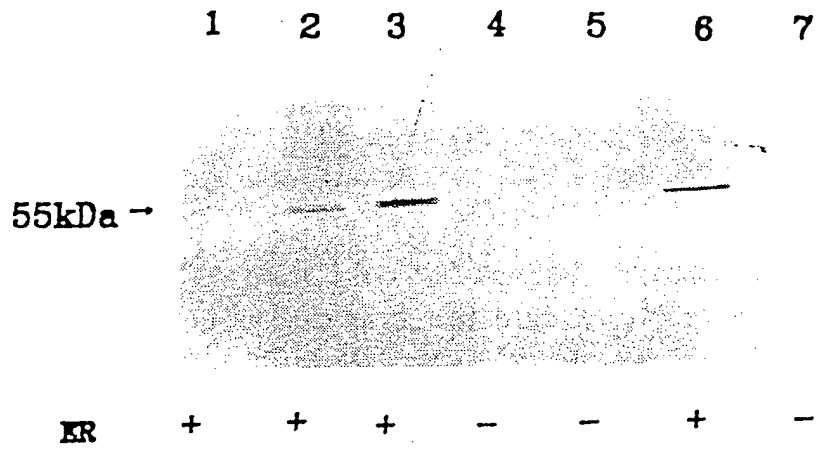

FIG. 3. Western blot analysis of *nmt55* in nuclear KCl-extracts of human breast tumors. Nuclear KCl-extracts from ER+ and ER− human breast tumors were prepared and analyzed by Western blot using NMT-1 antibody. Presence or absence of ER in these tumors is indicated at the bottom.

consisting of 50% formamide and 10% dextran sulphate. Probes were loaded onto the denatured chromosomes on slides. After overnight hybridization, slides were washed and the signal was detected and amplified. In the same field, FISH signals and DAPI banding patterns were recorded separately by fluorescent photomicroscopy using appropriate filters. The assignment of FISH mapping data with chromosomal bands was achieved by superimposing FISH signals with DAPI banded chromosomes (12).

RESULTS

Identification and Characterization of a 55 kDa Nuclear Protein in Human Breast Cancer

A monoclonal antibody (NMT-1) (36,38) raised to a unique peptide from the human ER did not recognize denatured ER on Western blots but reacted with a 55 kDa nonreceptor protein solubilized by extraction of nuclei from human MCF-7 cells with buffer containing 0.4 M KCl (Fig. 1, lane 3). The 55 kDa protein band was not detected by preimmune serum (Fig. 1, lane 1) or with antibodies to retinoic receptor (RARα) (26) (Fig. 1, lane 5), progesterone receptor (37) or with monoclonal antibodies directed to various regions of ER (1,40) (data not shown), suggesting that NMT-1 recognizes an epitope on this novel protein. Preincubation of the antibody with the peptide (amino acid 140–154 of human ER) effectively inhibited the binding of the antibody to this protein, as shown by the absence of the immunoreactivity (Fig. 1, lane 2). This protein was detected only in nuclear KCl-extracts but not in low-salt cytosolic extracts (Fig. 1, lane 4) suggesting that this protein is tightly bound to nuclear components. The inability of the monoclonal antibody NMT-1 to detect ER after SDS/PAGE was confirmed by using ER specific antibodies that detect ER in the same blots (data not shown). This suggests that NMT-1, while it detects *nmt55* protein, failed to detect ER on Western blots because its epitope on ER, once denatured by SDS, could not be renatured under these Western blot conditions.

To investigate if *nmt55* is conserved among various species and to determine its distribution in nuclear extracts from various tissues and cells, we analyzed nuclear extracts derived from various tissues and cells by Western blots. As shown in Figure 2, *nmt55* was detected in nuclear extracts of porcine brain, rat liver, spleen, testes, and uterus. This protein was present in MCF-7 cells, and in B16 melanoma cells. This protein was not detectable in CHO cells and was detected in prostate, kidney, and bladder, albeit at a lower abundance. We have also tested if this protein is expressed in normal mammary gland. Analysis of nuclear extracts of two tissue specimens from a normal breast by Western blot demonstrated the expression of *nmt55* (data not shown). Also, immunohistochemical analysis of normal rat mammary gland showed positive staining within the epithelial and stroma, suggesting that this protein is expressed in normal mammary gland cells (data not shown). These observations suggest that this protein is conserved among species and its presence in many normal tissues indicate that it may have an important biological function.

Tumor Pathologic Characteristics

The tumors analyzed were obtained from 63 patients who underwent surgery for treatment of breast cancer. The mean age of patients was 61.5 years (SD ± 15.8) with a range of 30–95 years. The racial composition of the patients in this study was 40 (87%) white, 4 (8.7%) black, 2 (4.3%) hispanics, and 18 (28.5%) of unknown race. Fifty-two (83.9%) of 62 tumors were characterized as infiltrating ductal carcinoma, 6 (9.7%) were infiltrating lobular carcinoma, 2 (3.2%) were ductal carcinoma in situ, 1 (1.6%) lobular carcinoma in situ, and one was inflammatory. The distribution of tumors based on size was as follows: 3.4% were between 0–0.9 cm, 52.5% between 1–1.9 cm, 33.9% between 2–4.9 cm and 10.2%

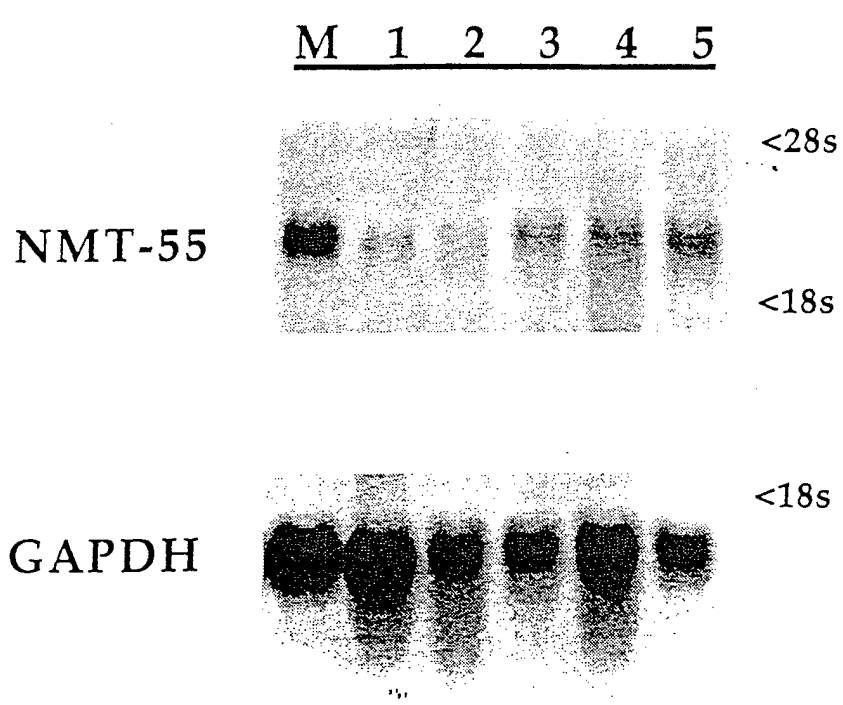

FIG. 4. Northern blot analysis of *nmt55* mRNA from MCF-7 cells and human breast tumors. Total RNA prepared from MCF-7 cells (Lane M) or from human breast tumor tissue (lanes 1–5) was analyzed by northern blots as described in "Materials and Methods." GAPDH was probed to indicate levels of RNA loading.

were ⩾5 cm. Tumor stage and grade were available for 48 and 47 of the 63 patients, respectively. Approximately 44% of tumors were stage I, 33% were stage IIA or IIB and 22.9% were stage IIIA or higher. Six of 47 tumors were classified as grade 1, 24 were classified as grade 2, and 17 were classified as grade 3.

Expression of ER, PR, and *nmt55* in Human Breast Tumors

Using Western blot analysis (Fig. 3), we have analyzed the nuclear KCl-extracts of 63 human breast tumors for the presence or the absence of *nmt55*. We have also measured ER and PR content in cytosolic extracts of these tumors. We have also reviewed the pathology records of these 63 patients, as discussed above and performed statistical analysis to determine if *nmt55* is associated with expression of biochemical markers (ER and PR) and pathologic characteristics. All tumors which expressed *nmt55* were ER+ (100%), whereas 60% of tumors lacking *nmt55* were ER+ ($p = 0.001$). Similarly, all tumors expressing *nmt55* were PR+ (100%) compared to 62.5% of tumors (PR+) in which *nmt55* was absent ($p = 0.001$). The mean tumor size was significantly greater (mean = 2.7 cm) in tumors lacking *nmt55* protein, than those in which *nmt55* was present (mean = 1.8 cm) ($p = 0.036$). The tumor hormone phenotype varied significantly by hormone status ($p = 0.001$) and all tumors expressing *nmt55* were ER+/PR+. Of tumors lacking *nmt55* 40% were ER+/PR+, 20% were ER+/PR−, 17.5% were ER−/PR− and 22.5% were ER−/PR+.

In order to predict the absence of *nmt55* using the biochemical and pathologic data available, the logistic regression analyses was limited to 45 patients from which most of the available information was collected. The model included the following determinants: PR, ER, tumor size, and tumor stage. Tumor type was not included in the model because the majority of tumors were infiltrating ductal carcinoma (83.9%). Tumor grade was also not included due to uneven distribution in this limited sample size. PR concentration independently and inversely predicted the loss of *nmt55* protein expression, after adjusting for tumor size and tumor stage ($p = 0.014$). This implies that as PR concentration decreases the likelihood of loss of *nmt55* increases.

Because loss of ER expression and/or function correlates with poor tumor differentiation (18–20), it is possible that loss of *nmt55* expression represents poor tumor differentiation. These observations suggest that loss of *nmt55* expression may be associated with tumor dedifferentiation, loss of ER and PR expression and possibly tumor metastases (18–20). Thus, understanding of the role of this protein in breast cell growth and function requires detailed studies to determine its biological and biochemical function. As a first step towards this goal, we have pursued cDNA cloning and characterization of *nmt55* gene in human breast cancer cells.

Cloning of *nmt55* From MCF-7 cDNA Library

Two clones were isolated and sequenced; one represented a full-length 2.5 kb clone and a 1.7 kb clone that was an internal fragment of the 2.5 kb. The 2.5 kb cDNA encompassed 115 bp 5′ untranslated, a 1,416 bp open

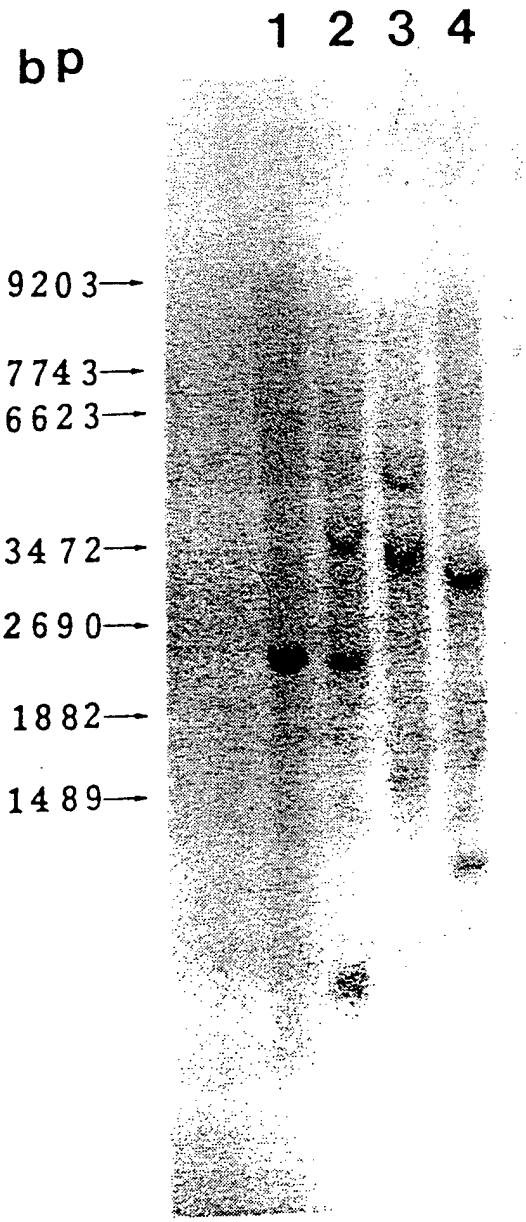

FIG. 5. Southern blot analysis of *nmt55* genomic DNA. Genomic DNA isolated from human placenta was digested with EcoRI (lane 1), HindIII (lane 2) PstI (lane 3) and NcoI (lane 4) and electrophoresed on 1% agarose gels. The DNA was transferred onto nylon-reinforced nitrocellulose and hybridized with the radiolabeled probe (a 499 bp SacI/BglII cDNA fragment). Subsequent to high-stringency washes the blot was dried and exposed to x-ray film. The size of the radiolabeled bands was determined by molecular weight markers (Lambda DNA digested with StyI).

reading frame, and ~970 bp of 3′ untranslated sequence terminating in poly A. The open reading frame was predicted to encode a 471 amino acid protein (54,197 Da), in good agreement with the observed 55 kDa apparent molecular weight determined by Western blots from nuclear KCl extracts. No unique sequences were identified with homology to ER, except 5 amino acids (Ala Ala Pro Gly Ala) which were found in the C-terminal region of *nmt55* and represent the epitope of NMT-1 (see below).

Characterization of *nmt55* mRNA Expression by Northern Blot Analysis

Figure 4 (lane M) shows that MCF-7 cells express a relatively abundant 2.6 kb mRNA transcript for *nmt55*. Analysis of total RNA from five ER+/PR+ human breast tumors (lanes 1–5) demonstrated different levels of nmt-55 mRNA expression. The low levels of expression observed in tumors represented by lanes 1 and 2 are not due to different RNA loading, since GAPDH mRNA levels were similar for all tumor samples. In preliminary experiment, tumors that were ER– and PR– did not express detectable *nmt55* transcripts (data not shown). The tumors used in these experiments also expressed different levels of *nmt55* protein, as determined by Western blot analysis (data not shown).

Southern Blot Analysis

Human female placental genomic DNA was digested with EcoRI (Figure 5, lane 1), HindIII (lane 2), PstI (lane 3) and NcoI (lane 4) and probed with a 499 bp SacI/BglII cDNA fragment. The product of EcoRI digestion hybridized to a single 2.3 kb band, suggesting the presence of a single copy of this gene. Deoxyribonucleic acid digested with HindIII showed three bands (3.5, 2.3, and 0.7 kb) despite the presence of a single HindIII site in the cDNA approximately 330 bp 3′ to the probe. This suggests the presence of one or more intervening sequences in this region. This observation is further supported by the hybridization products subsequent to digestion with PstI (~4.4, 3.2, and 1.4 kb), since PstI site is absent in the cDNA. Digestion with NcoI resulted in hybridization to a 2.9 and 1.1 kb bands. Since the two NcoI sites predicted from the cDNA sequence flank the probe and would be expected to yield only a 0.96 kb fragment, the hybridization pattern obtained suggests that the 2.9 and 1.1 kb bands must be the result of intervening sequences.

Structural Features of *nmt55* Protein: Amino Acid Sequences, Location of the RNA Binding Domains and Antibodies Binding Epitopes

The amino acid sequence of *nmt55*, deduced from the cDNA, is shown in Figure 6. Several interesting featuers are noted: glutamine- and histidine-rich regions (Q/H) located in the amino terminus (residues 19–35); a predicted bipartite RNA binding domain (RBD), residues 75–147 and 149–228; a putative helix-turn-helix motif (HTH), residues 287–335; and a region rich in acidic

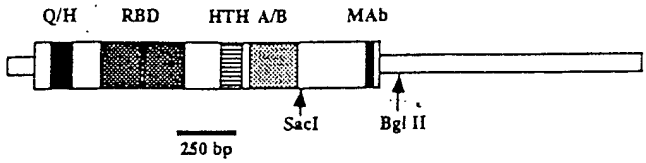


```
86/1                                                                116/11
ATG CAG AGT AAT AAA ACT TTT AAC TTG GAG AAG CAA AAC CAT ACT CCA AGA AAG CAT CAT
 M  Q  S  N  K  T  F  N  L  E  K  Q  N  H  T  P  R  K  H  H
146/21                                                              176/31
CAA CAT CAC CAC CAG CAG CAG CAC CAC CAG CAG CAA CAG CAG CAG CCG CCA CCA CCG CCA
 Q  H  H  H  Q  Q  Q  H  H  Q  Q  Q  Q  Q  Q  P  P  P  P  P
206/41                                                              236/51
ATA CCT GCA AAT GGG CAA CAG GCC AGC AGC CAA AAT GAA GGC TTG ACT ATT GAC CTG AAG
 I  P  A  N  G  Q  Q  A  S  S  Q  N  E  G  L  T  I  D  L  K
266/61                                                              296/71
AAT TTT AGA AAA CCA GGA GAG AAG ACC TTC ACC CAA CGA AGC CGT CTT TTT GTG GGA AAT
 N  F  R  K  P  G  E  K  T  F  T  Q  R  S  R  L  F  V  G  N
326/81                                                              356/91
CTT CCT CCC GAC ATC ACT GAG GAA GAA ATG AGG AAA CTA TTT GAG AAA TAT GGA AAG GCA
 L  P  P  D  I  T  E  E  E  M  R  K  L  F  E  K  Y  G  K  A
386/101                                                             416/111
GGC GAA GTC TTC ATT CAT AAG GAT AAA GGA TTT GGC TTT ATC CGC TTG GAA ACC CGA ACC
 G  E  V  F  I  H  K  D  K  G  F  G  F  I  R  L  E  T  R  T
446/121                                                             476/131
CTA GCG GAG ATT GCC AAA GTG GAG CTG GAC AAT ATG CCA CTC CGT GGA AAG CAG CTG CGT
 L  A  E  I  A  K  V  E  L  D  N  M  P  L  R  G  K  Q  L  R
506/141                                                             536/151
GTG CGC TTT GCC TGC CAT AGT GCA TCC CTT ACA GTT CGA AAC CTT CCT CAG TAT GTG TCC
 V  R  F  A  C  H  S  A  S  L  T  V  R  N  L  P  Q  Y  V  S
566/161                                                             596/171
AAC GAA CTG CTG GAA GAA GCC TTT TCT GTG TTT GGC CAG GTA GAG AGG GCT GTA GTC ATT
 N  E  L  L  E  E  A  F  S  V  F  G  Q  V  E  R  A  V  V  I
626/181                                                             656/191
GTG GAT GAT CGA GGA AGG CCC TCA GGA AAA GGC ATT GTT GAG TTC TCA GGG AAG CCA GCT
 V  D  D  R  G  R  P  S  G  K  G  I  V  E  F  S  G  K  P  A
686/201                                                             716/211
GCT CGG AAA GCT CTG GAC AGA TGC AGT GAA GGC TCC TTC CTG CTA ACC ACA TTT CCT CGT
 A  R  K  A  L  D  R  C  S  E  G  S  F  L  L  T  T  F  P  R
746/221                                                             776/231
CCT GTG ACT GTG GAG CCC ATG GAC CAG TTA GAT GAT GAA GAG GGA CTT CCA GAG AAG CTG
 P  V  T  V  E  P  M  D  Q  L  D  D  E  E  G  L  P  E  K  L
806/241                                                             836/251
GTT ATA AAA AAC CAG CAA TTT CAC AAG GAA CGA GAG CAG CCA CCC AGA TTT GCA CAG CCT
 V  I  K  N  Q  Q  F  H  K  E  R  E  Q  P  P  R  F  A  Q  P
866/261                                                             896/271
GGC TCC TTT GAG TAT GAA TAT GCC ATG CGC TGG AAG GCA CTC ATT GAG ATG GAG AAG CAG
 G  S  F  E  Y  E  Y  A  M  R  W  K  A  L  I  E  M  E  K  Q
926/281                                                             956/291
CAG CAG GAC CAA GTG GAC CGC AAC ATC AAG GAG GCT CGT GAG AAG CTG GAG ATG GAG ATG
 Q  Q  D  Q  V  D  R  N  I  K  E  A  R  E  K  L  E  M  E  M
986/301                                                             1016/311
GAA GCT GCA CGC CAT GAG CAC CAG GTC ATG CTA ATG AGA CAG GAT TTG ATG AGG CGC CAA
 E  A  A  R  H  E  H  Q  V  M  L  M  R  Q  D  L  M  R  R  Q
1046/321                                                            1076/331
GAA GAA CTT CGG AGG ATG GAA GAG CTG CAC AAC CAA GAG GTG CAA AAA CGA AAG CAA CTG
 E  E  L  R  R  M  E  E  L  H  N  Q  E  V  Q  K  R  K  Q  L
1106/341                                                            1136/351
GAG CTC AGG CAG GAG GAA GAG CGC AGG CGC CGT GAA GAA GAG ATG CGG CGG CAG CAA GAA
 E  L  R  Q  E  E  E  R  R  R  R  E  E  E  M  R  R  Q  Q  E
1166/361                                                            1196/371
GAA ATG ATG CGG CGA CAG CAG GAA GGA TTC AAG GGA ACC TTC CCT GAT GCG AGA GAG CAG
 E  M  M  R  R  Q  Q  E  G  F  K  G  T  F  P  D  A  R  E  Q
1226/381                                                            1256/391
GAG ATT CGG ATG GGT CAG ATG GCT ATG GGA GGT GCT ATG GGC ATA AAC AAC AGA GGT GCC
 E  I  R  M  G  Q  M  A  M  G  G  A  M  G  I  N  N  R  G  A
1286/401                                                            1316/411
ATG CCC CCT GCT CCT GTG CCA GCT GGT ACC CCA GCT CCT CCA GGA CCT GCC ACT ATG ATG
 M  P  P  A  P  V  P  A  G  T  P  A  P  P  G  P  A  T  M  M
1346/421                                                            1376/431
CCG GAT GGA ACT TTG GGA TTG ACC CCA CCA ACA ACT GAA CGC TTT GGT CAG GCT GCT ACA
 P  D  G  T  L  G  L  T  P  P  T  T  E  R  F  G  Q  A  A  T
1406/441                                                            1436/451
ATG GAA GGA ATT GGG GCA ATT GGT GGA ACT CCT CCT GCA TTC AAC CGT GCA GCT CCT GGA
 M  E  G  I  G  A  I  G  G  T  P  P  A  F  N  R  A  A  P  G
1466/461                                                            1496/471
GCT GAA TTT GCC CCA AAC AAA CGT CGC CGA TAC TAA
 A  E  F  A  P  N  K  R  R  R  Y  *
```

FIG. 6. Schematic representation of *nmt55* cDNA and the predicted amino acid sequence. The locations of the glutamine- and histidine-rich region (Q/H), the RNA binding domain (RBD), the helix-turn-helix mofit (HTH), the acidic/basic residues region (A/B) are indicated. The 499 bp SacI/BglII fragment used as a probe for Northern and Southern blots is also shown. The peptide sequences used to develop antibodies were underlined.

(A)

RNA Binding Domain

```
nmt55          75 RLFVGNLPPD ITEEEMRKLF EKYGKAGEVF IHKDKGFGFI RLETRTLAEI
HeLa p54nrb    75 RLFVGNLPPD ITEEEMRKLF EKYGKAGEVF IHKDKGFGFI RLETRTLAEI
Mouse NonO     77 RLFVGNLPPD ITEEEMRKLF EKYGKAGEVF IHKDKGFGFI RLETRTLAEI
PSF           298RLFVGNLPAD ITEDEFKRLF AKYGEPGEVF INKGKGFGFI KLESRALAEI
NonA/BJ6      303RLYVGNLTND ITDDELREMF KPYGEISEIF SNLDKNFTFL KVDYHPNAEK

nmt55         125AKVELDNMPL RGKQLRVRFA CHSASLTVRN LPQYVSNELL EEAFSVFGQV
HeLa p54nrb   125AKVELDNMPL RGKQLRVRFA CHSASLHVRN LPQYVSNELL EEAFSVFGQV
Mouse NonO    127VKVELDNMPL RGKQLRVRFA CHSASLTVRN LPQYVSNELL EEAFSVFGQV
PSF           348AKAELDDTPM RGRQLRVRFA THAAALSVRN LSPYVSNELL EEAFSQFGPI
NonA/BJ6      353AKRALDGSMR KGRQLRVRFA PNATILRVSN LTPFVSNELL YKSFEIFGPI

nmt55         175ERAVVIVDDR GRPSGKGIVE FSGKPAARKA LDRCSEGSFL LTTFPRPVTV
HeLa p54nrb   175ERAVVIVDDR GRPSGKGIVE FSGKPAARKA LDRCSEGSFL LTTFPRPVTV
Mouse NonO    177ERAVVIVDDR GRPSGKGIVE FSGKPAARKA LDRCSEGSFL LTTFPRPVTV
PSF           398ERAVVIVDDR GRSTGKGIVE FASKPAARKA FERCSEGVFL LTTTPRPVIV
NonA/BJ6      403ERASITVDDR GKHMGEGIVE FAKKSSASAC LRMCNEKCFF LTASLRPCLV

nmt55         225EPMD
HeLa p54nrb   225EPMD
Mouse NonO    227EPMD
PSF           448EPLE
NonA/BJ6      453EPME
```

(B)

Helix Turn Helix Motif

```
nmt55          287 RNIKEAREKL EMEMEAARHE HQVMLMRQDL MRRQEELRRM EELHNQEVQ
HeLa p54nrb    287 RNIKEAREKL EMEMEAARHE HQVMLMRQDL MRRQEELRRM EELHNQEVQ
Mouse NonO     289 RNIKEAREKL EMEMEAARHE HQVMLMRQDL MRRQEELRRM EELHNQEVQ
```

FIG. 7A. Homologies between *nmt55* RNA recognition motif and other related proteins.
FIG. 7B. Homologies between *nmt55* helix-turn-helix motif and other related proteins.

(glutamic) and basic (arginine) residues (A/B) extending from residue 318 to residue 368. These structural features, together with its nuclear localization, suggest that this protein may play a role as a nucleic acid binding protein (42).

When the open reading frame was screened against the GenBank database, two clones of high homology were found, one murine (42) and one human (4). One of these clones isolated from HeLa cells has high homology to PSF family of RNA splicing factors and contains a bipartite RNA binding motif (23,24). The murine candidate had high homology to the OCT-2 family of transcription factors as well as RNA binding motifs. As shown in Figure 7A, the RNA recognition motifs of *nmt55* share considerable homologies with those of HeLa p54^{nrb} (4) PSF (24), *NonO* (42) and NonA/BJ6 (28). Also, *nmt55* has a homologous region in the predicted helix-turn-helix motif with HeLa p54^{nrb}, and *NonO* (Figure 7B).

Using the deduced amino acid sequence, we have developed two new polyclonal antibodies to *nmt55;* one antibody (NMT-4) raised to a peptide in the N-terminal region that encompasses amino acids 56–72 of *nmt55* and another antibody (NMT-5) raised to a peptide in the carboxyl terminal region and spans amino acids 371–386 of *nmt55.* The peptides were chosen to avoid cross-reactivity of the generated antibodies with other RNA binding proteins that share homology with *nmt55* (e.g. PSF). Western blot analysis showed that only one band was detected with these antibodies when nuclear extracts from MCF-7 cells and human breast tumors were tested (data not shown). These antibodies should be useful in developing enzyme-linked immunosorbent assay (ELISA) sandwich assays for routine and quantitative detection of this protein in human breast tumors nuclear extracts. Immunocytochemical analysis of rat mammary gland tissues showed only nuclear localization in both epithelial and stromal cells (data not shown).

Chromosomal Mapping with the FISH Method.

Seventy-four of 100 mitotic figures showed signal on one pair of the X chromosome (Figure 8, panels A and B). Since DAPI was used to identify the specific chro-

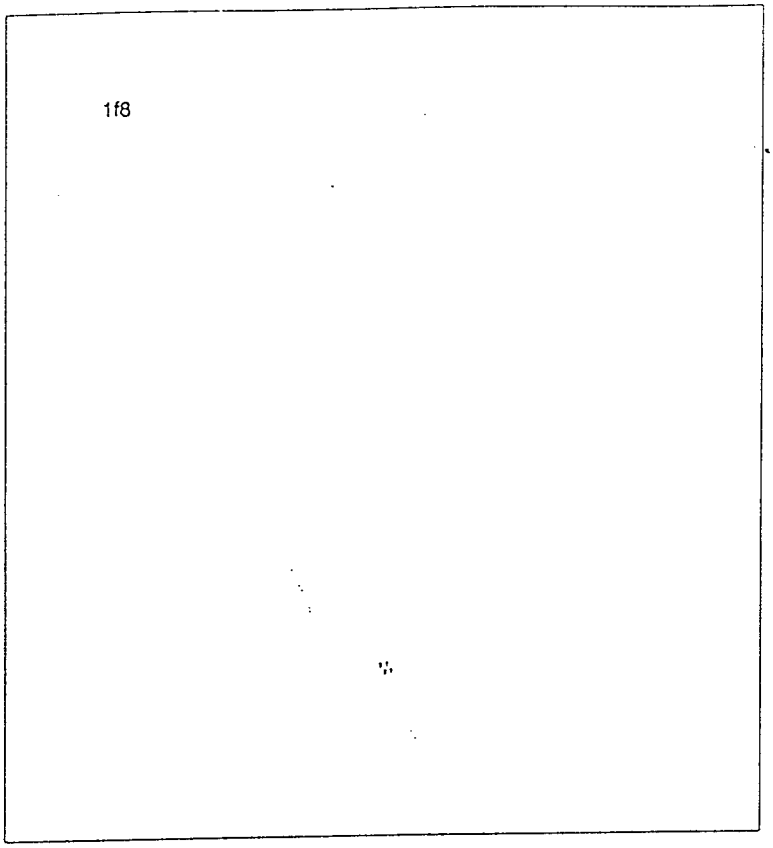

FIG. 8. Chromosomal location of *nmt55* gene. Fluorescent in situ hybridization (FISH) mapping of nmt55 gene showed signals on chromosome X (Panel A). Mitotic figures stained with DAPI are shown in Panel B).

mosomes, the assignment between signal form the cDNA probe and the long arm of chromosome X was obtained. The detailed position of the *nmt55* gene was further assessed from the summary analyses of 10 photographs, and was assigned to the long arm of chromosome X q13, as depicted in Figure 9. We did not detect additional loci for *nmt55* using the FISH method.

DISCUSSION

In this study we have identified and characterized a 55 kDa protein (*nmt55*) using a site-directed monoclonal antibodies to a unique peptide derived from human ER. Although NMT-1 monoclonal antibody was raised against a peptide from ER, NMT-1 failed to react with denatured ER in Western blot analyses. This observation suggests that the epitope for this antibody on ER is very sensitive to conformational changes, and once denatured by SDS it could not be recognized in ER. In contrast, this epitope appears to be stable or capable of renaturation in *nmt55*, as demonstrated by consistent detection by Western blot analyses. Nuclear protein *nmt55* did not bind estradiol, and did not cross-react with antibodies specific to ER (1,40). These observations suggested that *nmt55* was not an ER variant. It also did not associate with ER, as assessed by sucrose density gradient analysis and subsequent Western blotting. In addition, *nmt55* was localized mainly to the nucleus and is found in many tissues of animal species. This suggests that *nmt55* is conserved and may have an important role in cellular regulation. Nuclear protein *nmt55* expression was detected in normal breast tissue biopsies, and in most ER+/PR+ breast tumors, but not expressed in all of ER– human breast tumors. Loss of ER expression in human breast tumors is often associated with poor prognosis, while continued expression of ER is associated with disease-free survival and correlates well with tumor state of differentiation (18–20). It is possible that the loss of *nmt55* expression in the majority of ER– human breast tumors is related to loss of regulation of normal cellular growth and function.

Evaluation of tumor pathologic characteristics and hormonal status and the relationship with *nmt55* expression showed an association with ER status, PR status, tumor hormone phenotype, and mean tumor size. The association of tumor size with loss of *nmt55* expression suggests that a possible role for this protein in tumor growth, invasion, or metastases. Since it has been proposed that tumor size is an indicator of tumor metastases (15), it is possible that loss of *nmt55* expression in large tumors may be indicative of tumor progression to metastases. This would raise the possibility that loss of *nmt55* may be a potential marker for tumor metastases. The PR was an independent predictor of *nmt55* protein expression. Because PR is under estrogen control, it is possible that the observed relationship between tumor hormonal status and *nmt55* expression is related to es-

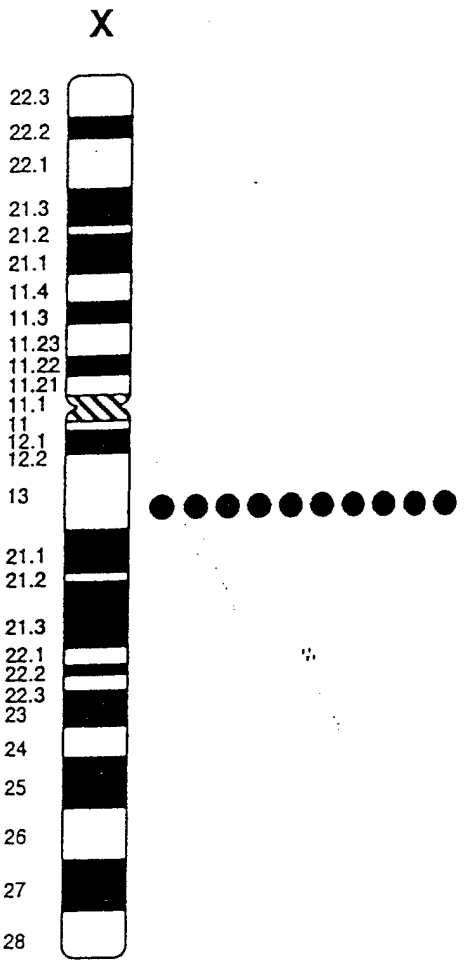

FIG. 9. Diagram of fluorescent in situ hybridization (FISH) chromosomal location of *nmt55* gene. Each dot represents the double FISH signals detected on human chromosome X.

trogen receptor function. Tumors that continue to express ER but not PR (ER+/PR−) may express nonfunctional ER and that these tumors are progressing to a poor state of differentiation (6,18–20,30).

We have cloned the cDNA for *nmt55* from a human breast tumor cell line. The predicted open reading frame encodes a 471 amino acid protein with a calculated molecular weight of 54,169 Da. The deduced amino acid sequence of this protein indicated that it is a basic protein with an estimated pI of 9.5. Based on homology with other proteins, *nmt55* has two RNA recognition motifs (RRM), suggesting that it is an RNA binding protein. The presence of a region with helix-turn-helix structure in *nmt55* suggests that *nmt55* binds to DNA. While the structural features are suggestive of RNA binding proteins (14), further work is necessary to demonstrate that *nmt55* indeed binds specifically to RNA.

A homology search of the GenBank/EMBL databases identified two other related genes. One was described by Dong et al., (4) cloned from HeLa cells and another is a mouse *NonO* (42). Nuclear protein *nmt55* had amino acid sequence identity >97 and 99% with *NonO* (42) and HeLa $p54^{nrb}$ (4), respectively. Nuclear protein *nmt55* differed from HeLa $p54^{nrb}$ in one amino acid; in *nmt55*, amino acid 151 was Thr while in HeLa $p54^{nrb}$ amino acid 151 is His. The mRNA for *nmt55* and HeLa $p54^{nrb}$ (4) detected by northern blot analysis revealed a similar size mRNA (~2.6 kb). Comparison of Southern blot analysis of *nmt55* and HeLa $p54^{nrb}$ (4), however, revealed subtle differences. While EcoRI digest of genomic DNA revealed a single 2.3 kb with an *nmt55* cDNA probe, EcoRI digest of genomic DNA probed by a homologous $p54^{nrb}$ cDNA probe showed >8.5 kb, 6 kb and 2.3 kb bands (4). When digested with PstI, *nmt55* showed three bands (~4.4, 3.2, and 1.4 kb) while $p54^{nrb}$ showed only two bands (~4.9 and 3.3 kb). Fluorescent in situ hybridization analyses of *nmt55* localized the gene to only one chromosomal locus on Xq13. The high degree of sequence homology and the detection of only one locus for *nmt55* by FISH suggest that *nmt55* and $p54^{nrb}$ are either the same gene or closely related genes tandemly arranged on Xq13.

Although the role of *nmt55* in cellular function is unknown at present, the striking homology between *nmt55* and HeLa $p54^{nrb}$ (4), 60 kDa murine *NonO* (42), and the PSF (24) suggest that *nmt55* may be a member of a family of splicing factors. These proteins exhibit conserved bipartite RNA binding domains common to proteins implicated in RNA splicing (4,24,42). HeLa $p54rnb^{nrb}$ was cloned using antibodies to yeast splicing factor PRP18 and has high homology to PSF and the Drosophila puff protein BJ6-$nonA^{diss}$ (28). *NonO* is a 60 kDa murine homologue of Drosophila $nonA^{diss}$ which has a bipartite RNA binding motifs, and an OCT-2-like helix-turn-helix lacking the POU domain (42). PSF is a 100 kDa protein shown to be essential for RNA splicing, but lacks the transcription factor-like domains and interacts with a 60 kDa RNA binding protein PTB (8). While *nmt55* and PTB have similar molecular weights, they share little amino acid homologies (8). Nuclear protein, hnRNP-A2/B1, which belongs to a family of RNA processing proteins was shown to be marker for detection of lung cancer (43). It is therefore, possible that proteins involved in pre-mRNA processing may be important in development or progression of neoplasm.

Several studies have attempted to elucidate the function of RNA binding proteins (e.g. PSF, PTB, U2AF, Drosophila Sex Lethal [*SxL*]) (14,32). These proteins recognize distinct polypyrimidine tracts in the 3′ splice sites of hnRNAs. These proteins are thought to regulate alternative splicing by selectively repressing 3′ splice sites containing a binding site for their respective RNA binding proteins (32). It has been suggested that proteins that contain RRM share a common fold in a similar protein-RNA interface, and may participate in pre-

mRNA processing via a common mechanism of function (14).

In summary, loss of *nmt55* expression may be an early marker for loss of ER expression or function. The strong association between *nmt55* and PR expression clearly indicates that *nmt55* may be an important marker in breast cancer. The ER gene encompasses more than 140 kb and is subdivided into 8 exons yielding a 6.32 kb mRNA (25). It is possible that *nmt55* is involved in pre-mRNA processing of ER, and loss of its expression in tumor cells may result in loss of ER expression due to lack of proper mRNA splicing. This may explain tumor heterogeneity, especially with respect to hormonal interventions in the course of treatment and further illustrates the heterogeneity of this disease. Also, since loss of *nmt55* expression is associated with increased tumor size, it is possible that this gene may be involved in tumor metastases. Therefore, *nmt55* may represent a new marker of tumor progression and prognostic information. While the function of *nmt55* remains unknown at present, its potential role as a splicing factor may be critical to cell growth and function and its loss of expression in human breast tumors may indicate loss of normal growth. The exact function of this protein and the significance of its gene location on the X chromosome q13 near the centromere are currently under investigation. □

Acknowledgment: This work was supported in part by a grant from the US Army Material Research Command DAMD 17 94 J4468 and by Hemagen Diagnostic, Waltham, Massachusetts.

REFERENCES

1. Abbondanza C, de Falco A, Nigro V, et al. Characterization and epitope mapping of a new panel of monoclonal antibodies to estradiol receptor. *Steroids* 1993;58:4–12.
2. Barnes R, Masood S, Barker E, et al. Low nm23 protein expression in infiltrating ductal breast carcinomas correlates with reduced patient survival. *Am J Pathol* 1991;139:245–50.
3. Chomczynski P, Sacchi N. Single step method of RNA isolation by acid guanidinium thiocyanate-phenol-chloroform extraction. *Anal Biochem* 1987;162:156–59.
4. Dong B, Horowitz DS, Kobayashi R, Krainer AR. Purification and cDNA cloning of HeLa cell p54^{nrb}, a nuclear protein with two RNA recognition motifs and extensive homology to human splicing factor PSF and *Drosophila* NONA/BJ6. *Nucleic Acids Res* 1993;21:4085–92.
5. Dong J, Lamb PW, Rinker-Schaeffer CW, Vukanovic J, Ichikawa T, Isaacs JT, Barrett JC. KAI1, a metastasis suppressor gene for prostate cancer on human chromosome 11p11.2. *Science* 1995; 268:884–86.
6. Foster BD, Cavener DR, Parl FF. Binding analysis of the estrogen receptor to its specific DNA target site in human breast cancer. *Cancer Res* 1991;51:3405–10.
7. Fu X-D, Maniatis T. Isolation of complementary DNA that encodes the mammalian splicing factor SC35. *Science* 1992;256: 535–38.
8. Ghetti A, Pinal-Roma S, Michael WM, Morandi C, Dreyfuss G. hn RNP I, the polypyrimidine tract-binding protein: distinct nuclear localization and association with hnRNA. *Nucleic Acid Res* 1992; 20:3671–78.
9. Gould MN. Cellular and molecular aspects of the multistage progression of mammary carcinogenesis in humans and rats. *Semin Cancer Biol* 1993;4(3):161–69.
10. Heng HHQ, Squire J, Tsui L-C. High resolution mapping of mammalian genes by in situ hybridization to free chromatin. *Proc Natl Acad Sci* 1992;89:9509–13.
11. Heng HHQ, Tsui L-C. Modes of DAPI banding and simultaneous in situ hybridization. *Chromosoma* 1993;102:325–32.
12. Heng HHQ, Tsui L-C. FISH detection on DAPI banded chromosomes. In: Choo KHA, ed. *Methods in Moelcular Biology: In situ Hybridization Protocols.* Clifton, NJ: Humana Press, 1994:35–49.
13. Horak ER, Leek R, Klenk N, et al. Angiogenesis, assessed by platelet/endothelial cell adhesion molecule antibodies, as indicator of node metastases and survival in breast cancer. *Lancet* 1992;340: 1120–24.
14. Kenan DJ, Query CC, Deene JD. RNA recognition: towards identifying determinants of specificity. *Trends Biochem Sci* 1991;16: 214–20.
15. Koscienly S, Tubiana M, Le MG. Breast Cancer: relationship between the size of the primary tumor and the probability of metastatic dissemination. *Br J Cancer* 1984;49:709–15.
16. Laemmli UK. Cleavage of structural proteins during the assembly of the head of the bacteriophage T4. *Nature* 1970;227:680–85.
17. Maniatis T, Fritsch EF, Sambrook J. *Molecular cloning a laboratory manual.* New York: Cold Spring Harbor Laboratory Press, 1982:280–81, 382–89.
18. McGuire WL. Hormone Receptors: their role in predicting prognosis and responses to endocrine therapy. *Semin Oncol* 1978;5: 428–33.
19. McGuire WL. Prognostic factor for recurrence and survival in human breast cancer. *Breast Cancer Res Treat* 1987;10:5–9.
20. McGuire WL, Pearson OH, Segaloff A. Predicting hormone responsiveness in human breast cancer. In: McGuire WL, Carbone PP, Vollmer ED, eds.) *Estrogen receptors in breast cancer.* NY: Raven Press, 1975:17–30.
21. Mierendorf RC, Percy C, Young RA. Gene isolation by screening lambda gt11 libraries with antibodies. *Methods Enzymology* 1987; 152:458–68.
22. Muller RE, Traish AM, Bebee DA, Wotiz HH. Reversible inhibition of estrogen receptor activation by molybdate. *J Biol Chem* 1982;257:1295–1300.
23. Patton JG, Mayer SA, Tempst P, Nadal-Ginard B. Characterization and molecular cloning of polypyrimidine tract-binding protein: a component of a complex necessary for pre-mRNA splicing. *Genes Dev* 1991;5:1237–51.
24. Patton JG, Porro EB, Galceran J, Tempst P, Nadal-Ginard B. Cloning and characterization of PSF, a novel pre-mRNA splicing factor. *Genes and Development* 1993;7:393–406.
25. Ponglikitmongkol M, Green S, Chambon P. Genomic organization of the human estrogen receptor gene. *EMBO J* 1988;7:3385–88.
26. Quick TC, Traish AM, Niles RM. Characterization of human retinoic acid receptor α1 expressed in recombinant baculovirus-infected Sf9 insect cells. *Receptor* 1994;4:65–80.
27. Ramshaw IA, Carlsen S, Wang HC, Badenoch-Jones P. The use of cell fusion to analyze factors involved in tumor cell metastasis. *Int J Cancer* 1983;32:471–78.
28. Rendahl KG, Jones KR, Kulkarni SJ, Bagully SH, Hall JC. The dissonance mutation at the no-on-transient-a locus of D. melanogaster: genetic control of courtship song and visual behaviors by a protein with putative RNA-binding motifs. *J Neuroscience* 1992; 12(2):390–407.
29. Santes K, Salmon D. Radiolabeled antibody targeting of the HER2/neu oncoprotein. *Cancer Res* 1992;52:1916–20.
30. Scott GK, Kushner P, Vigne J-L, Benz CC. Truncated forms of DNA-binding estrogen receptors in human breast cancer. *J Clin Invest* 1991;88:700–07.
31. Seymour L, Bezwoda WR, Meyer K. Tumor factors predicting for prognosis in metastatic breast cancer. The presence of P24 predicts for response to treatment and duration of survival. *Cancer* 1990; 66:2390–94.
32. Singh R, Valcarcel J, Green MR. Distinct binding specificities and functions of higher eukaryotic polypyrimidine tract-binding proteins. *Science* 1995;268:1173–76.

33. Salmon DJ, Godolphin W, Jones LA, et al. Studies of the HER-2/neu protooncogene in human breast and ovarian cancer. *Science* 1989;244:707–12.
34. Tso J, Sun X-H, Kao T-H, Reese K, Wu R. Isolation and characterization of rat and human glyceraldehyde-3-phosphate dehydrogenase cDNAs: genomic and molecular evolution of the gene. *Nucleic Acids Res* 1985;13:2485–2502.
35. Traish AM, Muller RE, Wotiz HH. Binding of 7 alpha, 17, alpha dimethyl-19-nortestoserone to androgen and progesterone receptors in human and animal tissues. *Endocrinology* 1986;118:1327–33.
36. Traish AM, Netsuwan N. Antibodies to human estrogen receptor recognize the native receptor form and a 55 kDa nuclear protein in estrogen target tissues. *75th Annual Meeting of Endocrine Society. Programs and Abstracts* P. 517, Abst. #1863, 1993.
37. Traish AM, Netsuwan N. 7 alpha-17 alpha-dimethyl-19-nortestosterone (mibolerone) induces conformational changes in progesterone receptors distinct from those induced by ORG 2058. *Steroids* 1994;59:362–70.
38. Traish AM, Al-Fadhli S, Klinge C, Kounine M, Quick TC. Identification of structurally-altered estrogen receptors in human breast cancer by site-directed monoclonal antibodies. *Steroids* 1995;60: 467–74.
39. Traish AM, Newton AW, Styperek K, Beazley R, Kavanah M. Estrogen receptor functional status in human breast cancer. *Diagn Mol Pathol* 1995;4:220–28.
40. Traish AM, Pavao M. Binding of site directed monoclonal antibodies to an epitope located in the A/B region (amino acids 140-154) of human estrogen receptor induced conformational changes in an epitope in the DNA-binding domain. *Steroids* 1996;61:549–56.
41. Weinberg RA. Tumor suppressor genes. *Science* 1991;254:1138–46.
42. Yang YS, Hanke JH, Caryannopoulos L, Craft CM, Capra JD, Tucker PW. *NonO*, a Non-POU-domain-containing, octamer binding protein, is a mammalian homolog of Drosophila nonA^{diss}. *Mol Cell Biol* 1993;13:5593–5603.
43. Zhou J, Mulshine JL, Unworth EJ, Scott FM, Avis IM, Vos MD. Purification and characterization of a protein that permits early detection of lung. *J Biol Chem* 1996;271:10760–766.

ESTROGEN AND PROGESTERONE RECEPTOR CONCENTRATIONS AND PREVALENCE OF TUMOR HORMONAL PHENOTYPES IN OLDER BREAST CANCER PATIENTS

Running head: Hormone Receptors in Breast Cancer

Jacqueline Ashba[1,2] MPH and Abdulmaged M. Traish[1], PhD.

Department of Biochemistry[1] Boston University School of Medicine, and the Data Coordinating Center[2], Boston University School of Public Health, Boston, MA 02118

All inquiries should be addressed to:

Dr. A. Traish

Department of Biochemistry Boston University School of Medicine

80 East Concord St.

Boston, MA 02118

Tel: (617) 638-4578

Fax: (617) 638-5412

ABSTRACT

We have examined the expression of estrogen (ER) and progesterone receptors (PR) and the distribution of tumor phenotypes as a function of age in breast cancer patients. ER and PR concentrations were determined in tissue biopsies from 1739 specimens of patients with primary breast cancer, using ligand binding assays. Tumors were classified as receptor positive (ER+) or negative (ER-) and PR+ or PR- based on the presence or absence of receptor binding activity. Tumors were stratified into four phenotypes based on the combined ER and PR status: ER+ PR+; ER+ PR-; ER- PR+; and ER- PR-. Significant positive associations were found between ER and age ($p=0.0001$) and between PR and age ($p=0.0002$). The median ER levels were statistically different age groups, with the greatest levels older versus younger patients. The prevalence of ER+PR+ tumor phenotype increased with age. In contrast, the prevalence of ER-PR- and ER-PR+ tumor phenotypes decreased with age. The median PR to ER ratio decreased with age ($p=0.0001$) and this trend was attributed to increased ER levels with age. The prevalence of ER-PR- and ER-PR+ tumor phenotypes in younger patients suggest that hormonal regulation of ER gene expression may be responsible for the observed disparity of tumor phenotypes in breast cancer.

Key terms: Breast cancer, estrogen receptors, progesterone receptors, risk.

INTRODUCTION

Breast cancer is the second leading cause of cancer death among women in the U.S. The incidence of breast cancer has been increasing since the 1980's with the highest incidence occurring in postmenopausal women (1-2). It has been well documented that ovarian hormones play a major role in the growth of breast cancer. Tumor expression of ER and PR is associated with favorable response to endocrine therapy (3-4), survival (5-7), histological differentiation (8-10) and is associated with certain risk factors for breast cancer (11-12). Of all the risk factors studied, age is a strong independent predictor of estrogen receptor levels and breast cancer incidence (12).

Most studies on the effects of age on hormone receptors have examined only the presence or absence of ER and PR (19-22), while fewer studies addressed the relationship between age and concentrations of ER and PR . Furthermore, the paucity of data regarding the effects of age on tumor phenotypes in breast cancer suggests the need for better understanding of the relationship between age and tumor hormonal responsiveness.

In this study, we have examined the relationship between age and ER and PR concentrations in a sample of hospital-based breast cancer patients. Since the combination of ER and PR status is thought to characterize tumors with different clinical outcomes (23), we also analyzed the relationship between age and tumor phenotype. This study sample included a substantial representation of patients beyond the seventh decade of life. Further, we used data generated by ligand binding assays, which unlike the enzyme immunoassay (EIA) or immunocytochemical assays, can distinguish between functional and non-functional hormone receptors. Also, all the data were generated in a single laboratory using one standard assay method, thereby reducing data variations when compared to data gathered from several different laboratories, in which different assays may have been employed.. The objective of this study is to determine the effects of age on the changes in the ER and PR concentrations and the distribution of tumor phenotypes, within various age groups, in breast cancer patients. Together with other prognostic factors, the concentrations of ER and PR within a given tumor phenotype, may serve as a better guide for the appropriate therapeutic modality in the management of breast cancer patients.

MATERIALS AND METHODS

Patient Population

Human breast tumors from 1740 patients were assayed for ER and PR content at Boston University School of Medicine Hormone Assay Laboratory, between December 1988 and December 1993 and the data were used in the final analyses. All data were obtained from primary breast cancer patients under going surgery for treatment of breast cancer in several Boston area hospitals. This study was approved by the Institutional Review Board of Boston University School of Medicine.

Estrogen and Progesterone Receptor Assays

The concentration of unoccupied ER and PR were determined by ligand binding analysis as described previously (24). [^{3}H]estradiol was used as a ligand for ER and [^{3}H] ORG 2058 was used as ligand for PR (24). The binding data were normalized as femtomoles of specifically bound ligand per milligram (fmol/mg) of cytosol proteins. We have chosen cut-off values for ER as 10 fmol/mg protein and for PR as 2 fmol/mg proteins since these value were reported to the American Collage of Pathologists (CAP) as a part of our laboratory certification. These cut off values were chosen because they reflect the sensitivity of the assays using ligands with high specific activity.

Stratification of Tumor Hormonal Phenotypes based on ER and PR Status

Tumors were stratified into four groups according to their ER and PR status: 1) ER+PR+; 2) ER-PR- ; 3) ER+PR- ; and 4) ER-PR+. Similar stratification was reported by others using ligand binding and gel shift assay (25). Patients were stratified into five age groups: Group I, less than 45 ; Group II, 45-54, Group III, 55-64, Group IV, 65-74, and Group V, > 74 years. The choice of this breakdown in age was chosen to reflect the clinical application of endocrine therapy and other risk factors and possible linkage to clinical trials of breast cancer.

Statistical Analyses

Separate linear regression analyses were performed to examine the association between age and ER and PR concentrations. In addition, for each age group, linear regressions were performed between ER, PR concentration and age. Multiple linear regression analyses were used to test the possibility of a non-linear function of hormone receptor levels and age, by adding

$(age)^2$ and $(age)^3$ to the model. Test for normality of the distribution of ER and PR levels was performed. A nonparametric test (Kruskal-Wallis test) was used to compare the median values of ER and PR by age groups Chi-square analysis was used to examine differences in age and the combined ER and PR status of tumors. For tumors with ER+PR+ status, the ratio of PR to ER was calculated for each age group and analysis of variance was used to compare the median PR/ER ratios, as well as the median ER and PR levels, by age group. .All statistical analyses were performed using mainframe SAS version 6.10 at the Boston University Medical Center.

RESULTS

This study examined the estrogen and progesterone receptor content of tumors from 173 breast cancer patients who underwent surgery for treatment of breast cancer. The mean age of patients was 64 (range 18-106 years), and after stratification of age, there were 219 patients (13%) less than 45 years of age; 266 patients (15%) between ages 45 and 54 years; 330 patients (19%) between ages 55 and 64 years; 469 patients (27%) between ages 65 and 74 years; and 455 (26%) above the age of 74 years.

Analyses of ER and PR expression and content in tumors from patients with various age using simple linear regression analysis showed a highly significant positive association between ER and age ($p = 0.0001$, $r=0.26$, slope = 2.90) and PR and age ($p = 0.0002$, $r=0.09$, slope = 1.77). The possibility of a non-linear relationship between age and either ER or PR was tested , however, we did not find statistically significant associations by multiple linear regression analysis. The normality test of the distribution of ER and PR levels did not show evidence for normality, therefore we used the median values for ER and PR and PR/ER ration rather than the means in all statistical comparisons. When analyzed by the Kruskal-Wallis test, the median ER increased with age (Table 1), and the medians were statistically different across age groups (Chi square 156.7; $p= 0.0001$). The mean and median values for PR were statistically significant across age groups (Chi square 18.86, $p=.0008$). However, the patterns were different between these two receptors across age groups (Table 1; Figure 5). Chi-square analyses showed statistical significance ($X^2 = 67.4$, $p < 0.001$) when age group were cross tabulated with tumor phenotype (combined ER and PR status). Overall, ER+PR+ (1200/1739) phenotype was the most prevalent (69%), followed by ER-PR+ (338/1739) or (19%); 7% were ER-PR- and 5% were ER+PR- .

The prevalence of ER+PR+ tumors increased with age, reaching 80% in the >74 year age group (Fig. 1). For ER-PR+ tumors (Fig. 2) and ER-PR- tumors (Fig.3) a decreasing trend in age group specific prevalence was observed. Among ER+PR- tumors but no consistent trend was observed (Fig. 4).

It is well recognized that PR synthesis is under estrogen regulation. For this reason, we examined the effects of age on PR expression. The ratio of PR to ER was calculated as a function of age (1200 subjects) only for the ER+PR+ tumors . Regression analysis showed a statistically significant negative association ($p = 0.0001$, $r = 0.21$, slope = -0.06) between the PR/ER ratio and age. The median PR/ER ratios were compared by age groups (Table 2; Fig. 5) and were statistically different ($X^2 = 106.32$, $p = 0.0001$). To determine which hormone receptor had a stronger influence on the observed changes in the PR/ER ratio with age, the median for ER and PR levels were compared by age groups (Table 2). The same linear trend was observed for ER+PR+ tumors; median ER concentrations increased with age were statistically different across age groups (Chi square =129.9; $p = 0.0001$). Comparisons of median PR levels by age group did not show a linear trend, and was not statistically different across age groups (Chi square = 6.82; $p=0.1457$).

The slopes obtained from the linear regressions of ER and PR with age were plotted versus age groups (Fig. 6). The slope for ER was smallest in the younger patients (<45 years) and greatest in patients aged 45-54 years, and declines thereafter. In contrast, the slopes for PR were greatest in the younger patients, least in 45-54 age group, and shows a similar trend as ER in the older patients.

DISCUSSION

The goal of this study was to investigate the age related changes in the concentrations and status of ER and PR in human breast tumors. Data from this study provide evidence that ER and PR concentrations, as well as tumor hormonal phenotypes, are significantly associated with age. The median ER level was greater in older patients compared to younger patients suggesting changes in the regulation of ER expression. This may be interpreted as increased availability of

unoccupied ER binding sites due to lower levels of circulating estrogens in postmenopausal patients or to regulation by endocrine hormones. The decreased levels of ER in tumors from younger patients are attributed to down-regulation of ER expression by progestins or other endocrine hormones. It is unlikely that the observed prevalence of ER- tumors in the younger patients is due to occupancy of ER by circulating estrogens in these pre-menopausal patients, since immunochemical analyses (8) which detect occupied and unoccupied ER correlated well with ligand binding studies. This suggests that loss of ER expression is a consequence of regulation of ER in tumors of premenopausal patients.

The point of inflection of the median PR concentration at the 45-54-year age group may reflect biological changes occurring in the perimenopausal years, as reported previously (23,28). Also the slopes of PR with age reflected this physiopathological changes during the peri-menopausal years. We speculate that breast cancer may be a disease with a dichotomous nature represented by hormonal insensitive tumors in the premenopausal patients and hormone dependent tumors in the postmenopausal patients. The observation that PR/ER ratio was greatest in younger patients and least in older patients is attributed to decreased levels of ER in younger patients and increased ER in older patients. In contrast, the smaller PR/ER ratio in patients 55 years or older can be explained by the increased ER levels. Whether increased ER concentration in older patients is due to increased expression of ER or to availability of unoccupied sites due to decreased circulating levels of estrogens remains unclear. Progesterone is known to down-regulate ER expression. Thus, it is possible that plasma progestins levels are reduced in older patients and progesterone may not down-regulate ER expression. Because ER regulates PR expression, the reduced levels of circulating estrogens in this older group may not induce PR expression.

Normal breast cells express reduced levels of ER and PR. The transformation of normal cells into neoplastic cells may lead to retention or loss of expression of regulatory proteins such as ER and PR. The ability of tumor cells to retain expression of regulatory proteins reflects the state of tumor differentiation (10,13, 15-17). Thus, during tumor growth and progression, four possible hormonal phenotypes may emerge. Tumor cells that retain ER and PR expression remain ER+ and PR+ and are expected to remain differentiated. Tumor progression may lead to loss of expression of ER and PR leading to an ER- and PR- phenotype with some de-differentiation. Progression of tumors from ER+ PR+ phenotype to ER- PR+ or ER+ PR-

suggests that loss of expression of regulatory proteins and this may reflect varying stages of tumor differentiation.

The increased prevalence of ER+PR+ tumor phenotype with age may be attributed to up-regulation of ER expression by decreased circulating levels of endocrine hormones. The decrease in the prevalence of ER- PR- and ER- PR+ tumor phenotypes with age may represent a different mechanism of regulation of ER expression when endocrine hormones are altered with age (30). Thus the progression of tumor phenotype from ER+ PR+ to ER- PR- may be the result of tumor cell de-differentiation in response to other endocrine factors or a manifestation of tumor progression to acquire growth advantages, becoming less dependent on estrogens. Fine needle aspirate studies (30,31) of normal and breast cancer tissue in premenopausal women have shown that in normal subjects, ER synthesis is cyclic and is mainly produced while plasma estrogen and progesterone concentrations are reduced (during the early follicular phase). In contrast to normal breast tissue where estrogen levels may regulate ER expression, in older patients, ER expression in breast cancer tissue may occur constitutively. Hence, among premenopausal patients, information on the menstrual cycle stage at the time of biopsy may be important in understanding the possible effects on tumor hormonal sensitivity.

The discordant tumors (ER+PR- and ER-PR+) are not clearly defined. Tumors with ER-PR+ phenotype were found mostly in the <55 year age group, and the prevalence decreases with age. This may be explained by other factors, such as the use of oral contraceptives, higher plasma estradiol levels due to use of estrogen replacement therapy in the postmenopausal groups, or by cyclic changes in plasma estradiol and progesterone levels in premenopausal women. These observations are in agreement with previous reports (23, 26-29).

The presence of tumor phenotypes with ER+ PR- may represent the expression of non-functional ER in such tumors (25,32,33,34). PR expression is dependent on ER function, thus lack of expression of PR is attributed to the presence of ER which has the ability to bind the hormone but elicits no biological function. Similarly, the presence of the ER- PR+ tumor phenotype may represent the expression of ER with an altered hormone binding domain but which remains biologically active. Indeed such phenotypes have been described (25,32,34). The prevalence of ER+ PR- tumors did not exhibit any consistent trend with age, and perhaps the

results are an effect of confounding by other risk factors for breast cancer. Another explanation may be that ER+PR- tumors represent a transition phase in cell differentiation or a stage in the growth of breast cancer. These tumors may also characterize the population of breast cancer patients that do not respond to endocrine therapy due to the presence of dysfunctional ER. Since there are significant differences in the prevalence of tumor phenotype among the various age groups, it is likely that lack of ER expression or function is associated with disease progression and tumor phenotypic changes with age. We were unable to correlate these finding with other risk factors (e.g. family history, age at menarche, parity) for these breast cancer patients because the data regarding these risk factors were inaccessible.

ER content, coupled with PR levels, provides a useful prognostic index in patients with metastatic disease, and is associated with disease-free survival (15-17). However, approximately 65% of all patients with ER+ tumors respond to hormonal intervention (15-17). The lack of response to hormonal interventions in approximately one-third of all patients with ER+ tumors may be attributed, at least in part, to the presence of nonfunctional ER or the inability of ER to recruit other transcriptional activation factors. The observations that several tumor phenotypes exist based on ER and PR status, suggest that it is likely that tumors exhibiting ER+PR- phenotype express significantly lower concentrations of ER than tumors exhibiting ER+PR+ phenotypes, and this may indicate different degrees of cell differentiation associated with each phenotype.

The discrepancies in the prevalence of tumor phenotypes between our studies and others, may be attributed to limitations of receptor assay techniques, choice of different cut-off values for ER and PR status, or the age distribution of the population studied. Further, other factors such as tumor tissue procurement and handling, assay conditions, previous radiotherapy treatment prior to surgery or treatment with antiestrogens prior to surgery may affect the values of ER and PR. Our study confirms and extends the observations made in previous reports (5,9,13,23,28) in which ER+PR+ tumors were shown to be most prevalent in older age groups. However, our study shows that ER-PR- tumors were less prevalent with age, contrary to other reports (29). In addition, the issue of referral bias in hospital versus community-based populations may have influenced our results, yet one study (12) found similar outcomes between the two types of samples. Additional prospective studies are needed to address the question of whether the four

tumor phenotypes represent multiple forms of cancer or different stages in the de-differentiation process of one form of cancer.

ACKNOWLEDGEMENTS: This work was supported by a grant from the Department of the Army DAMD 1794J4468 and b Hemagen Diagnostic, Waltham, Massachusetts.

REFERENCES

1. Qualters JR, Lee NC, Smith RA, et al. Breast and cervical cancer surveillance, united states, 1973-1987. MMWR CDC Surveillance Summaries 1992; 41(2):1-15. 1992

2. Miller BA, Feuer EJ, Hankey BF. Recent incidence trends for breast cancer in women and the relevance of early detection. CA-a cancer journal for clinicians 1993; 43(1):27-41.

3. Brooks SC, Saunders DE, Singhakowinta A, et al. Relation of tumor content with response of patient to endocrine therapy. Cancer 1980; 46:2775-2778.

4. Degenshein GA, Bloom N, Tobin E. The value of progesterone receptor assays in the management of advanced breast cancer. Cancer 1980; 46:2789-2793.

5. Gelbfish GA, Davidson AL, Kopel S, et al. Relationship of estrogen and progesterone receptors to prognosis in breast cancer. Ann Surg 1988; 207(1):75-79.

6. Williams MR, Todd JH, Ellis IO, et al. Oestrogen receptors in primary and advanced breast cancer: an eight year review of 704 cases. Br J Cancer 1987; 55:67-73.

7. Kohail HM, Elias EG, El-Nowiem SA, et al. A multifactorial analysis of steroid hormone receptors in stages I and II breast cancer. Ann Surg 1985; 201(5):611-617.

8. Anderson J, Bentzen SM, Poulsen HS. Relationship between radioligand binding assay, immunoenzyme assay and immunohistochemical assay for estrogen receptors in human breast cancer and association with tumor differentiation. Eur J Cancer Oncol 1988; 24:377-384.

9. Millis RR. Correlation of hormone receptors with pathological features in human breast cancer. Cancer 1980; 46:2869-2871.

10. McCarty KS, Barton TK, Fetter BF, et al. Reeves W, et al. Correlation of estrogen and progesterone receptors with histologic differentiation in mammary carcinoma. Cancer 1980; 46:2851-2858.

11. Cooper JA, Rohan TE, Cant EL, et al. Risk factors for breast cancer by oestrogen receptor status: a population-based case-control study. Br J Cancer 1989; 59:119-125.

12. Ballard-Barbash R, Griffin MR, Fisher LD, et al. Estrogen receptors in breast cancer. Am J Epidemiol 1986; 124:77-84.

13. Witliff JL. Steroid-hormone receptors in breast cancer. Cancer 1984; 53:630-643.

14. Beattie GW, Bride HA, Hart G, et al. Estradiol and progesterone in human breast cancer cytosols and their relationship to receptor incidence. Cancer Invest 1983; 1:199-206.

15. McGuire WL, Pearson OH, Segaloff. Predicting hormone responsiveness in human breast cancer. In: McGuire WL. Carbone PP. Vollmer eds. Estrogen Receptors In Breast Cancer. New York: Raven Press, 1975: 17-30.

16. McGuire WL. Prognostic factor for recurrence and survival in human breast cancer. Breast Cancer Res & Treat 1987; 10: 5-9.

17. McGuire WL. Hormone Receptors: Their role in predicting prognosis and responses to endocrine therapy. Semin. Onco 1978; 5: 428-433.

18. Habel LA, Stanford JL. Hormone receptors and breast cancer. Epidemiol Rev 1993; 15(1):209-219.

19. Sutherland CM, Mather F. Charity hospital experience and prognostic factors in patients with breast cancer with localized or regional disease. Ann Surg 1988; 207:569-579.

20. McKeown-Eyssen GE, Rogers-Melamed I, Clarke EA. Estrogen receptor status of breast cancer in Ontario. Can Med Assoc J 1985; 133:997-1000.

21. Stanford JL, Grenberg RS. Breast cancer incidence in young women by estrogen receptor status and race. Am J Public Health 1989; 79(1):71-73.

22. Stanford JL, Szklo M, Boring CC, et al. A case-control study of breast cancer stratified by estrogen receptor status. Am J Epidemiol 1987; 125(2):184-194.

23. Thorpe SM. Estrogen and progesterone receptor determinations in breast cancer. Acta Oncol 1988; 27:1-19.

24. Traish AM, Wotiz HH. Monoclonal and polyclonal antibodies to human progesterone receptor-peptide 533-547 recognize a specific site in unactivated (8S) and activated (4S) progesterone receptor and distinguish between intact and proteolyzed receptors. Endocrinology 1990; 127:1167-1175.

25. Foster BD, Cavener DR, Parl FF. Binding analysis of the estrogen receptor to its specific DNA target site in human breast cancer. Cancer Res 1991; 51:3405-3410.

26. Alghanem AA, Hussain S. The effect of age on estrogen and progesterone receptor in primary

breast cancer. J Surg Oncol 1985; 30:29-32.

27. Navarro MA, Huget J, Valero J, et al. Clinical and methodological considerations in the quantification of estrogen and progesterone receptors using monoclonal antibodies in breast cancer. Medicina Clinica 1991; 97(2):41-44.

28. Ferno M, Borg A, Johanson U, et al. Estrogen and progesterone receptor analyses in more than 4,000 human breast cancer samples. A study with special reference to age at diagnosis and stability of analyses. Southern Swedish Breast Cancer Study Group. Acta Oncol 1990; 29(2):129-135.

29. Redkar AA, Kabre SS, Mittra I. Estrogen & progesterone receptors measurement in breast cancer with enzyme-immunoassay correlation with other prognostic factors. Ind J Med res 1992; 96:1-8.

30. Markopoulos C, Berger U, Wilson P, et al. Oestrogen receptor content of normal breast cells and breast carcinomas throughout the menstrual cycle. Brit J Med 1988; 296:1349-1351. 31. Ricketts D, Turnbull L, Ryall G, et al. Estrogen and progesterone receptors in the normal female breast. Cancer Res 1991; 51:1817-1822.

32. Fuqua SAW, Fitzgerald SD, Chamness GC, et al. Variant human breast tumor estrogen receptor with constitutive transcriptional activity. Cancer Res. 1991; 51:105-109.

33. Traish AM Al-Fadhli S Klinge C, Kounine M and Quick TC. Identification of structurally altered estrogen receptors in human breast cancer by site-directed monoclonal antibodies. Steroids

34. Faqua SAW, Chamness GC and McGuire WL. Estrogen receptor mutations in breast cancer. J. Cell. Biochem. 51: 135-139, 1993.

TABLE 1

MEAN AND MEDIAN ER AND PR CONCENTRATIONS (fmol/mg) BY AGE GROUP FOR ALL TUMORS (N=1739)

Age Group (years)	N	MEAN ER	MEDIAN ER	MEAN PR	MEDIAN PR
<45	219	36.3	14	126.7	31
45-54	266	69.4	19	136.6	39
55-64	330	105.1	37	115.5	25.5
65-74	469	124.6	62	156.5	36
>74	455	159.7	92	191.3	54

Kruskal-Wallis Chi square = 156.73, p=0.0001 for median ER values..

Kruskal-Wallis Chi square = 18.85, p=0.0008 for median PR values..

TABLE 2

MEDIAN OF PR, ER AND PR/ER RATIO IN ER+PR+ TUMORS BY AGE GROUP (1200 Patients)

Age Group (years)	N	MEDIAN ER (fmol/mg)	MEDIAN PR (fmol/mg)	MEDIAN PR/ER
<45	122	34	108	3.1
45-54	159	49	98	1.7
55-64	223	87	64	0.9
65-74	334	104	83.5	0.8
>74	362	138	83	0.83

Kruskāl-Wallis Chi square =129.9, p=0.0001, for ER values.

Kruskal-Wallis Chi square =6.82, p=0.1497, for PR values.

Kruskal-Wallis Chi square =106.3, p=0.0.0001, for median PR/ER ration.

Figure 1. Prevalence of ER+PR+ in breast cancer patients of various age groups. (n=1200 patients),

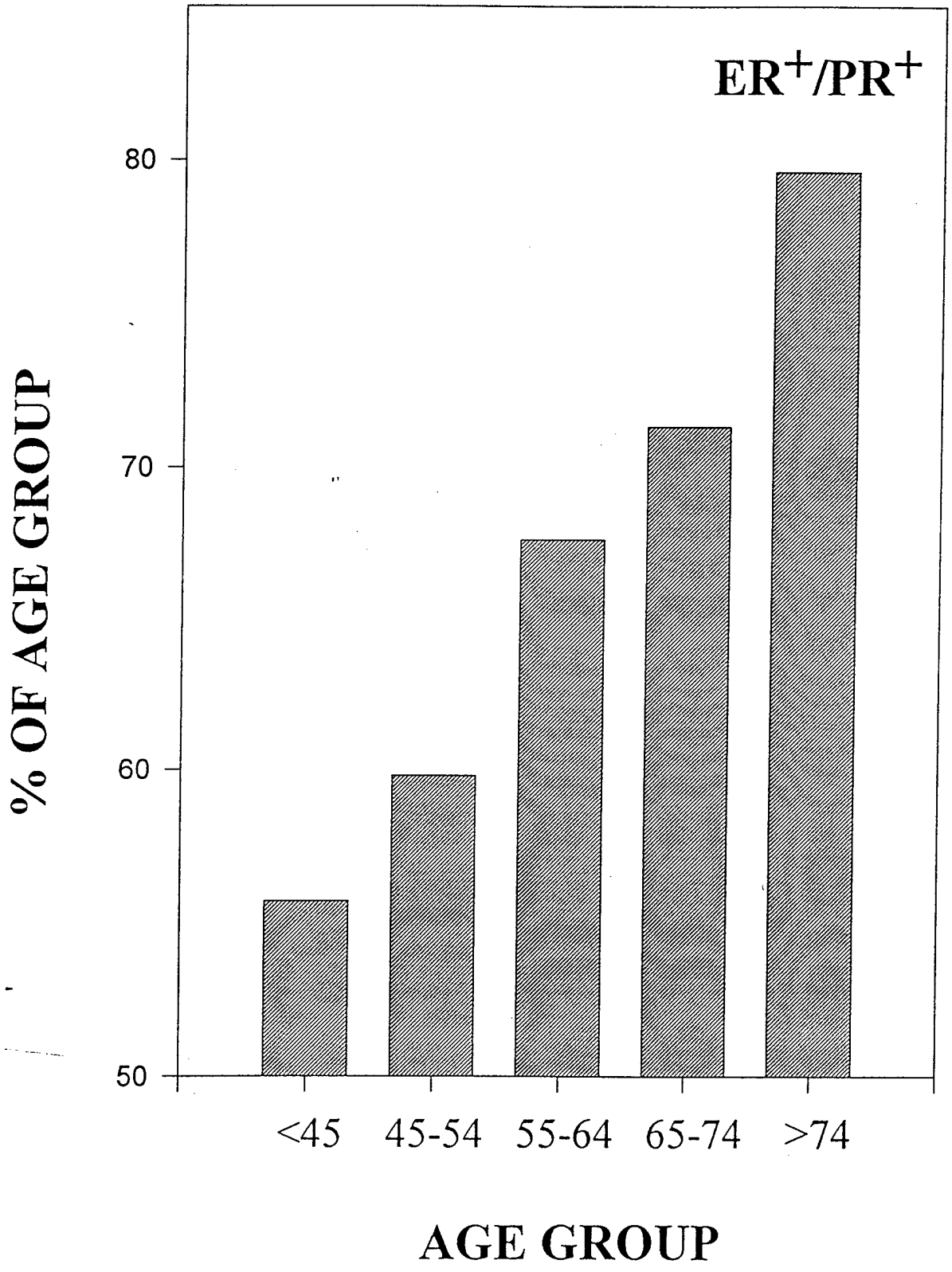
ER+/PR+
80
70
60
50
% OF AGE GROUP
<45
45-54
55-64
65-74
>74
AGE GROUP

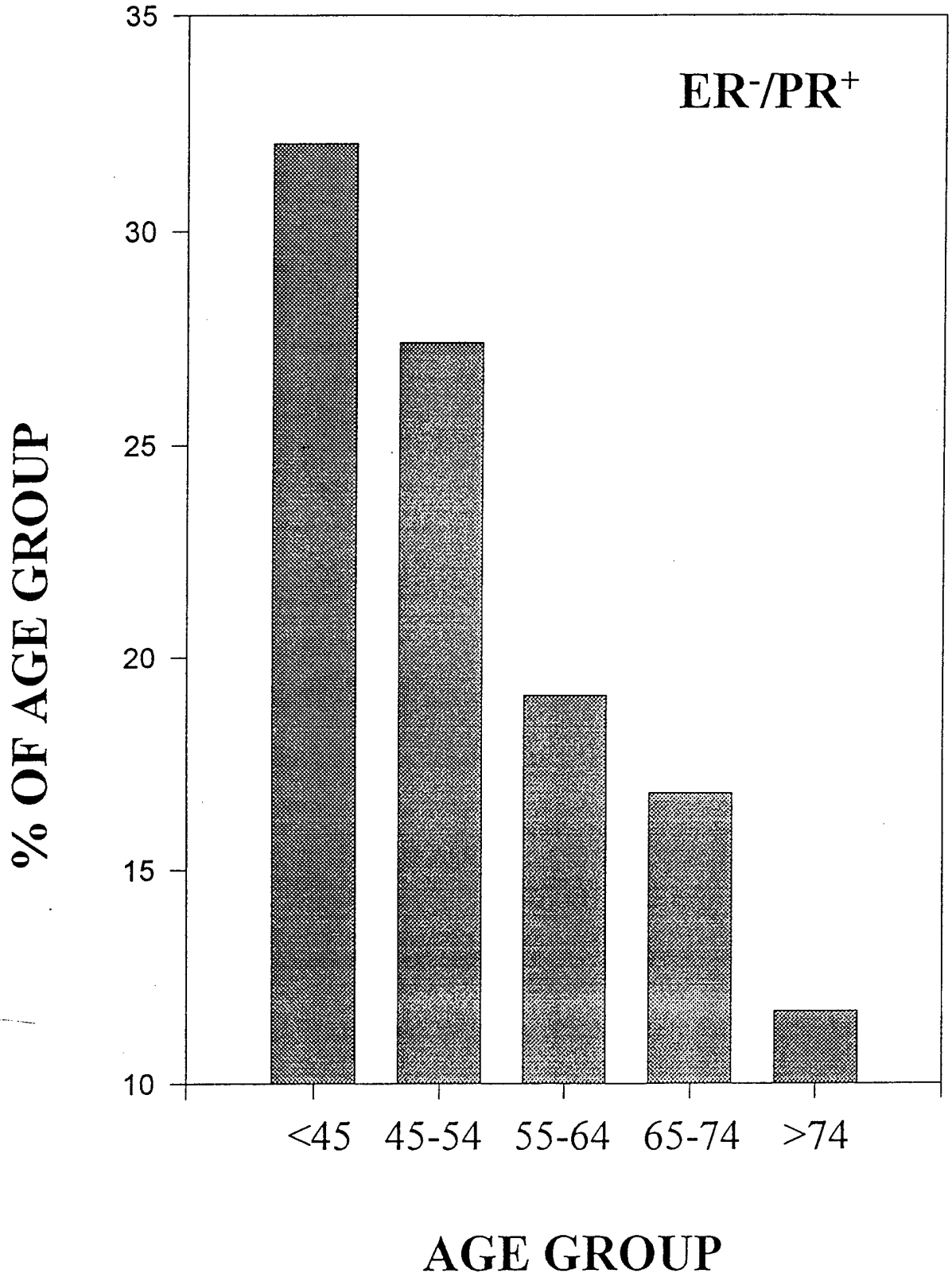
ER-/PR+
35
30
25
20
15
10
% OF AGE GROUP
<45
45-54
55-64
65-74
>74
AGE GROUP

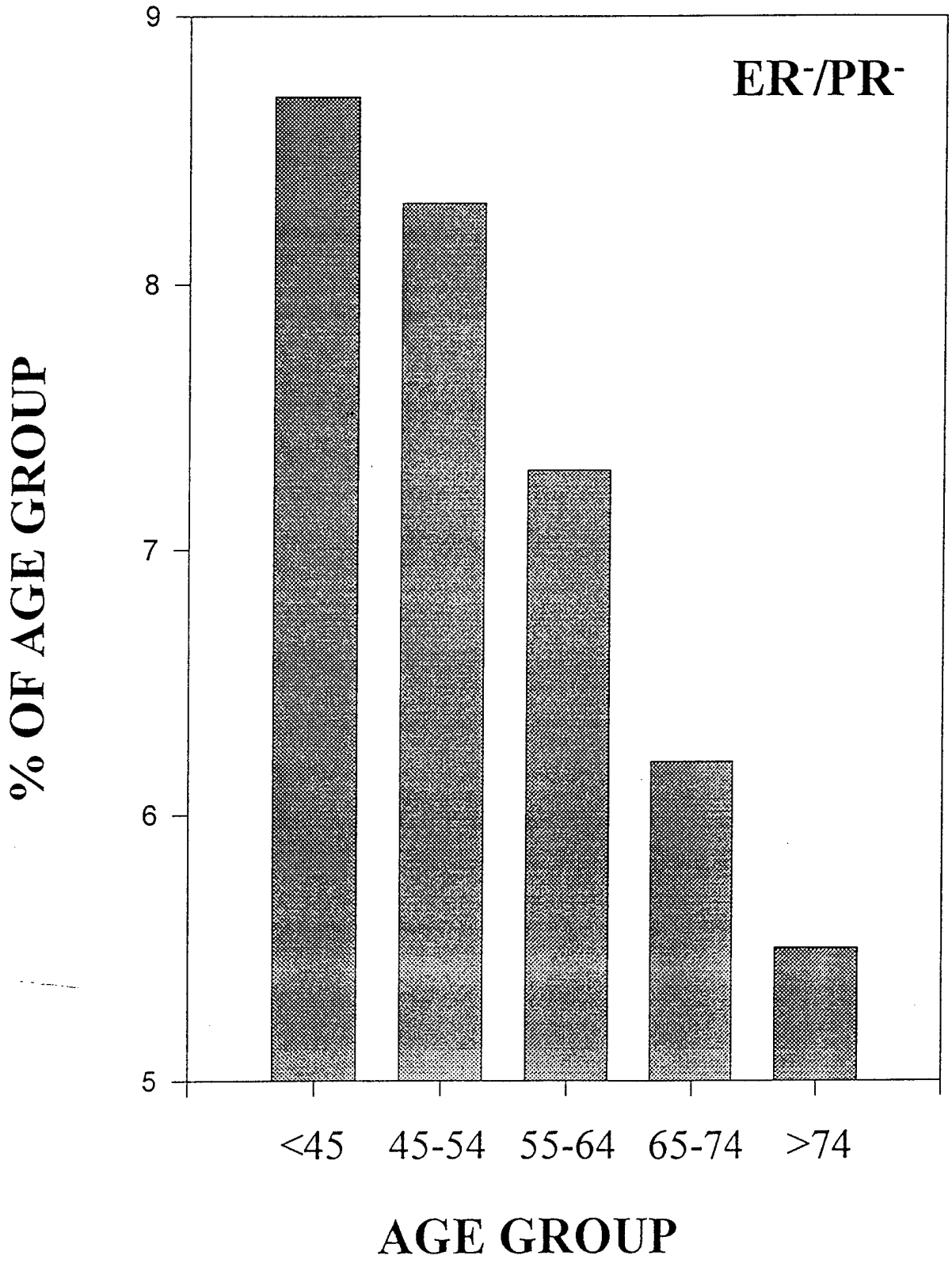
ER-/PR-
% OF AGE GROUP
9
8
7
6
5
<45
45-54
55-64
65-74
>74
AGE GROUP

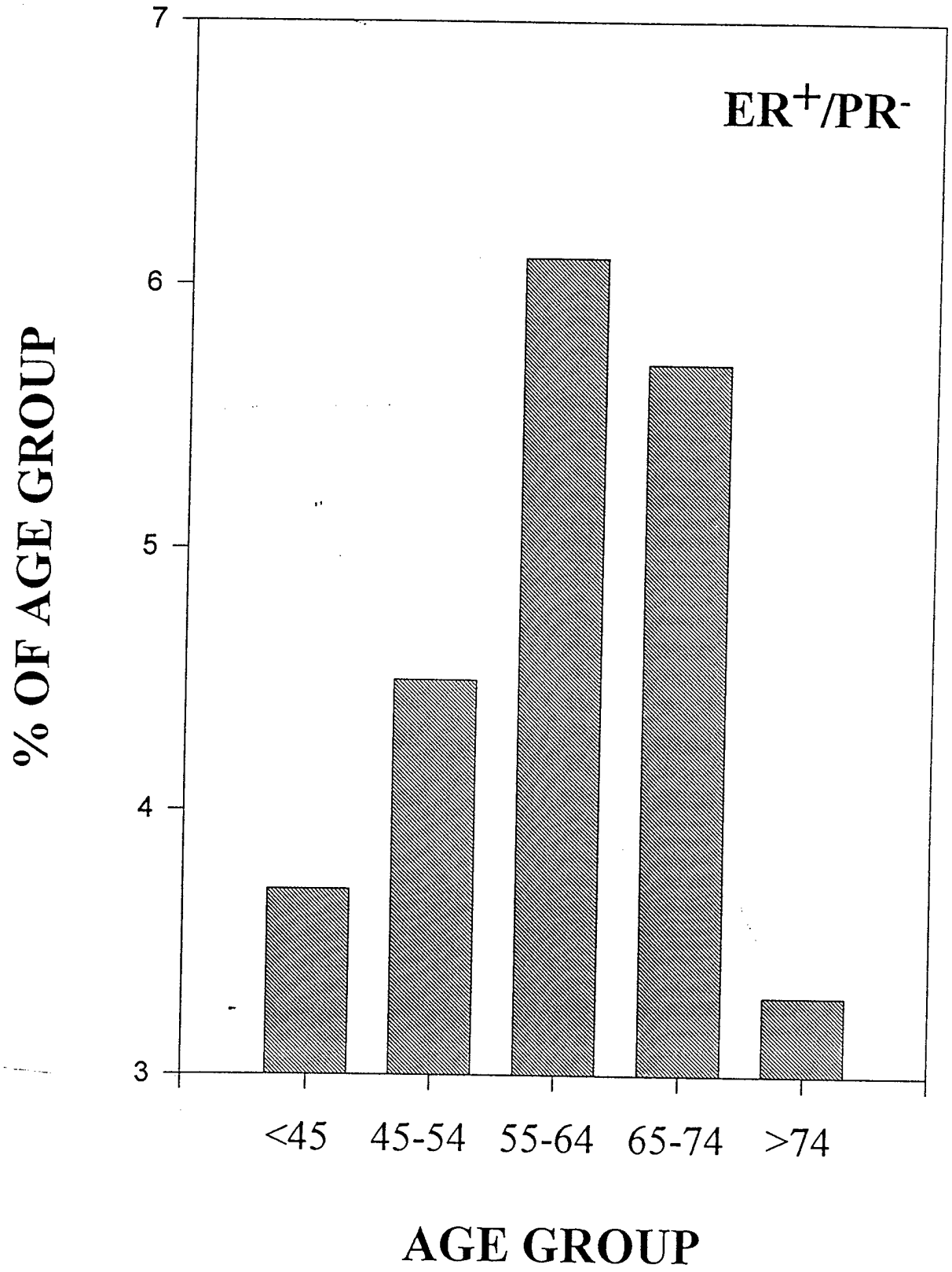
ER+/PR-
% OF AGE GROUP
7
6
5
4
3
<45
45-54
55-64
65-74
>74
AGE GROUP

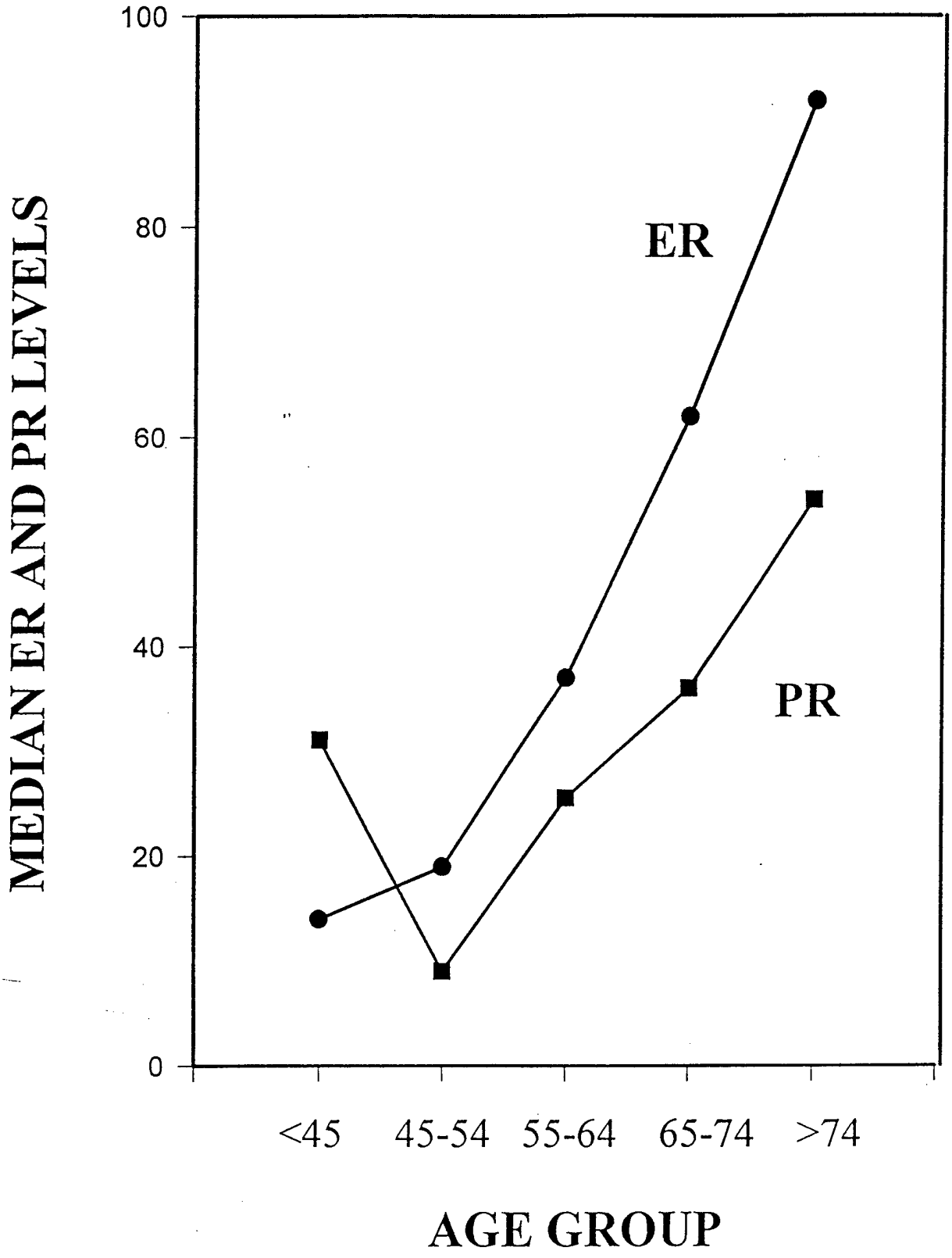
MEDIAN ER AND PR LEVELS
100
80
60
40
20
0
ER
PR
<45
45-54
55-64
65-74
>74
AGE GROUP

Linear regression analyses slopes for ER and PR

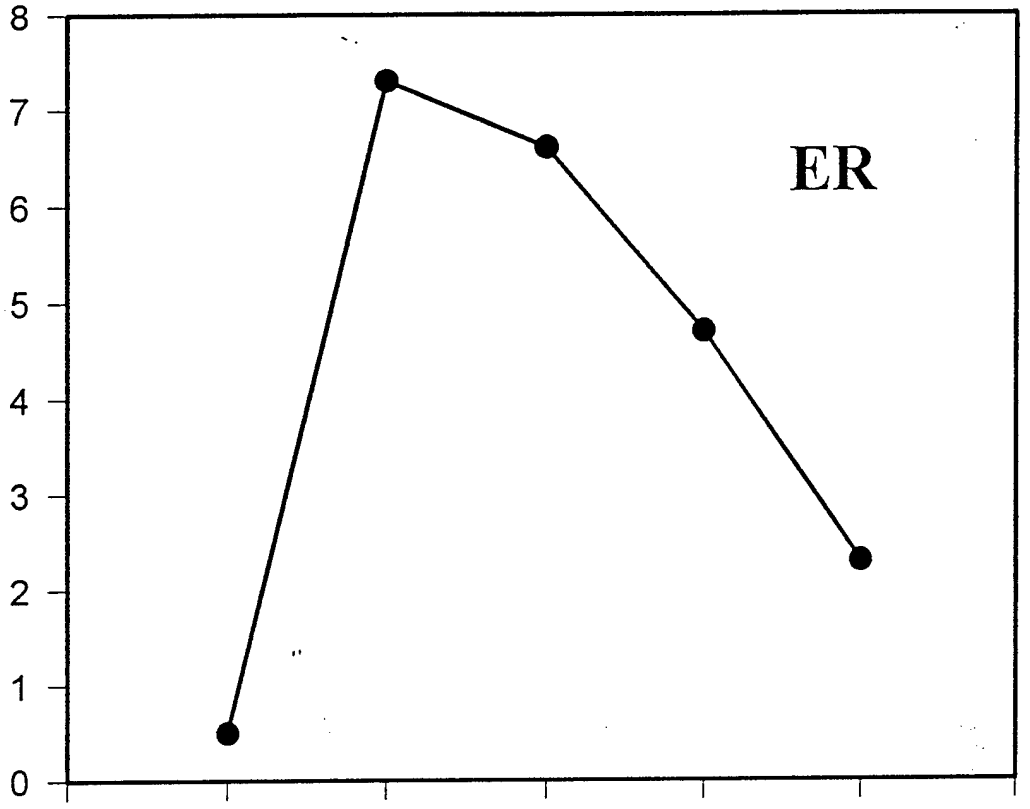

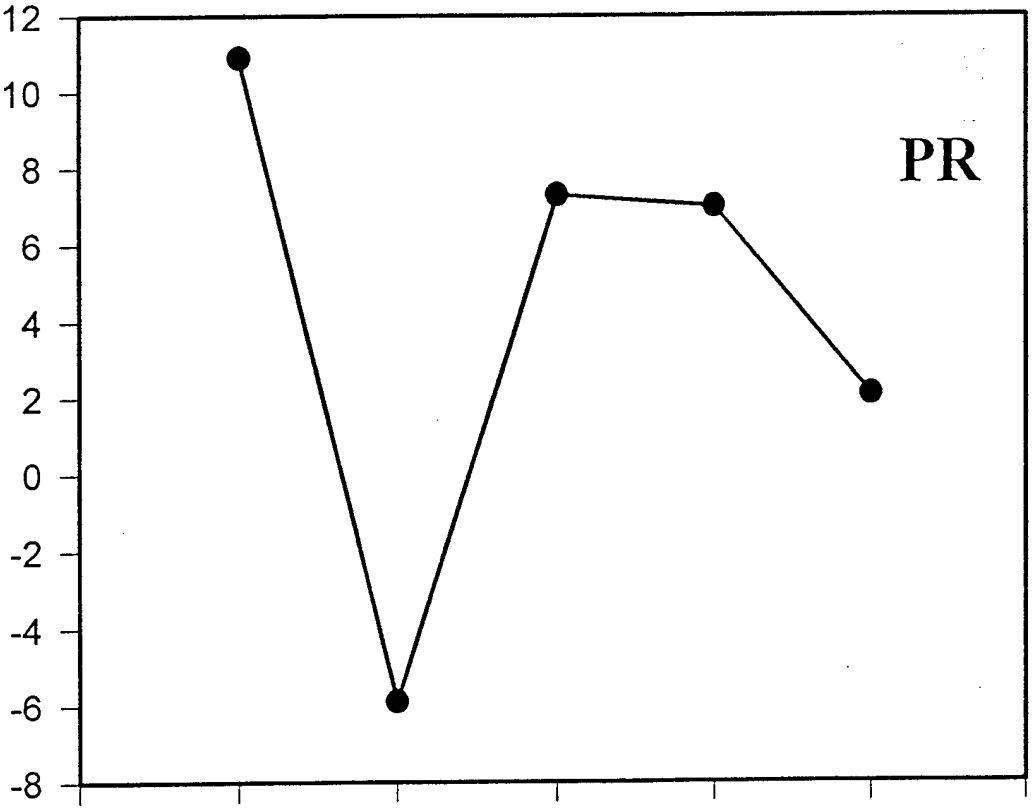

J. Clin. Invest. (in press)

Aberrant NF-κB/Rel Expression and the Pathogenesis of Breast Cancer

Mika A. Sovak*, Robert E. Bellas@, Dong W. Kim@, Gregory J. Zanieski@, Adrianne E. Rogers*, Abdulmaged M. Traish@ and Gail E. Sonenshein@τ

from the Departments of Pathology and Laboratory Medicine* and Biochemistry@, and the Program in Research on Women's Health, Boston University School of Medicine, 80 East Concord Street, Boston, MA 02118

Running Title: NF-κB/Rel Expression in Breast Cancer

τCorresponding author. Mailing address: Department of Biochemistry, Boston University Medical School, 80 East Concord St., Boston, MA 02118-2394. Phone: (617) 638-4120. Fax: (617) 638-5339. Electronic mail address: gsonensh@acs.bu.edu.

Abstract

Expression of Nuclear Factor-κB(NF-κB)/Rel transcription factors has recently been found to promote cell survival, inhibiting the induction of apoptosis. In most cells other than B lymphocytes, NF-κB/Rel is inactive, sequestered in the cytoplasm. For example, nuclear extracts from two human untransformed breast epithelial cell lines expressed only very low levels of NF-κB. Unexpectedly, nuclear extracts from two human breast tumor cell lines displayed significant levels of NF-κB/Rel. Direct inhibition of this NF-κB/Rel activity in breast cancer cells induced apoptosis. High levels of NF-κB/Rel binding were also observed in carcinogen-induced primary rat mammary tumors, whereas only expectedly low levels were seen in normal rat mammary glands. Furthermore, multiple human breast cancer specimens contained significant levels of nuclear NF-κB/Rel subunits. Thus, aberrant nuclear expression of NF-κB/Rel is associated with breast cancer. Given the role of NF-κB/Rel factors in cell survival, this aberrant activity may play a role in tumor progression, and represents a possible therapeutic target in the treatment of these tumors.

Keywords: Apoptosis/Aromatic hydrocarbons/7,12-dimethylbenz(*a*)anthracene/ Rat model/Transcription factors

Introduction

The incidence of breast cancer has been steadily increasing over the past 50 years, and is now one of the leading causes of death among American women between the ages of 40-55 (1). In an attempt to find the causes of this increased incidence, both genetic and environmental factors are being studied. Attention has recently focused on the mechanism by which increased exposure to and bioaccumulation of pollutants might have an etiologic role in breast cancer (2-5). The polycyclic aromatic hydrocarbons (PAHs)[1] such as 7,12-dimethylbenz(*a*)anthracene (DMBA) are specifically of interest with respect to breast cancer (4). The most proximal event in PAH tumorigenesis is the binding of the chemicals to a cytosolic aromatic hydrocarbon receptor (AhR) (6-8). The receptor-ligand complex is translocated to the nucleus where it can bind to and alter the transcriptional activity of DNA that has AhR-responsive elements. One battery of enzymes whose transcriptional induction is a hallmark of DMBA and other PAH exposure is the Phase I cytochrome P450 enzymes (9-12). These enzymes aid in the oxidative metabolism of both endogenous substances such as steroids, as well as in the breakdown of exogenous substances such as drugs, chemical carcinogens, and environmental pollutants. The products formed by this oxidative metabolism are often reactive oxygen intermediates. The potential for increased levels of oxidative stress within the cell resultant from exposure to environmental carcinogens led us to

[1] *Abbreviations used in this paper:* AhR, Aromatic hydrocarbon receptor; BSAP; B cell specific activator protein; CAT, chloramphenicol acetyl transferase; dm, double mutant; DMBA, 7,12-dimethylbenz(*a*)anthracene; EMSA, electrophoretic mobility shift analysis; GST, glutathione-S-transferase; IκB-α, NF-κB/Rel inhibitor-α; NF-κB, Nuclear Factor-κB; PAH, polycyclic aromatic hydrocarbon; RHD, Rel homology domain; URE, upstream regulatory element.

hypothesize that this might activate expression of the NF-κB/Rel family of transcription factors.

NF-κB/Rel is a family of dimeric transcription factors whose DNA binding domains have considerable homology with an approximately 300 amino acid region of the v-Rel oncoprotein and was thus termed the Rel homology domain (RHD) (13-15). Classical NF-κB is a heterodimer composed of a 50 kDa (p50) and a 65 kDa (p65 or RelA) subunit (16). Other members of the mammalian Rel family include c-Rel, p52, and RelB (16-19). The activity of many of these factors is controlled post-translationally by their subcellular localization. In most cells other than mature B lymphocytes, NF-κB/Rel proteins are sequestered as inactive forms in the cytoplasm by association with inhibitory proteins, termed IκB's, for which IκB-α represents the prototype (16, 20-22). Activation involves IκB degradation, and nuclear translocation of the NF-κB/Rel protein. Many signals that activate NF-κB/Rel do so through a final common pathway of increasing cellular oxidative stress (23). Genes regulated by NF-κB/Rel include those involved in immune and inflammatory responses, cellular proliferation, and adhesion molecules (16, 20, 21). More recently NF-κB/Rel has been implicated in control of apoptosis. For example, we have shown that inhibition of constitutive expression of NF-κB/Rel in B cell lymphomas leads to the induction of apoptosis, and that ectopic c-Rel expression promotes cell survival (24, 25). Recently we have obtained similar data with two untransformed hepatocyte cell lines, which express classical NF-κB constitutively (26,27). Activation of NF-κB/Rel by TNF-α has recently been linked to protection of multiple types of cells from apoptosis (28-31). Here we report that NF-κB/Rel is aberrantly activated in human breast cancer and in rat mammary tumors from the aromatic hydrocarbon induced model of breast cancer. Inhibition of this activity in human breast cancer cell lines leads

to apoptosis. These results suggest an important role for NF-κB/Rel in the pathogenesis of breast cancer and in potential treatment modalities.

Methods

Cell lines. The MCF7 cell line, the prototype of estrogen-dependent breast cancer cells, was established from the pleural effusion of a patient with metastatic adenocarcinoma (33). The 578T tumor cell line was established from a patient with infiltrating ductal carcinoma and does not express estrogen receptors (33); normal breast tissue from this same patient was taken to establish the untransformed breast cell line 578Bst (33). The MCF 10F cell line was established from mammary tissue from a patient with fibrocystic breast disease and is also estrogen receptor negative (34, 35).

Electrophoretic Mobility Shift Analysis. Nuclear extracts for electrophoretic mobility shift analyses (EMSA) were prepared by the method of Dignam et al. (36). URE (5'-GATCCAAGTCCGGGTTTTCCCCAACC-3'; core sequence is underlined) (37), and PU.1 (GATCTACTTCTGCTTTTG, where the core element is underlined) oligonucleotides were end labeled with large Klenow fragment of DNA polymerase and [^{32}P]dNTPs. The electrophoretic mobility shift assay was performed using approximately 2 ng of labeled oligonucleotide (20,000 dpm), 5 μg of nuclear extract, 5 ul of sample buffer (10mM HEPES, 4mM dithiothreitol, 0.5% Triton X-100, and 2.5% glycerol), 2.5 ug poly dI-dC as nonspecific competitor and adjusted to 100 mM with KCl in a final volume of 25 ul. This mixture was incubated at room temperature for 30 min. Complexes were resolved in a 4.5% polyacrylamide gel using 0.5x TBE running buffer (90 mM Tris, 90 mM boric acid, 2 mM EDTA pH 8.0). Specificity of binding was tested using

competition analyses in which 10-fold molar excess of wild type or double mutant URE (URE 1, see below) was added to a binding reaction. For IκB-α blocking experiments, 1 ug of IκB-α-GST fusion protein was added to the reaction after the 30 min incubation, and the mixture allowed to incubate for an additional 1-2 h at 4°C.

Microinjection analysis. Exponentially growing 578T cells were plated on tissue culture dishes. After 24 hours, the medium was supplemented with 20 mM HEPES (pH 7.3) to maintain pH when exposed to open air. All cell nuclei in a defined grid were microinjected at 1.4 psi at a rate of approximately 20 cells per minute as described previously (38). Successful microinjection was estimated to occur more than 90% of the time. Purified IκB-α-glutathione-S-transferase (IκB-α-GST), kindly provided by U. Siebenlist, or GST protein was used at 1 ug/ul. Affinity purified antibodies to p65 or c-Rel, SC109 and SC070, respectively (Santa Cruz Biotechnology) were used at 4 ug/ul in the absence or presence of 4 ug/ul cognate peptide. Double-stranded oligonucleotides were microinjected at a concentration of 200 ng/μl. Oligonucleotides used were: NF-κB, wild type element from the immunoglobulin κ light chain enhancer (39); wt URE, see above; UREm1 (5'-GATCCAAGTCCGCCTTTTCCCCAACC-3') and UREm2 (5'-GATCCAAGTCCGGGTTGGCCCCAACC-3'), mutant forms of the URE κB element (mutated bases are indicated in bold), which fail to bind NF-κB factors.

Cells were stained with 10 ug/ml propidium iodide (Sigma), 0.1% Triton X-100, 50 ug/ml RNase A in PBS for 15 minutes and visualized on a Nikon Optiphot Fluorescence microscope and fluorescent images recorded at 200x using Kodak Tmax 3200 film. For trypan blue analysis, cloning rings were placed over the microinjected areas. At various time points after microinjection, the supernatant containing cells that lost adherence during incubation were

transferred to a 96-well plate for trypan blue analysis. The adherent cells were removed by trypsinization and added to the same well. Trypan blue was added to 0.04% and the plate incubated at 37°C. After 30 minutes, the percentage of positively staining cells was determined by microscopic visualization at 100X magnification under brightfield illumination.

Transfection analysis. 578T and MCF7 cells were transfected using the modified calcium phosphate procedure of Chen and Okayama (40) as we have described previously (41). The total amount of plasmid DNA transfected into the cells was adjusted to 25 ug using either pBlueScript or pUC19 plasmid DNA where necessary. Results were normalized to a TK-luciferase construct and are presented as percent of URE_2-TK-CAT or p1.6 Bgl-CAT wt activity (mean $\pm$ SD), which have been set at 100%. Data shown are representative of three independent experiments.

Rat mammary gland and tumor analysis. Virgin female Sprague-Dawley rats fed AIN76 diet were treated according to a protocol approved by the Boston University Institutional Animal Care and Use Committee. Animals were given a single intragastric dose of 15 mg/kg DMBA at 8 weeks of age. Tumors, which were first detected by palpation after 7 weeks, were rapidly removed at necropsy following sacrifice by CO_2 inhalation. Normal mammary glands, similarly excised from untreated control rats, and tumors were frozen in liquid nitrogen. Animals were sacrificed 16 weeks post DMBA treatment at 24 weeks of age, except when tumors appeared ulcerated. Samples were pulverized on dry ice using a Bessman Tissue Pulverizer (Spectrum). Frozen tissue powder was homogenized (0.5g/ml) in TEGT/MO buffer [50 mM Tris/HCl, 1 mM EDTA, 10% (v/v) glycerol, 10 mM monothioglycerol, 10 mM sodium molybdate, pH 7.4 containing 0.02% sodium azide] using a Polytron. After the initial burst proteolytic inhibitors were added to a final concentration of: 0.5 mM PMSF, 1 ug/ml leupeptin, 100 ug/ml aprotinin, 10 ug/ml pepstatin and

100 ug/ml bacitracin. Homogenates were centrifuged for 10 min at 3,000 rpm at 2°C. Nuclear pellets were extracted via the procedure of Dignam et al. (36) and analyzed as described above.

Human breast cancer specimen analysis. Primary human breast cancer tissue, obtained with IRB approval, was frozen in dry ice and stored frozen until samples were processed for nuclear protein extraction. Nuclear pellets were obtained as described above and washed twice with TEGT/MO buffer and proteins extracted in TEGT/MO buffer plus protease inhibitors adjusted to 0.4 M KCl for 45 min. The debris was removed by centrifugation at 30,000 rpm and the nuclear extract stored frozen. For immunoblot analysis, 20-100 ug of protein were resolved on a 10% polyacrylamide gel and transferred to a 0.45-um pore PVDF membrane (Millipore). Blots were blocked for one hour at room temperature in 5% milk (Carnation) in Tris-buffered saline (TBS), then probed with antibody diluted (1:1000) in 5% milk in TBS for 1 hour at room temperature. After 3 washes in 0.5% NP-40 in TBS, blots were incubated in secondary horseradish peroxidase (HRP)-conjugated goat anti-rabbit antibody at 1:1000 dilution for 1 hour at room temperature. Bands were visualized by chemiluminescence.

Results

Human breast epithelial tumor cell lines constitutively express high levels of functional nuclear NF-κB/Rel activity. To begin to analyze the role of NF-κB/Rel in regulation of epithelial cell proliferation, we performed EMSA on nuclear extracts of untreated, exponentially growing breast tumor and untransformed breast epithelial cell lines to assess basal NF-κB/Rel binding activity. The oligonucleotide containing the NF-κB upstream regulatory element (URE) from the c-*myc* gene (37) was employed as probe; this oligonucleotide has been shown to bind multiple NF-κB/Rel complexes efficiently (41-44). Significant levels of nuclear NF-κB/Rel complexes were detected in MCF7 (32) and 578T (33) human breast tumor cell lines, but not in untransformed MCF 10F (34, 35) and 578Bst (33) breast epithelial cell lines (Fig. 1A). This finding was unexpected since nuclear NF-κB/Rel is thought to be restricted primarily to B lymphocytes (16, 21, 39). Nuclear extracts from MCF7 cells displayed several complexes that resolved as a broad lower band and a faint upper band. The ratio and intensity of these two bands varied with different isolates of this line (compare Figs. 1A and 2B, and data not shown), which is known to change phenotype in culture. Multiple complexes were also seen with nuclear extracts from 578T cells. Nuclear extracts from the untransformed MCF 10F and 578Bst cell lines displayed only very low levels of NF-κB/Rel binding, as expected. The bands observed with all cell lines tested comigrated with complexes obtained using nuclear extracts from WEHI 231 B lymphoma cells (data not shown), a cell line known to express high levels of NF-κB/Rel (37, 39, 44). Binding specificity of these proteins to URE was confirmed by successful competition with 10-fold excess unlabeled wild type oligonucleotide, whereas excess unlabeled mutant oligonucleotide essentially had no effect on binding (Fig. 1B and data not shown).

Transient transfection analyses were performed to test functional Rel activity in the tumor lines. The URE_2-TK-CAT wild type (wt) and URE_2-TK-CAT double mutant (dm) constructs have 2 copies of the URE NF-κB binding element from the c-*myc* gene in either wild type or mutant form, respectively, linked to the heterologous thymidine kinase (TK) promoter and the chloramphenicol acetyltransferase reporter gene (CAT) (37). Cultures of 578T cells at 70% confluence were transiently transfected in duplicate (Fig. 2A). The wild type element vector gave approximately 7-fold higher levels of activity than the double mutant; an average of 9 ± 2-fold higher levels of activity were obtained in 6 experiments. A similar value of 11 ± 3-fold (n= 6) was obtained using MCF7 cells. To further confirm the observed transactivation was indeed due to constitutive NF-κB/Rel activity, cells were cotransfected in duplicate with URE_2-TK-CAT wt and increasing amounts of an IκB-α expression vector (45). A decrease in relative CAT activity of the wild type construct to that of the double mutant vector was observed upon cotransfection of as little as 3 ug of the IκB-α vector, indicating that the observed activity of the URE_2-TK-CAT wt construct was due to constitutively functional NF-κB/Rel in the cells (Fig 2A). Similarly, cotransfection of MCF7 cells was performed with a natural promoter construct responsive to NF-κ B, the c-*myc* promoter/exon1 p1.6 Bgl-CAT construct (46). Increasing concentrations of the IκB-α expression vector brought the activity of the wild type construct down to that of the construct with mutated NF-κB elements (Fig. 2B). Consistent with the effects of the inhibitor in transient transfection, addition of IκB-α-GST protein to the binding reactions with nuclear extracts from either transformed cell line abrogated formation of the upper complexes and significantly reduced the level of the more rapidly migrating complex (insets, Figs. 2A and B). This finding is expected as IκB-α protein has been shown to prevent binding via selective interaction with p65, c-Rel and

RelB (present in slower migrating complexes); inhibition of binding of p50 or p52 appears to require somewhat higher concentrations of inhibitor protein (rev. in 16). Lastly, the specific activation of NF-κB/Rel binding as opposed to a general elevation in B cell transcription factors was confirmed by EMSA for the Ets transcription factor member PU.1, expressed predominantly in B lymphocytes and myeloid cells (47-49). No PU.1 binding was observed with nuclear extracts from the breast epithelial cell lines, whereas binding of nuclear extracts from the Burkitt lymphoma Raji B cells to the PU.1 oligonucleotide was easily detected (Fig. 1C). Similarly, we failed to detect binding of the B-cell-specific activator protein (BSAP) with nuclear extracts from the untransformed or transformed breast epithelial lines (50) (data not shown). Thus, MCF7 and 578T breast cancer cells have selectively activated constitutive nuclear NF-κB/Rel factors.

Inhibition of the constitutive NF-κB/Rel activity in 578T cells induces apoptosis. Recently, we demonstrated that NF-κB/Rel rescues immature B lymphoma cells and hepatocytes from undergoing apoptosis (24-27) and a similar role in cell survival has been demonstrated upon its induction following TNF-α treatment of various cell lines (28-31). If the aberrant NF-κB/Rel expression we detect in breast cancer cells plays a similar role, specific inhibition of its activity should result in cell death. Thus, we used a microinjection strategy to selectively inhibit NF-κB/Rel expression in breast cancer cells. Areas of approximately 4 mm^2 were defined and all 578T breast cancer cells within the grid were microinjected with either the specific NF-κB/Rel inhibitory IκB-α-GST fusion protein or GST protein alone as control. After 3.5 hours, the nuclear morphology of the cells was examined by microscopic observation following staining with propidium iodide. Nuclear condensation, a hallmark of apoptosis, was clearly visualized in a field of cells microinjected with IκB-α-GST protein (Fig. 3A, left bottom panel), but not with GST

protein or in non-injected cells (Fig. 3A, top panels). Typical cells with condensed chromatin after microinjection of IκB-α-GST are shown in Fig. 3A (right bottom panel). A marked drop in cell density with time was noted following microinjection with IκB-α-GST protein but not control GST protein, possibly reflective of the observation that cells undergoing apoptosis detach and float off the dish surface.

To obtain more quantitative analysis, trypan blue staining was used as a measure of cell viability following microinjection with IκB-α-GST or GST protein, as above, or with affinity purified antibodies to either the p65 or c-Rel subunit. We noted that the adherent cell density was reduced by about 50-60% after injection with IκB-α-GST (Fig 3A), whereas only 4-5% of the cell population injected with GST protein alone lost adherence (data not shown). Therefore, non-adherent and adherent cells were combined and analyzed for loss of cell viability 20-22 hours after microinjection (Fig. 3B). Twenty percent of the cells microinjected with IκB-α-GST stained positive for trypan blue, compared to less than 3% of cells microinjected with GST or non-microinjected cells. Thus, IκB-α-mediated inhibition of NF-κB/Rel caused death of 578T breast cancer cells by apoptosis. In a preliminary supershift EMSA analysis, 578T cells were found to express significant levels of p65 whereas only low levels of c-Rel subunits were detected (data not shown). Microinjection with an affinity purified antibody to p65 induced cell death in approximately 45% of 578T cells within 20-22 hrs, which was inhibited by preincubation of the antibody with 40-fold molar excess of its cognate peptide (Fig. 3B). In contrast, microinjection of the antibody against c-Rel induced only modest additional loss of cell viability over background levels seen with microinjection with GST protein alone.

To further evaluate the effects of specific inhibition of NF-κB/Rel activity, we also monitored loss of cell viability after microinjection of double-stranded (ds) oligonucleotides

harboring either wild type or mutated NF-κB elements. Recent studies have demonstrated that microinjection of ds oligonucleotides containing a transcription factor binding site can compete *in vivo* and inhibit the activity of the factor (51, 52). Microinjection of oligonucleotides containing the wild type element from the κ light chain enhancer (κB) or from the c-*myc* gene (URE) induced significant levels of apoptosis within 20 hrs (Fig. 3C). In contrast, microinjection of oligonucleotides containing two mutations of the URE (UREm1 and UREm2) that prevent binding of NF-κB/Rel factor (41) did not significantly increase cell death above background levels seen with uninjected cells. In summary, selective inhibition of NF-κB/Rel activity by these three different strategies resulted in apoptosis of 578T breast cancer cells.

DMBA-induced rat mammary tumors express high levels of nuclear NF-κB/Rel binding activity. To verify that the observed nuclear expression of NF-κB/Rel factor complexes in the breast cancer cell lines was not the result of *in vitro* cell culturing, we have extended these observations to a widely used *in vivo* rat model of breast cancer. Treatment of female Sprague-Dawley rats with a single dose of the polycyclic aromatic hydrocarbon DMBA results in the induction of mammary gland (breast) tumors within 7-20 weeks (53). These tumors are generally well-differentiated and retain their hormonal responsiveness. Nuclear extracts were prepared from multiple DMBA-induced rat mammary tumors and from normal mammary glands from untreated rats as controls. High levels of binding to the URE NF-κB oligonucleotide, essentially comparable to that seen with WEHI 231 B cells, were obtained with nuclear extracts from 86% of the 35 tumor specimens analyzed (Fig. 4A, lanes T1-T4 and data not shown). In contrast, no significant levels of NF-κB/Rel binding were observed with nuclear extracts from the normal mammary gland, as expected (Fig. 4A, lanes N1-N3 and data not shown). The specificity of the NF-κB/Rel binding

was confirmed by competition with excess unlabelled oligonucleotides containing wild type but not mutant NF-κB elements and the ability of an antibody against the p50 subunit and addition of I κB-α-GST protein to significantly ablate binding activity (Fig. 4B). No binding to the PU.1 oligonucleotide was seen with nuclear extracts from either normal mammary gland or mammary tumors (Fig. 4C). These results indicate that the observed NF-κB/Rel binding is not due to contaminating B cells. Thus, NF-κB/Rel expression is selectively induced *in vivo* within rat mammary gland tumors but is not present normally in mammary glands, suggesting a significant association between the activation of NF-κB/Rel expression and mammary tumor formation.

Nuclei of primary human breast tumor specimens contain NF-κB/Rel subunits. To determine whether NF-κB/Rel factors are constitutively expressed in nuclei of primary human breast cancer tissue, samples procured following surgical removal of breast tumors were analyzed for potential NF-κB/Rel subunit expression by immunoblotting. Nuclear extracts from 13 patient tumor samples were tested with an antibody against the p65 subunit (#1226 (54), kindly provided by N. Rice, NCI, Frederick MD) (Fig. 5A and data not shown). Eight tumors had detectable levels of a band that comigrated with the p65 subunit derived from 578T cells. A second antibody against p65 (SC372, Santa Cruz Biotechnology) was used with its cognate peptide to confirm the specificity of the positive signal seen with the tumor samples (data not shown). Detection of p65 in the nuclear extracts is not due to contamination with cytoplasmic proteins as nuclear extracts from 8 tumors were tested and found negative for the cytoplasmic IκB-α protein (data not shown). Overall, nuclear extracts from 15 of 23 specimens displayed positive staining for p65: 8 of 13 specimens were found positive using the #1226 antibody (and 4 confirmed with SC372) and 7 of 10 specimens were positive using the SC372 antibody (Table 1).

Expression of the c-Rel subunit was also assessed by immunoblotting (Fig. 5B). A band that migrated marginally slower than the mouse c-Rel protein was detected with antibody SC070 (Santa Cruz Biotechnology), which was competed away upon addition of cognate peptide (data not shown). Of 23 specimens tested, 20 were found to contain nuclear c-Rel protein (Fig. 5B and data not shown); the level of this expression was in many cases comparable to that seen in WEHI 231 cells, which express very high levels of this subunit (37, 39). In addition, nuclear extracts from tumors contained significant levels of the p50 subunit (Fig. 5C and data not shown), which was shown to be specific by successful competition with cognate peptide (data not shown). Overall, 19 of 21 tumors were positive for this subunit. The absence of detectable p105 precursor, as seen in the cytoplasmic extracts of WEHI 231 B cells (WEHI c), further confirms the absence of cytoplasmic contamination of these nuclear extracts (Fig. 5C). The results, summarized in Table 1, indicate that most primary human breast cancer tissue samples express the transactivating p65 and/or c-Rel subunits of NF-κB/Rel. Some samples were negative for both subunits; however, a more complete analysis of breast tumors for all of the NF-κB/Rel subunits may reveal the presence of additional subunits. Preliminary EMSA, which is more sensitive than immunoblotting, has confirmed variable levels of NF-κB/Rel binding in multiple human patient samples (data not shown). Overall, these findings indicate that the nuclear localization of NF-κB/Rel expression is a characteristic of human breast tumor cell lines, DMBA-induced rat mammary tumors and primary human breast cancer tissue.

Discussion

We have analyzed three different systems of breast cancer: *in vitro* human breast cancer cell lines, an *in vivo* rat model of breast cancer, and human tissue samples from primary breast tumors. All three have revealed an association between activated NF-κB/Rel and breast cancer. Direct inhibition of the functional NF-κB/Rel factors expressed in 578T cells by microinjection of IκB-α protein, an antibody to the p65 subunit, or ds oligonucleotides containing NF-κB elements led to induction of death of these cells via apoptosis. This study extends our recent work demonstrating that inhibition of the normal constitutive NF-κB/Rel activity in B cell lymphomas leads to cell death (24, 25), to breast cancer where NF-κB/Rel has been aberrantly activated. Our findings suggest that down-regulation of NF-κB/Rel may be useful in the treatment of this disease. Many antioxidants such as pentoxifylline (55) and N-acetyl cysteine (56), which are already in clinical use, have been found to repress NF-κB/Rel activity. Preliminary evidence suggests that these agents have significant inhibitory effects on proliferation of breast cancer cells in culture (unpublished observations). Thus, while the efficacy of a specific agent may depend on the nature of the NF-κB/Rel and IκB subunits expressed, our studies suggest NF-κB/Rel is a novel therapeutic target for the treatment of breast cancer.

There has been a steady increase in the incidence of breast cancer over the last several decades, and it has been proposed that this may reflect an increased exposure to environmental carcinogens such as DMBA (5, 57, 58). Our study of DMBA-induced tumors in rats shows an association between DMBA exposure, breast tumor formation and activation of NF-κB/Rel. It has been proposed that carcinogens promote tumor progression through DNA damage. The activation of NF-κB/Rel in the tumors, which would promote cell survival, suggests an additional indirect

effect of this carcinogen on tumor progression. The mechanism of NF-κB/Rel activation by DMBA remains to be determined. As discussed above, however, a hallmark of DMBA exposure is an increase in P450 enzyme levels with a resultant increase in oxidative stress, which is known to activate NF-κB/Rel (11, 23, 59).

We have recently reported that ectopic expression of c-Rel in WEHI 231 B cells leads to extensive protection from apoptosis induced by engagement of surface immunoglobulin, treatment with TGF-β1, or addition of the protease inhibitor TPCK (24, 25). Ectopic c-Rel expression plays a similar role in protection of hepatocytes from TGF-β1-induced cell death (26). Furthermore, inhibition of endogenous p50/p65 NF-κB activity within these hepatocytes leads to cell death via apoptosis (27). Thus, the finding that many of the breast cancer specimens express c-Rel and p65 suggests that NF-κB/Rel factors play a similar role as a survival gene in these tumors. The primary target(s) of these factors remain a major question. Candidate genes include the known anti-apoptotic genes, Bcl-2 and Bcl-X_L. One additional candidate for target is the c-*myc* gene, which is extensively regulated through its two NF-κB/Rel elements (42, 44, 46). Recently, we have shown that ectopic c-*myc* expression protects against apoptosis of B cells (60). Interestingly, studies on patient material and transgenic mice have implicated overexpression of the c-*myc* gene in the etiology of breast cancer (61-66). In human breast cancer, analysis of tumors shows an association between overexpression of the c-*myc* gene and poor prognosis, especially in node-negative patients (61, 62, 67, 68). These findings raise the possibility that the activation of c-*myc* gene by NF-κB may serve to promote both tumor cell protection from apoptosis as well as neoplastic transformation.

With the expanded use of sensitive mammographic and tissue sample screening procedures, there has been a significant rise in detection of potentially premalignant lesions. The prevalence of benign breast conditions or fibrocystic changes is estimated at over 85% in women in the U.S. Approximately one third of U.S. women undergo breast biopsies; the vast majority of these biopsies show benign disease that are not associated with an increased risk of cancer (69). The quest for markers to positively identify which of these lesions will progress to malignancy is critical to help develop strategies for treatment of benign breast disease and to improve early detection of breast cancer. Nuclear NF-κB/Rel expression is associated with neoplastic breast tissue in both human and laboratory rats. Studies are underway to elucidate any association between the stages of neoplastic transformation and expression of NF-κB/Rel factors as markers of disease.

Acknowledgments. We thank M. Fenton, U. Siebenlist, and N. Rice for generously providing PU.1 oligonucleotide, purified IκB-α protein and expression vector, and NF-κB/Rel specific antibodies, respectively. We gratefully acknowledge M. Arsura for providing extracts and helpful discussions. This work was supported by grants from the National Institutes of Health Grant (G.E.S.), Department of Army Grant (G.E.S.), Commonwealth of Massachusetts Department of Public Health Grant (M.A.S.), and the Tea Trade Health Research Association.

References

1. Harris, J. R., M. E. Lippman, U. Veronesi, and W. Willett. 1992. Breast cancer (1). *New Eng. J. Med.* 327:319-328.

2. DiAugustine, R., and D. L. Davis. 1993. A holistic approach to breast cancer. *Env. Health Persp.* 101:116-120.

3. Falck, F., Jr., A. Ricci, Jr., M. S. Wolff, J. Godbold, and P. Deckers. 1992. Pesticides and polychlorinated biphenyl residues in human breast lipids and their relation to breast cancer. *Arch. Env. Health.* 47:143-146.

4. Morris, J. J., and E. Seifter. 1992. The role of aromatic hydrocarbons in the genesis of breast cancer. *Med. Hypoth.* 38:177-184.

5. Wolff, M. S., P. G. Toniolo, E. W. Lee, M. Rivera, and N. Dubin. 1993. Blood levels of organochlorine residues and risk of breast cancer. *J. Nat. Cancer Inst.* 85:648-652.

6. Burbach, K. M., A. Poland, and C. A. Bradfield. 1992. Cloning of the Ah-receptor cDNA reveals a distinctive ligand-activated transcription factor. *Proc. Nat. Acad. Sci. USA.* 89:8185-8189.

7. Ema, M., K. Sogawa, N. Watanabe, Y. Chujoh, N. Matsushita, O. Gotoh, Y. Funae, and Y. Fujii-Kuriyama. 1992. cDNA cloning and structure of mouse putative Ah receptor. *Biochem. Biophys. Res. Comm.* 184:246-253.

8. Safe, S. 1984. Polychlorinated biphenyls (PCBs) and polybrominated biphenyls (PBBs): biochemistry, toxicology, and mechanism of action. *Crit. Rev. Tox.* 13:319-395.

9. Buening, M. K., R. L. Chang, M. T. Huang, J. G. Fortner, A. W. Wood, and A. H. Conney. 1981. Activation and inhibition of benzo(a)pyrene and aflatoxin B1 metabolism in human liver microsomes by naturally occurring flavonoids. *Cancer Res.* 41:67-72.

10. Le Bon, A. M., M. H. Siess, and M. Suschetet. 1992. Inhibition of microsome-mediated binding of benzo[a]pyrene to DNA by flavonoids either in vitro or after dietary administration to rats. *Chem.-Bio. Inter.* 83:65-71.

11. Nebert, D. W., and F. J. Gonzalez. 1987. P450 genes: structure, evolution, and regulation. *Ann. Rev. Biochem.* 56:945-993.

12. Nebert, D. W., D. D. Petersen, and A. J. Fornace, Jr. 1990. Cellular responses to oxidative stress: the [Ah] gene battery as a paradigm. *Env. Health Persp.* 88:13-25.

13. Ghosh, S., A. M. Gifford, L. R. Riviere, P. Tempst, G. P. Nolan, and D. Baltimore. 1990. Cloning of the p50 DNA binding subunit of NF-κB: homology to *rel* and *dorsal*. *Cell.* 62:1019-1029.

14. Kieran, M., V. Blank, F. Logeat, J. Vandekerckhove, F. Lottspeich, O. Le Bail, M. B. Urban, P. Kourilsky, P. A. Baeuerle, and A. Israel. 1990. The DNA binding subunit of NF-κB is identical to factor KBF1 and homologous to the rel oncogene product. *Cell.* 62:1007-1018.

15. Ruben, S. M., P. J. Dillon, R. Schreck, T. Henkel, C. H. Chen, M. Maher, P. A. Baeuerle, and C. A. Rosen. 1991. Isolation of a rel-related human cDNA that potentially encodes the 65-kD subunit of NF-κB. *Science*. 251:1490-1493.

16. Grilli, M., J. J. Chiu, and M. J. Lenardo. 1993. NF-κB and Rel: participants in a multiform transcriptional regulatory system. *Internat. Rev. Cytol.* 143:1-62.

17. Gilmore, T. D. 1991. Malignant transformation by mutant Rel proteins. *Trends in Genetics*. 7:318-322.

18. Schmid, R. M., N. D. Perkins, C. S. Duckett, P. C. Andrews, and G. J. Nabel. 1991. Cloning of an NF-κB subunit which stimulates HIV transcription in synergy with p65. *Nature*. 352:733-736.

19. Ryseck, R. P., P. Bull, M. Takamiya, V. Bours, U. Siebenlist, P. Dobrzanski, and R. Bravo. 1992. RelB, a new Rel family transcription activator that can interact with p50-NF-κB. *Mol. Cell. Biol.* 12:674-684.

20. Baeuerle, P. A. 1991. The inducible transcription activator NF-κB: regulation by distinct protein subunits. *Biochem. Biophys. Acta.* 1072:63-80.

21. Blank, V., P. Kourilsky, and A. Israel. 1992. NF-κB and related proteins: Rel/dorsal homologies meet ankyrin-like repeats. *Trends Biochem. Sci.* 17:135-140.

22. Verma, I. M., J. K. Stevenson, E. M. Schwarz, D. Van Antwerp, and S. Miyamoto. 1995. Rel/NF-κB/IκB family: intimate tales of association and dissociation. *Genes and Dev.* 9:2723-2735.

23. Baeuerle, P. A., and T. Henkel. 1994. Function and activation of NF-κB in the immune system. *Ann. Rev. Immunol.* 12:141-179.

24. Wu, M., H. Lee, R. E. Bellas, S. L. Schauer, M. Arsura, D. Katz, M. J. FitzGerald, T. L. Rothstein, D. H. Sherr, and G. E. Sonenshein. 1996. Inhibition of NF-κB/Rel induces apoptosis of murine B cells. *EMBO J.* 15:4682-4690.

25. Arsura, M., M. Wu, and G. E. Sonenshein. 1996. TGF-β1 inhibits NF-κB/Rel activity inducing apoptosis of B cells: transcriptional activation of IκB-α. *Immunity*. 5:31-40.

26. Arsura, M., M. J. FitzGerald, N. Fausto, G.E. Sonenshein. 1997. NF-κB/Rel blocks transforming growth factor-β1-induced apoptosis of murine hepatocyte cell lines. *Cell Growth Diff.* (In press).

27. Bellas, R. E., M. J. FitzGerald, N. Fausto, G.E. Sonenshein. 1997. Inhibition of NF-κB activity induces apoptosis in murine hepatocytes. *Am. J. Path.* (In press).

28. Wang, C. Y., M. W. Mayo, and A. S. Baldwin, Jr. 1996. TNF-α and cancer therapy-induced apoptosis: potentiation by inhibition of NF-κB. *Science*. 274:784-787.

29. Van Antwerp, D. J., S. J. Martin, T. Kafri, D. R. Green, and I. M. Verma. 1996. Suppression of TNF-α-induced apoptosis by NF-κB. *Science*. 274:787-789.

30. Liu, Z. G., H. Hsu, D. V. Goeddel, and M. Karin. 1996. Dissection of TNF receptor 1 effector functions: JNK activation is not linked to apoptosis while NF-κB activation prevents cell death. *Cell*. 87:565-576.

31. Beg, A. A., and D. Baltimore. 1996. An essential role for NF-κB in preventing TNF-α-induced cell death. *Science*. 274:782-784.

32. Soule, H. D., J. Vazguez, A. Long, S. Albert, and M. Brennan. 1973. A human cell line from a pleural effusion derived from a breast carcinoma. *J. Nat. Cancer Inst.* 51:1409-1416.

33. Hackett, A. J., H. S. Smith, E. L. Springer, R. B. Owens, W. A. Nelson-Rees, J. L. Riggs, and M. B. Gardner. 1977. Two syngeneic cell lines from human breast tissue: the aneuploid mammary epithelial (Hs578T) and the diploid myoepithelial (Hs578Bst) cell lines. *J. Nat. Cancer Inst.* 58:1795-1806.

34. Calaf, G., and J. Russo. 1993. Transformation of human breast epithelial cells by chemical carcinogens. *Carcinogen.* 14:483-492.

35. Soule, H. D., T. M. Maloney, S. R. Wolman, W. D. Peterson, Jr., R. Brenz, C. M. McGrath, J. Russo, R. J. Pauley, R. F. Jones, and S. C. Brooks. 1990. Isolation and characterization of a spontaneously immortalized human breast epithelial cell line, MCF-10. *Cancer Res.* 50:6075-6086.

36. Dignam, J. D., R. M. Lebovitz, and R. G. Roeder. 1983. Accurate transcription initiation by RNA polymerase II in a soluble extract from isolated mammalian nuclei. *Nuc. Acids Res.* 11:1475-1489.

37. Duyao, M. P., A. J. Buckler, and G. E. Sonenshein. 1990. Interaction of an NF-κB-like factor with a site upstream of the c-*myc* promoter. *Proc. Nat. Acad. Sci. USA*. 87:4727-4731.

38. Bellas, R. E., J. S. Lee, and G. E. Sonenshein. 1995. Expression of a constitutive NF-κB-like activity is essential for proliferation of cultured bovine vascular smooth muscle cells. *J. Clin. Investig.* 96:2521-2527.

39. Sen, R., and D. Baltimore. 1986. Multiple nuclear factors interact with the immunoglobulin enhancer sequences. *Cell*. 46:705-716.

40. Chen, C., and H. Okayama. 1987. High-efficiency transformation of mammalian cells by plasmid DNA. *Mol. Cell. Biol.* 7:2745-2752.

41. Lawrence, R., L. J. Chang, U. Siebenlist, P. Bressler, and G. E. Sonenshein. 1994. Vascular smooth muscle cells express a constitutive NF-κB-like activity. *J. Biol. Chem.* 269:28913-28918.

42. La Rosa, F. A., J. W. Pierce, and G. E. Sonenshein. 1994. Differential regulation of the c-*myc* oncogene promoter by the NF-κB rel family of transcription factors. *Mol. Cell. Biol.* 14:1039-1044.

43. Kunsch, C., S. M. Ruben, and C. A. Rosen. 1992. Selection of optimal κB/Rel DNA-binding motifs: interaction of both subunits of NF-κB with DNA is required for transcriptional activation. *Mol. Cell. Biol.* 12:4412-4421.

44. Lee, H., M. Arsura, M. Wu, M. Duyao, A. J. Buckler, and G. E. Sonenshein. 1995. Role of Rel-related factors in control of c-*myc* gene transcription in receptor-mediated apoptosis of the murine B cell WEHI 231 line. *J. Exp. Med.* 181:1169-1177.

45. Brown, K., S. Gerstberger, L. Carlson, G. Franzoso, and U. Siebenlist. 1995. Control of IκB-α proteolysis by site-specific, signal-induced phosphorylation. *Science*. 267:1485-1488.

46. Duyao, M. P., D. J. Kessler, D. B. Spicer, C. Bartholomew, J. L. Cleveland, M. Siekevitz, and G. E. Sonenshein. 1992. Transactivation of the c-*myc* promoter by human T cell leukemia virus type 1 *tax* is mediated by NF-κB. *J. Biol. Chem.* 267:16288-16291.

47. Simon, M. C., M. Olson, E. Scott, A. Hack, G. Su, and H. Singh. 1996. Terminal myeloid gene expression and differentiation requires the transcription factor PU.1. *Curr. Top. Micro. & Immunol.* 211:113-119.

48. Moreau-Gachelin, F. 1994. Spi-1/PU.1: an oncogene of the Ets family. *Biochem. Biophys. Acta.* 1198:149-163.

49. Buras, J. A., W. R. Reenstra, and M. J. Fenton. 1995. NF-βA, a factor required for maximal interleukin-1β gene expression is identical to the ets family member PU.1. Evidence for structural alteration following LPS activation. *Molec. Immunol.* 32:541-554.

50. Michaelson, J. S., M. Singh, C. M. Snapper, W. C. Sha, D. Baltimore, and B. K. Birshtein. 1996. Regulation of 3' IgH enhancers by a common set of factors, including κB-binding proteins. *J. Immunol.* 156:2828-2839.

51. Lamb, N. J., A. Fernandez, N. Tourkine, P. Jeanteur, and J. M. Blanchard. 1990. Demonstration in living cells of an intragenic negative regulatory element within the rodent c-*fos* gene. *Cell.* 61:485-496.

52. Gilman, M. Z., L. A. Berkowitz, J. R. Feramisco, B. R. Franza, Jr., R. M. Graham, K. T. Riabowol, and W. A. Ryan, Jr. 1988. Intracellular mediators of c-*fos* induction. *Cold Spring Harbor Symposia on Quantitative Biology.* 53:761-767.

53. Rogers, A. E., and B. H. Conner. 1990. Dimethylbenzanthracene-induced mammary tumorigenesis in ethanol-fed rats. *Nut. Res.* 10:915-928.

54. Rice, N. R., and M. K. Ernst. 1993. In vivo control of NF-κB activation by IκB-α. *EMBO J.* 12:4685-4695.

55. Biswas, D. K., B. J. Dezube, C. M. Ahlers, and A. B. Pardee. 1993. Pentoxifylline inhibits HIV-1 LTR-driven gene expression by blocking NF-κB action. *J. AIDS.* 6:778-786.

56. Staal, F. J., M. Roederer, and L. A. Herzenberg. 1990. Intracellular thiols regulate activation of NF-κB and transcription of human immunodeficiency virus. *Proc. Nat. Acad. Sci. USA.* 87:9943-9947.

57. Manz, A., J. Berger, J. H. Dwyer, D. Flesch-Janys, S. Nagel, and H. Waltsgott. 1991. Cancer mortality among workers in chemical plant contaminated with dioxin. *Lancet.* 338:959-964.

58. Willett, W. 1989. The search for the causes of breast and colon cancer. *Nature*. 338:389-394.

59. Conney, A. H. 1982. Induction of microsomal enzymes by foreign chemicals and carcinogenesis by polycyclic aromatic hydrocarbons: G. H. A. Clowes Memorial Lecture. *Cancer Res.* 42:4875-4917.

60. Wu, M., M. Arsura, R. E. Bellas, M. J. FitzGerald, H. Lee, S. L. Schauer, D. H. Sherr, and G. E. Sonenshein. 1996. Inhibition of c-*myc* expression induces apoptosis of WEHI 231 murine B cells. *Mol. Cell. Biol.* 16:5015-5025.

61. Roux-Dosseto, M., S. Romain, N. Dussault, C. Desideri, L. Piana, P. Bonnier, N. Tubiana, and P. M. Martin. 1992. c-*myc* gene amplification in selected node-negative breast cancer patients correlates with high rate of early relapse. *Europ. J. Cancer*. 28A:1600-1604.

62. Berns, E. M., J. G. Klijn, W. L. van Putten, I. L. van Staveren, H. Portengen, and J. A. Foekens. 1992. c-*myc* amplification is a better prognostic factor than *Her2/neu* amplification in primary breast cancer. *Cancer Res.* 52:1107-1113.

63. Bonilla, M., M. Ramirez, J. Lopez-Cueto, and P. Gariglio. 1988. In vivo amplification and rearrangement of c-*myc* oncogene in human breast tumors. *J. Nat. Cancer Inst.* 80:665-671.

64. Leder, A., P. K. Pattengale, A. Kuo, T. A. Stewart, and P. Leder. 1986. Consequences of widespread deregulation of the c-*myc* gene in transgenic mice: multiple neoplasms and normal development. *Cell*. 45:485-495.

65. Pavelic, Z. P., P. Steele, and H. D. Preisler. 1991. Evaluation of c-*myc* proto-oncogene in primary human breast carcinomas. *Anticancer Res.* 11:1421-1427.

66. Schoenenberger, C. A., A. C. Andres, B. Groner, M. van der Valk, M. LeMeur, and P. Gerlinger. 1988. Targeted c-*myc* gene expression in mammary glands of transgenic mice induces mammary tumours with constitutive milk protein gene transcription. *EMBO J.* 7:169-175.

67. Borg, A., B. Baldetorp, M. Ferno, H. Olsson, and H. Sigurdsson. 1992. c-*myc* amplification is an independent prognostic factor in postmenopausal breast cancer. *Internat. J. Cancer*. 51:687-691.

68. Pertschuk, L. P., J. G. Feldman, D. S. Kim, K. Nayeri, K. B. Eisenberg, A. C. Carter, W. T. Thelmo, Z. T. Rhong, P. Benn, and A. Grossman. 1993. Steroid hormone receptor immunohistochemistry and amplification of c-*myc* protooncogene. Relationship to disease-free survival in breast cancer. *Cancer*. 71:162-171.

69. Dupont, W. D., and D. L. Page. 1985. Risk factors for breast cancer in women with proliferative breast disease. *New Eng. J. Med.* 312:146-151.

70. Cai, Z., M. Koerner, N. Tarantino, and S. Chouaib. 1997. IκB-α overexpression in human breast carcinoma MCF7 cells inhibits nuclear factor-κB activation but not tumor necrosis factor-α -induced apoptosis. *J. Biol. Chem.* 272:96-101.

Figure legends.

Figure 1. Transformed human breast cancer cell lines constitutively display high levels of nuclear NF-κB/Rel factor binding. A) Nuclear extracts from transformed MCF7 and 578T and untransformed MCF 10F and 578Bst breast epithelial cell lines in exponential growth were used in EMSA analysis with URE NF-κB element oligonucleotide as probe. The level of binding varied amongst the several MCF7 isolates studied, which is in accordance with the recent inability of another group to detect significant levels in their nuclear preparations (70). B) Nuclear extracts from 578T and MCF10F cells were used in EMSA analysis with the URE NF-κB oligonucleotide as probe in the absence (control) or presence of 10-fold molar excess unlabelled wild type (wt) or double mutant URE m1 (dm) as competitor. C) EMSA of PU.1 binding was performed, as above. Nuclear extract from the Raji Burkitt lymphoma B cell line was used as a positive control.

Figure 2. Constitutive nuclear NF-κB/Rel in transformed breast cancer lines is functional.
A) 578T cells were transfected in duplicate with either 10 ug of the URE_2-TK-CAT wt reporter plasmid in the absence (bar 1) or presence of increasing amounts of IκB-α expression vector (3 and 9 ug, bars 2 and 3, respectively), or with 10 ug of the URE_2-TK-CAT dm plasmid (bar 4). The total amount of DNA transfected into the cells was adjusted to 25 ug using pBlueScript plasmid DNA. Results were normalized to a TK-luciferase construct and are presented as percent of URE_2-TK-CAT wt activity (mean ± SD), which is set at 100%.
Inset: Nuclear extracts from exponentially growing 578T cells were incubated in the absence (-) or presence (+) of 1 ug of IκB-α-GST protein and subjected to EMSA analysis using the URE oligonucleotide as probe.

B) MCF7 cells were transfected in duplicate with 13 ug of p1.6 Bgl-CAT wt plasmid in the absence (bar 1) or presence of 3, 6, or 12 ug of IκB-α expression vector (bars 2, 3, or 4, respectively). Additionally cells were transfected with 13 ug of p1.6 Bgl-CAT dm plasmid containing two G to C conversions in its two identified NF-κB elements (46) (bar 5). The total amounts of DNA transfected into cells were equalized to 25 ug using pUC19 DNA. The data are presented relative to p1.6 Bgl-CAT wt activity (mean ± SD), which is set at 100%.
Inset: Nuclear extracts from exponentially growing MCF7 cells were incubated in the absence (-) or presence (+) of 1 ug of IκB-α-GST protein and subjected to EMSA analysis using the URE oligonucleotide as probe.

Figure 3. Microinjection of 578T cells with IκB-α protein induces apoptosis. A) Propidium iodide staining of 578T cells in exponential growth (none), and 3.5 hrs after microinjection with 1 ug/ul GST protein alone or 1μg/μl IκB-α-GST fusion protein. All cells shown within these representative fields were microinjected. (The left bottom panel displays a representative region of the full field; however, since the numbers of cells microinjected with IκB-α protein were greatly reduced, individual clusters of cells are shown in the smaller panels.) B) 578T cells (between 76 and 141 cells per sample) were microinjected in duplicate and cells stained with trypan blue 20-22 hours after microinjection to assess cell viability. Data are expressed as mean ± SD and are representative of 2 experiments. C) 578T cells (between 84 and 164 cells per sample) were microinjected in duplicate with the indicated double stranded wild type or mutant NF-κB oligonucleotide, and analyzed for trypan blue staining 20 hours after treatment. Data are expressed as mean ± SD.

Figure 4. Nuclear expression of NF-κB/Rel in primary rat mammary tumors but not normal mammary gland. A) Nuclear extracts were prepared from mammary glands from three untreated control rats (N1-N3) or from mammary tumors from DMBA-treated rats (T1-T4) and equal amounts (5 μg) subjected to EMSA for binding to the URE oligonucleotide, as described above. B) EMSA was performed with a nuclear extract from tumor T1 in the absence (control) or presence of 1 μg IκB-α-GST protein (IκBα), 50x molar excess unlabelled oligonucleotide containing URE wild type (wt) or mutant (dm) sequences (left panel). Alternatively, the antibody to the p50 subunit in the absence (p50) or presence of cognate peptide (p50 + pep) was added to the binding reaction. C) EMSA was performed with nuclear extracts described in part A with the PU.1 oligonucleotide. WEHI 231 B cell nuclear extracts were used as a positive control.

Figure 5. Nuclear expression of NF-κB/Rel subunits in primary human breast cancer tissue. A) p65: Samples of nuclear extracts from multiple tumor specimens (100 ug/lane) were analyzed using the anti-p65 antibody #1226 (54). B) c-Rel: Immunoblot analysis was performed on nuclear extracts (50 μg/sample) using an antibody against c-Rel protein (SC070, Santa Cruz Biotechnology Co.). C) p50: Immunoblot analysis was performed on nuclear extracts (50 μg/sample) using an antibody against p50 protein (SC114, Santa Cruz Biotechnology Co.). Patient samples are indicated by four digit numbers. As controls for detection, a nuclear extract from exponentially growing 578T cells (20 ug) was used in panel A, and nuclear (n) or cytoplasmic (c) extracts (50 ug) from WEHI 231 murine B cells (WEHI) were used in panels B and C, respectively.

A

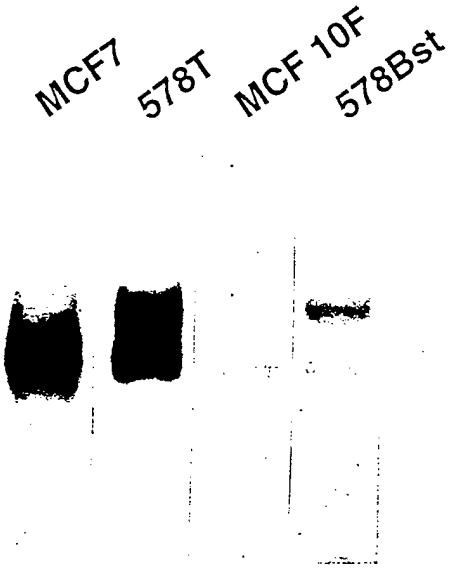
MCF7
578T
MCF 10F
578Bst

B

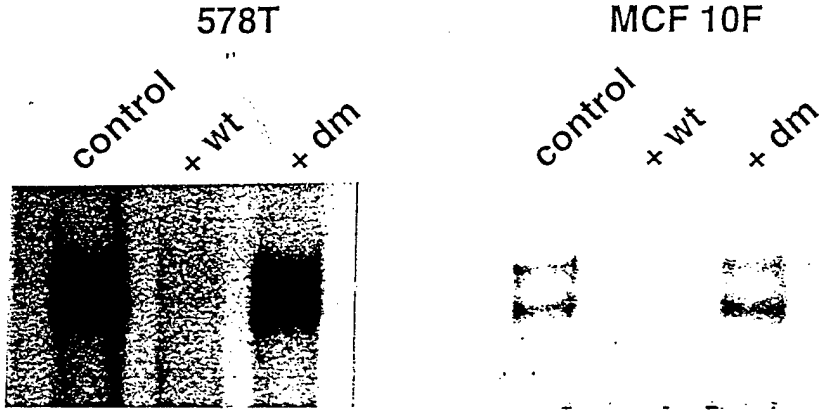
578T
MCF 10F
control
+ wt
+ dm
control
+ wt
+ dm

C

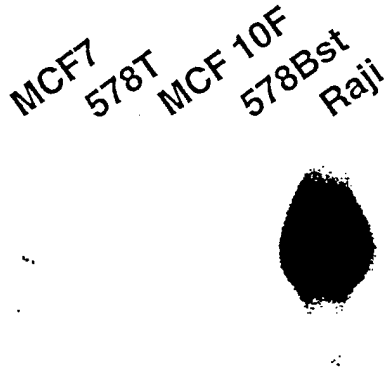
MCF7
578T
MCF 10F
578Bst
Raji

A

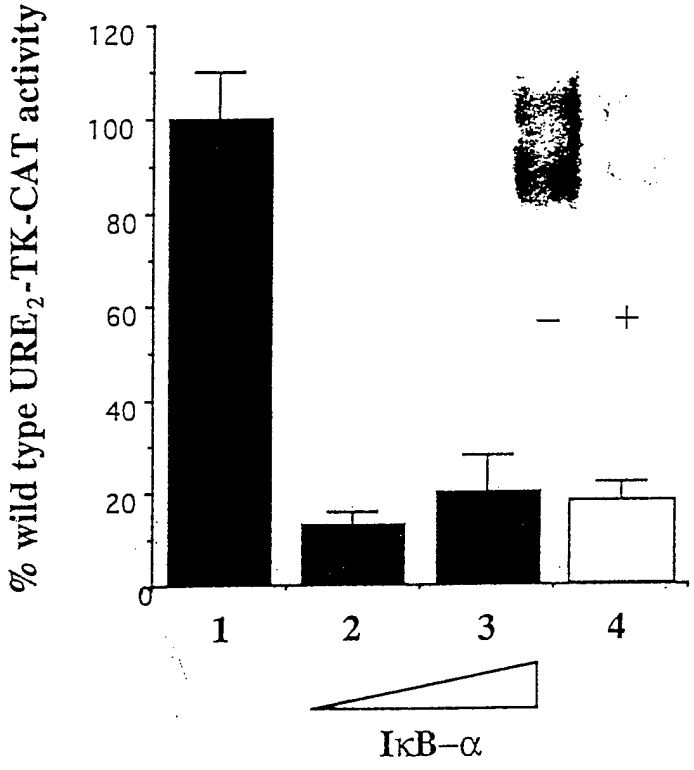
% wild type URE2-TK-CAT activity
120
100
80
60
40
20
0
1
2
3
4
IκB–α
–
+

B

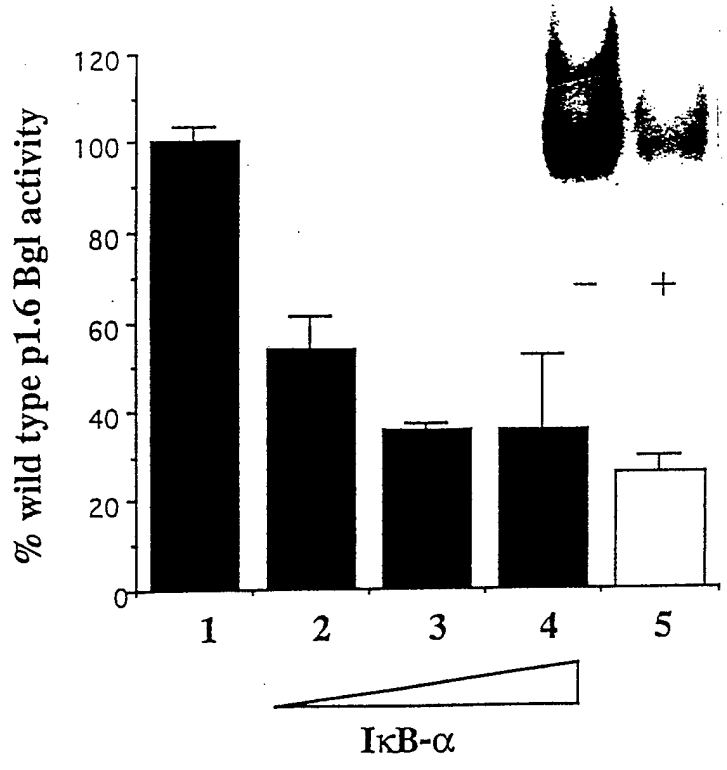
% wild type p1.6 Bgl activity
120
100
80
60
40
20
0
1
2
3
4
5
IκB-α
–
+

Figure 2

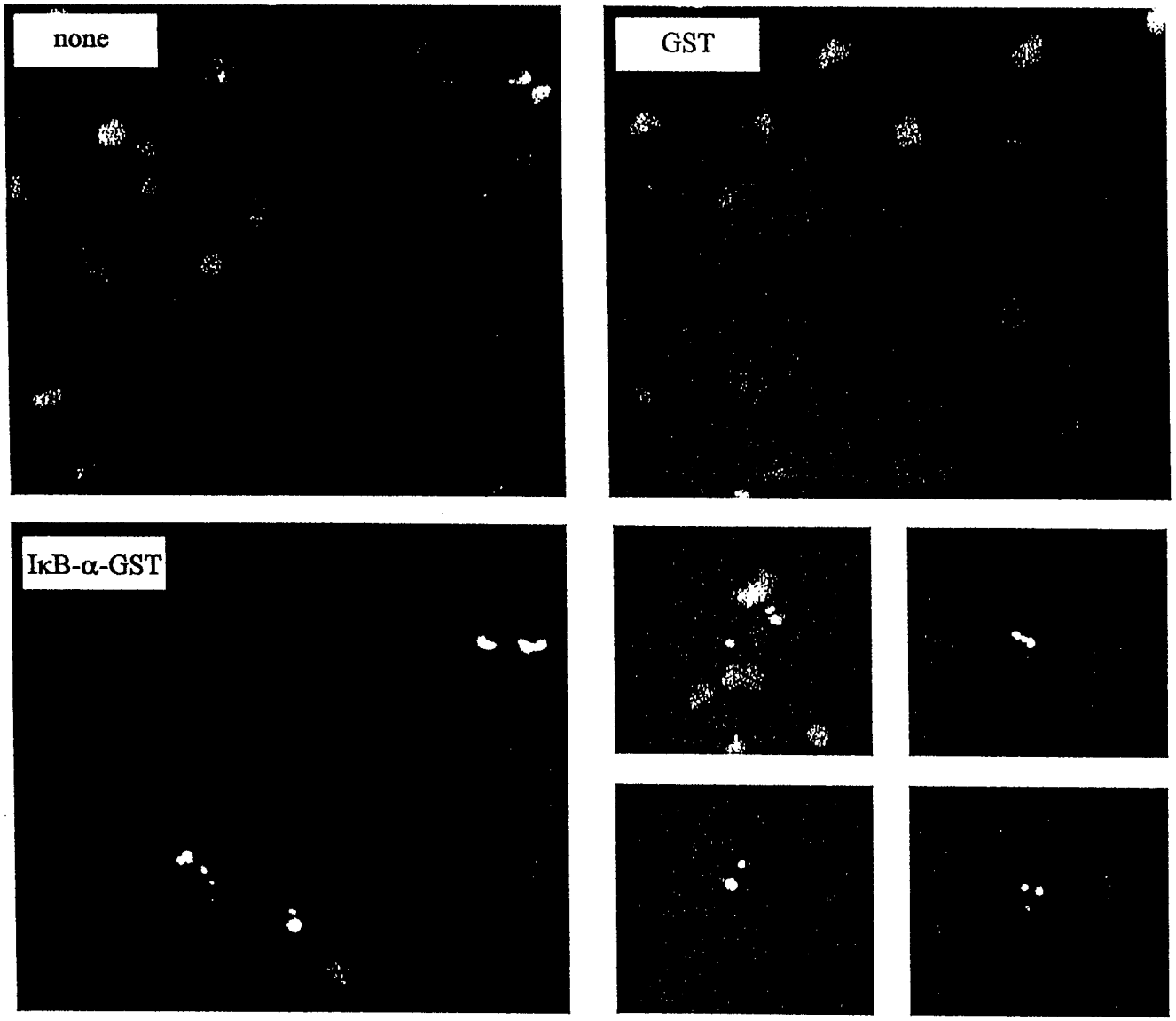
none
GST
IκB-α-GST

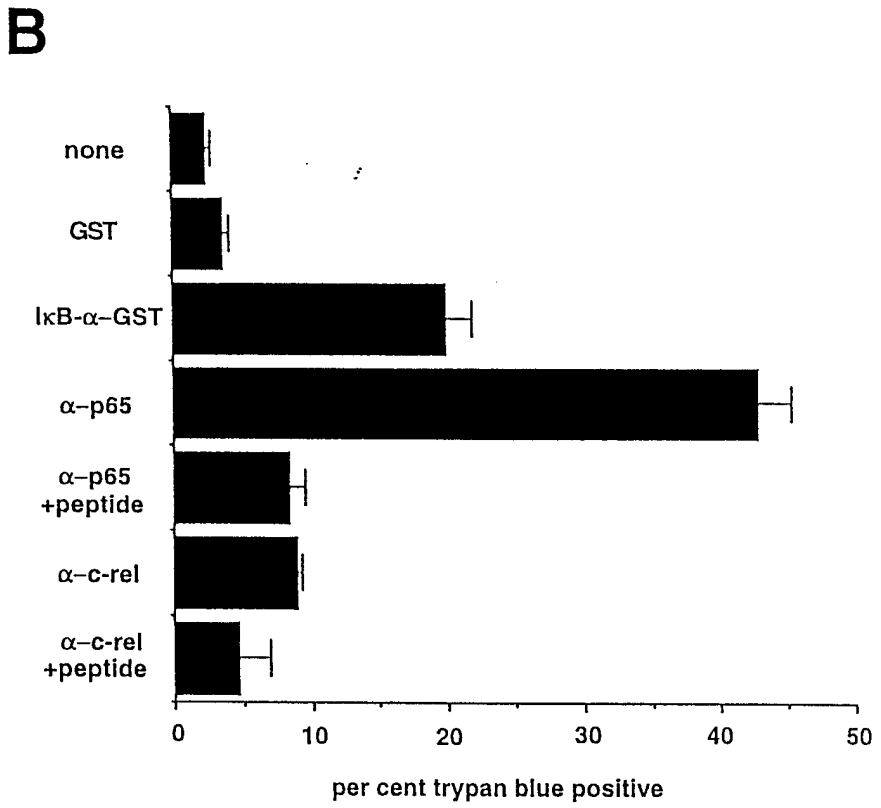
B
none
GST
IκB-α-GST
α-p65
α-p65
+peptide
α-c-rel
α-c-rel
+peptide
0
10
20
30
40
50
per cent trypan blue positive

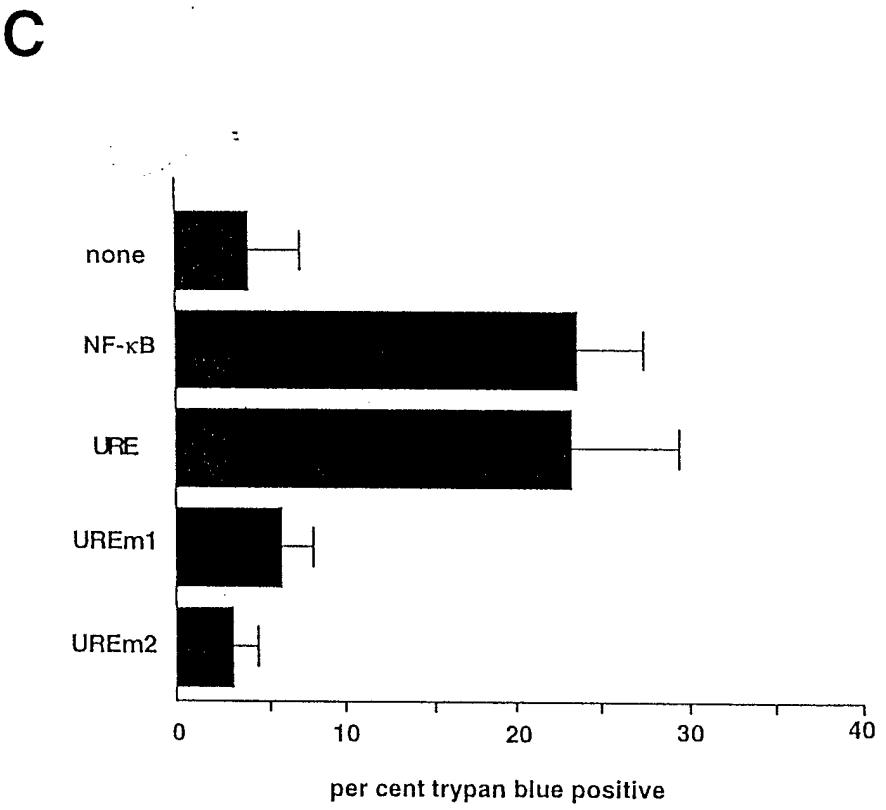
C
none
NF-κB
URE
UREm1
UREm2
0
10
20
30
40
per cent trypan blue positive

Figure 3B,C

A


N1
N2
N3
T1
T2
T3
T4

B

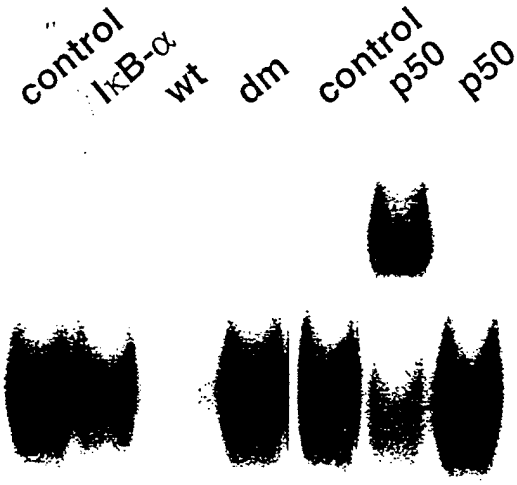
control
IκB-α
wt
dm
control
p50
p50 + pep

C

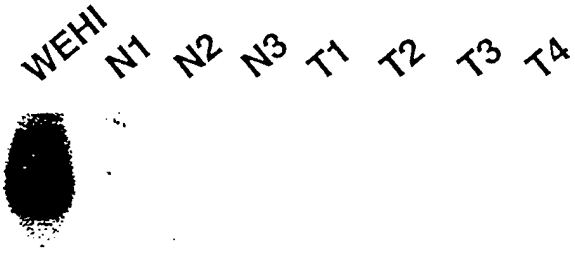
WEHI
N1
N2
N3
T1
T2
T3
T4

FIG. 4

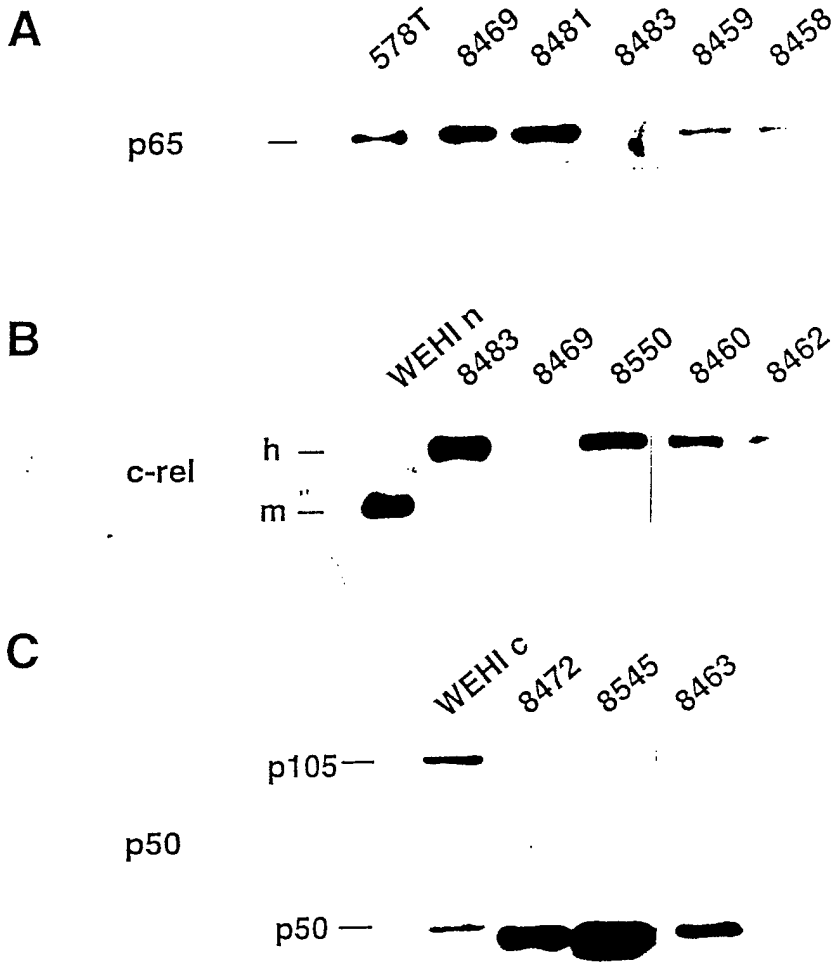

Figure 5

Sarkar et al

Table 1. Immunoblot analysis of nuclear NF-κB/Rel subunit expression in human breast cancer tissues.

CODE*	p65	c-Rel	p50
8445	+	+	+
8446	-	+	+
8448	+	+	+
8450	+	+	+
8458	+	+	+
8459	+	+	+
8460	+	+	+
8462	+	+	-
8463	-	+	+
8469	+	+	+
8470	-	+	+
8471	+	+	+
8472	-	+	+
8479	-	-	NA†
8481	+	+	-
8483	-	+	+
8484	+	+	+
8487	+	+	+
8488	+	+	+
8545	-	+	+
8547	+	-	+
8549	-	-	NA†
8550	+	+	+
Total Positive	15/23	20/23	19/21

* Patient samples are indicated by four digit numbers

† Not Available